INTERACTIONS BETWEEN ANTIWEAR AGENT AND NOVEL ADDITIVE IN ENGINE OILS

by

KAJAL PAREKH

Presented to the Faculty of the Graduate School of
The University of Texas at Arlington in Partial Fulfillment
of the Requirements
for the Degree of

MASTER OF SCIENCE IN MATERIAL SCIENCE AND ENGINEERING

THE UNIVERSITY OF TEXAS AT ARLINGTON

December 2005

ACKNOWLEDGEMENTS

The present research work is based on valuable inputs from several people. My advisor Prof. Pranesh Aswath has been a marvelous guide to me. His guidance has proved invaluable in helping me form the concepts of research and has been the main key to my findings. My deepest acknowledgments to him for the same.

I would like to thank Dr. Elsenbaumer for his expert counsel and timely tips that encouraged a ‘lateral thinking’ with all possible ways of approach and solving problems.

I wish to express my sincere gratitude to Dr. Goolsby for being a part of my thesis committee. His sense of discipline and sincerity have had a great impact on me.

Most of this work is based on the findings of Nuclear Magnetic Resonance Spectroscopy which was a completely a new characterization tool for me. Mr. Chuck Savage’s expert guidance on the instrumentation aspect of NMR including training to solving various technical problems helped me enormously in my work and finish it in a timely schedule. The TEM work involved another great contribution of Mr. Michael Coviello. It was through his efforts that it was possible to obtain TEM images and EDS spectrums for some samples. I am very grateful to Mr. Xin Chen, a doctorate student for valuable technical inputs in present research work. I wish to thank my colleagues Mr. Ramon Mourhatch, Mr. Krupal Patel, Ms Anuradha Somyaji for promoting a great team work. All the practical work involving experiments have received a significant helping hand from my fellow colleagues. My special thanks to the members of PRO team whose practical guidance and sponsorship has helped my thesis work greatly. I wish to thank Prudence Brett and Donna Woodhead for their continuous efforts in helping ship samples, place orders and official formalities.

Last but not the least I wish to thank my parents Arun Parekh, Urmila Parekh, my sister Hansika Parekh and my husband Jitesh Shah for being a constant source of love, support and encouragement to me. I also wish to thank my best friend Mr. Amith Kalaghatagi for being a great mental support in all times.

November 9, 2005

ABSTRACT

INTERACTIONS BETWEEN ANTIWEAR AGENT AND NOVEL ADDITIVE IN ENGINE OILS

Publication No. ______

KAJAL PAREKH, M.S.

The University of Texas at Arlington, 2005

Supervising Professor: Dr. Pranesh. B. Aswath, Dr. Ronald. L Elsenbaumer

Research has shown that side/end products of phosphorus and sulfur compounds in engine oils reduce effective life of exhaust catalysts of automobiles resulting in harmful emissions. Thus environmental regulations have been imposed on phosphorus levels in engine oils.

The main source of phosphorus in today's oils is the indispensable antiwear agent Zinc Dialkyl Dithiophosphate (ZDDP). To find cost-effective non-phosphorus substitute has not proven fruitful. A unique way of reducing phosphorus or ZDDP level while maintaining good antiwear performance has been achieved by introduction of a novel additive FeF_3 along with ZDDP. It appears that the interactions between FeF_3 and

ZDDP are strong enough not only in overshadowing the undesired interactions between ZDDP and additive package but result in more ‘protective film’ than the usual tribo-film from ZDDP decomposition products.

The objective of this research is to examine the chemical interactions between ZDDP and FeF_3 underlying their improved wear performance.

TABLE OF CONTENTS

Appendix

LIST OF ILLUSTRATIONS

LIST OF TABLES

CHAPTER 1

INTRODUCTION

Internal combustion engines dominate land transportation propulsion like cars, trucks, railroad, marine, motor bikes etc. Started from a simple design that consisted of a pair of overhead valves, the system was cheap reliable durable, space efficient and easy to service but consumed fuel heavily. So new ideas of system comprising of overhead camshafts and three or four valves per cylinder emerged which were worth the near-doubling of cost and complexity for the fuel efficiency gained [1]. Over the years engineers have tried to optimize internal design to make a major difference to economy, emissions, and power. But in the process, engine designers striving for greater efficiency have increased the stresses on engine components for e.g., the cam & lifter mechanisms commonly working at 1m/s speed experience as high as 1 GPa pressures or 1×10^9 Pascal's [2]. Today we drive thousands of miles comfortably in all weather conditions not being aware of these enormous stresses that exist inside our automobiles.

Simple lubricants are unable to sustain the enormous loads. Followed by major wear problems of engine components upon introduction of overhead valves and increased compression ratios in V8 engines in 1949, it was realized that oils containing Zinc Dialkyl Dithio phosphate or ZDDP generally gave less wear than oils without it [3]. The automobile industry revolutionized. Since then it has become the primary antiwear agent for 60 yrs in addition to being an antioxidant and a corrosion inhibitor.

These additives are incorporated into the lubricant packages and form surface films that protect the underlying material from the destructive forces applied under sliding condition [4]. The most widespread application of antiwear additives is in automobile engines, where the rubbing surfaces are almost exclusively composed of steel and cast iron.

The problem really began with the advent of exhaust after treatment catalysts (catalytic converter) in 1990. These catalysts are connected to the exhaust pipe present in automobiles. They are meant to convert the harmful emissions (CO, NOx, hydrocarbons) into harmless ones (CO_2, NO_2, H_2O) before releasing them into the atmosphere. It was realized that the side/after products like phosphorus oxides (and also sulfur oxides and ash) reduce the effective life of exhaust catalysts (poison it) thus resulting in more harmful tailpipe emissions [3]. This marked the beginning of regulations on levels of phosphorus in engine oils as evident from Table 1.1 [3].

Table 1.1 Phosphorus (P) and sulfur (S) limits in engine oil specifications

1989	SG	No P, S limits
1994	GF-1	≤ 0.12 % wt P
1997	GF-2	≤ 0.1 % wt P
2000	GF-3	≤ 0.1 % wt P
2004	GF-4	0.06% wt ≤ P ≤ 0.08% wt., ≤ 0.5%wt S

This has led to stricter controls on the concentrations of these elements in engine oils, which has limited the amount of ZDDP (a major source of these elements) that can be incorporated into motor oil formulation [4]. Consequences are that environmental action can be achieved at the cost of engine's life (significant wear). If the engine wears significantly, fuel/air mixture necessary to provide power through compression & combustion leaks into the sump and oil can similarly enter the combustion chamber and burn with the fuel [5]. The result is high oil and fuel consumption. It ultimately transforms into more power loss, more volatile hydrocarbons into the atmosphere, reduced drainage interval & low mileage!

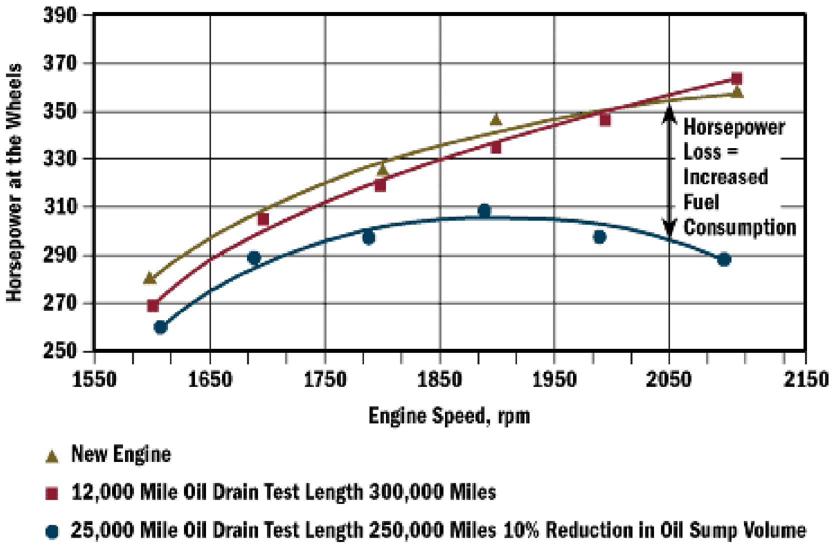

Figure 1.1 Loss in fuel economy due to power loss caused by significant engine wear

Fig 1.1 [6] shows an example of how increased engine wear, in this case due to overextended oil drains, contributes to power loss in the engine. At 2100 rpm, the severely worn engine horsepower at the wheels decreased from 365 hp to less than 300 hp (18 percent). Loss of horsepower translates directly to losses in fuel economy [6].

Reports from NASA indicate that loss due to wear is 100 billion dollars alone and savings that could be made by overcoming friction related losses could amount to 12-16 billion dollars per year in US [7]. So big is the driving force to balance the environmental and economy needs.

Until now several attempts have been made by researchers all over the world to reduce/eliminate phosphorus level in engine oils. Each is accompanied by some difficulty, resulting in no definite solution at present. Major attempts have been listed here.

1. Researches had initiated in the direction of innovative non phosphorus substitutes. Although none were found to be economically efficient and competent enough with ZDDP [3], strong research for a practical non phosphorus substitute still continues [8].
2. Attempts have also been made to understand the mode of antiwear action of ZDDP with a motive to make it more effective. To date (60 years) no unequivocal mechanism has emerged due to multidisciplinary nature of the wear process and complexity of ZDDP's antiwear reaction mechanism [2].
3. ZDDP is known to undergo competitive interactions with other surface active additives (used in engine oil) at the metal surface and direct reactions in the bulk [9]. More ZDDP is lost here by complexation/reaction with other additives rather than being available for the antiwear function. These are considered to be

antagonistic and result in unwanted consumption of ZDDP [10]. With a host of additives used in engine oils it becomes difficult to understand and thus control the multiple interactions occurring simultaneously. A lot of research is focused on understanding these interactions and overcoming the same [11, 12].

1.1 Drive for this research

A novel way of reducing the phosphorus or ZDDP level while maintaining a good antiwear performance has been achieved by the introduction of a second additive Iron fluoride FeF_3 along with ZDDP. Some features related to this new chemistry are:

1. The additive, iron (III) fluoride was found to significantly improve the antiwear performance of ZDDP even at very low levels of phosphorus [13]. The boundary condition wear performance of these oils containing 0.01 wt% phosphorus is comparable to oils without FeF_3 at much higher phosphorus levels of 0.1wt% phosphorus.
2. The beneficial effect was noticed even in presence of many other additives used in engine oil like the detergents, dispersants, etc [14]. Presumably the catalyst prevented the unwanted complexation between ZDDP and other additives at ambient temperatures.
3. It was considered to possess catalytic activities in decomposition of ZDDP i.e., facilitated the decomposition of ZDDP (decomposition process necessary for antiwear protection) at lower temperatures [15].

It appears that the interactions between FeF_3 and ZDDP are strong enough not only in overshadowing the undesired interactions between ZDDP and the additive package but result in more ‘protective film’ than the usual tribo-film from ZDDP decomposition products. It was a first incentive to look into the underlying mechanism.

It was also noticed that in presence of certain additives, the good effect vanished and instead the wear performance worsened. The ‘antagonistic effect’ in various formulations, could not be predicted forehand and thus the process could not be implemented in mass productions. It was necessary to acquire more knowledge about the mode of interaction of ZDDP with FeF_3 and interaction of the same with other additives.

1.2 Objective of research

At this stage it was necessary to understand the mechanism underlying the superior antiwear performance of the ZDDP-FeF_3 mix in engine oils. What can be possibly gained from this research can be summarized below.

Understanding underlying mechanism involved in the interaction of ZDDP and FeF_3

Differential Scanning Calorimetry data shows energy changes involved between the two components [14, 15]. Wear performance reflects a synergism between the two that results in an overall good wear performance [13]. This indicates some sort of interactions involved. It could be a simple catalytic effect or it could be Vanderwaals force of bonding. A chemical reaction resulting in new products is another possibility. In that case the knowledge of products and conditions under which they are formed would help understand the mechanism of the reaction. Identifying the nature of interaction involved will provide a chemical justification behind the improvement of antiwear performance of ZDDP in presence of FeF_3.

Attempting to solve dispersion problems or shelf life issues

Currently the blending of ZDDP and FeF_3 requires dispersing FeF_3 powder into the oil-ZDDP mix using a dispersing agent. This constitutes a complex step. Also it invariably gives rise to instability of dispersion or shelf life issues [13]. If any improvement could be made in the same area using the knowledge of mechanism study, it would prove very valuable.

Optimization of the wear performance of ZDDP-FeF_3 mix with preactivation conditions

The activity of the preactivated (heating the mix at 60-80 C for 1 hr) blend of ZDDP-FeF_3 (using FeF_3 powder) was found to be good in terms of wear performance. It was desired to optimize proper reaction conditions for 'preactivating' the blend with wear performance of the same based on the knowledge of mechanism studies.

1.3 Structure of thesis

The thesis comprises of eight chapters. Each chapter is included here with an outline summary of the contents detailed in the chapter later.

Chapter 1 Introduction This chapter is meant to introduce the reader to the drive and objective behind the whole research. It also includes what can be gained from such a study from research point of view.

Chapter 2 Background The conflicting needs of Wear vs. Emissions and Energy Economy pose a challenge and serve as the origin for this research. This chapter acquaints the reader with the fundamental issue of wear, economical impacts due to the same and combating it with proper lubrication system. Lubrication in automotive applications particularly at the 'start up' of an engine regarded to be critical is the prime focus area. Boundary lubrication most severe regime of lubrication, leads into the concept of ‘additives’ being added to engine oil to help achieve the diverse needs of an engine. How the additive ZDDP present in the lubrication system plays an important role in combating wear is discussed.

Chapter 3 Outline and Approach The approach adopted involves thermal degradation of ZDDP that helps in understanding the underlying mechanism in terms of the products formed in presence and absence of FeF_3. A layout of the entire work divided into four parts is outlined here.

Chapter 4 Experimental procedure: The experimental procedure is discussed here in details.

Chapter 5 Nuclear Magnetic Resonance Spectroscopy (NMR) The characterization tool that has been extensively used in this research is NMR. Theory and working principle of the same have been discussed briefly to acquaint the reader in the analysis of NMR spectra and understand the findings and the results.

Chapter 6 Results and Discussions: Results of all the experiments and characterization techniques have been discussed here.

Chapter 7 Conclusion This chapter concludes the thesis.

Chapter 8 Future Work It includes the scope of more work that could supplement and/or complement this work.

CHAPTER 2

BACKGROUND

2.1 Wear and Tribology

Whenever two surfaces slide past one another, the potential for the deterioration of one or both the surfaces exist. Wear is not an undesirable effect in all cases. For e.g. in rotating plain bearings, piston sliding in cylinders, automotive brake disks with break pads, processing of materials by machining, forging, extrusion wear is intentional [4, 16]. However in other cases wear is not desirable like some structural joints where small cyclic displacements (fretting) cause wear under oscillating loading, in biological artificial joints, computer hard drives , automobile engines where wear in crankcases is caused by metal-metal contact, abrasive particulate, and attack by corrosive acids, blow by gases from combustion chamber etc. [4, 16,17].

Friction, wear, lubrication and adhesion of engineering surfaces with a view to understanding surface interactions are all associated with the discipline of ‘Tribology’. Tribology is defined as the science and technology of interacting surfaces in relative motion and deals with force transference between surfaces moving relative to each other [7]. Many processes in nature and technology depend on the motion and the dynamic behavior of solids, liquids, and gases (Table 2) [7]. Bearings employ either sliding or rolling action and gears have both sliding and rolling action, a strong attempt is made to provide enough lubrication to keep the bearing and gear teeth surfaces separated by a film of solid lubricant, oil, or other lubricant such as grease [7].

Table 2.1 Type of surface motion and related objects

Related subject	Schematic representation of contact and motion		
	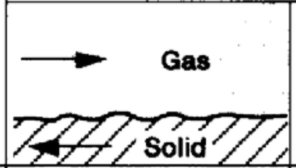		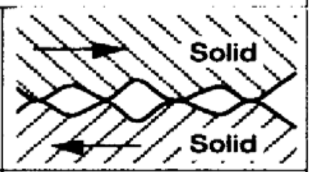
Lubrication	Gas or air film	Fluid film	Solid film
Resistance to motion	Gas or air friction	Viscous friction	Solid friction
Damage mechanism	Erosion; corrosion	Cavitation erosion; corrosion	Wear; erosion
Technical systems	Gas turbine; wind turbine	Hydraulic turbine	Seals; clutches; brakes; wheel and rail; tires

The subject of Tribology is multidisciplinary nature and thus has received insufficient attention. Some classical estimates of economic losses due to Tribology and savings through the same are presented in table 2.1 which indicate that the cost of tribological losses is large and should be reduced by national efforts.

Table 2.2 Economic impacts in Tribology

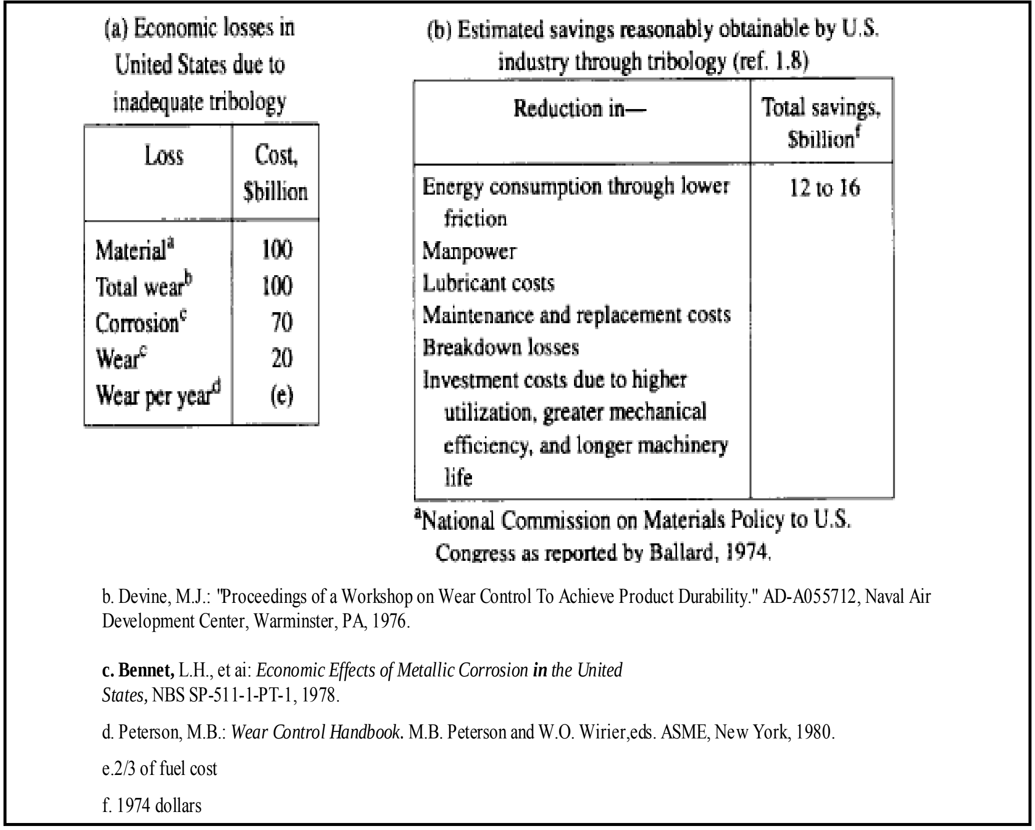

(a) Economic losses in United States due to inadequate tribology

Loss	Cost, $billion
Material[a]	100
Total wear[b]	100
Corrosion[c]	70
Wear[c]	20
Wear per year[d]	(e)

(b) Estimated savings reasonably obtainable by U.S. industry through tribology (ref. 1.8)

Reduction in—	Total savings, $billion[f]
Energy consumption through lower friction	12 to 16
Manpower	
Lubricant costs	
Maintenance and replacement costs	
Breakdown losses	
Investment costs due to higher utilization, greater mechanical efficiency, and longer machinery life	

[a]National Commission on Materials Policy to U.S. Congress as reported by Ballard, 1974.

b. Devine, M.J.: "Proceedings of a Workshop on Wear Control To Achieve Product Durability." AD-A055712, Naval Air Development Center, Warminster, PA, 1976.

c. Bennet, L.H., et ai: *Economic Effects of Metallic Corrosion **in** the United States,* NBS SP-511-1-PT-1, 1978.

d. Peterson, M.B.: *Wear Control Handbook.* M.B. Peterson and W.O. Wirier,eds. ASME, New York, 1980.

e.2/3 of fuel cost

f. 1974 dollars

2.2 Wear control vs. emissions and energy economy

2.2.1 Wear vs. emissions

In the past, oil formulators could make a premium product to improvise wear performance by simply adding more ZDDP, the antiwear agent. A similar move today would result in an oil formulation that would not support new car warranties. The reason is due to stringent emissions and fuel economy standards mandated by the U. S. Government. Automotive OEM's need better fuel economy to meet Corporate Average Fuel Economy (CAFÉ) limits [18].

Catalytic converters became part of the vehicle exhaust system in the mid-1970s to meet emission regulations mandated by the U.S. Environmental Protection Agency (EPA) [18]. Engineers and scientists have tried to optimize the performance and durability of these devices to meet increasingly stringent emissions and durability standards. As catalysts age, their ability to convert exhaust pollutants decreases and stringent regulations of today require the catalytic converters to provide reduced emissions for 120,000 miles [18]. There is no engine test that measures emission system stability, but the OEM's have data showing that sulfur and phosphorus are poisons for catalytic converters and must be limited. An experiment procedure demonstrated [19] the same. This involved automobile catalyst washing as the first step to remove the phosphorus. The washing (1-8) procedure is outlined below.

1. 1 Molar oxalic (weak acid) solution at 80 °C
2. 30 minute soak, rinse and collect wash solution (Repeat soak and rinse)
3. Measure total solution volume and collect sample to determine phosphorus concentration
4. Dry washed catalyst at 200 °C and Calcined at 500 °C
5. Removes ~ 90 % of Phosphorus

Used catalysts of automobiles (known mileage) were subjected to a washing treatment outlined (steps 1-8) to remove most of the deposited phosphorus. The concentration of removed phosphorus was measured and catalysts were tested for harmful emissions. ‘Aged catalyst’ under identical conditions without any washing treatment and thus phosphorus removal were used for comparison. Results in fig 2.1

[19] demonstrate that upon removal of phosphorus the used catalysts regained their efficiency as compared to aged catalysts in which phosphorus was still present. This proves the fact that presence of phosphorus on catalysts of automobiles reduces their efficiency in reducing harmful emissions.

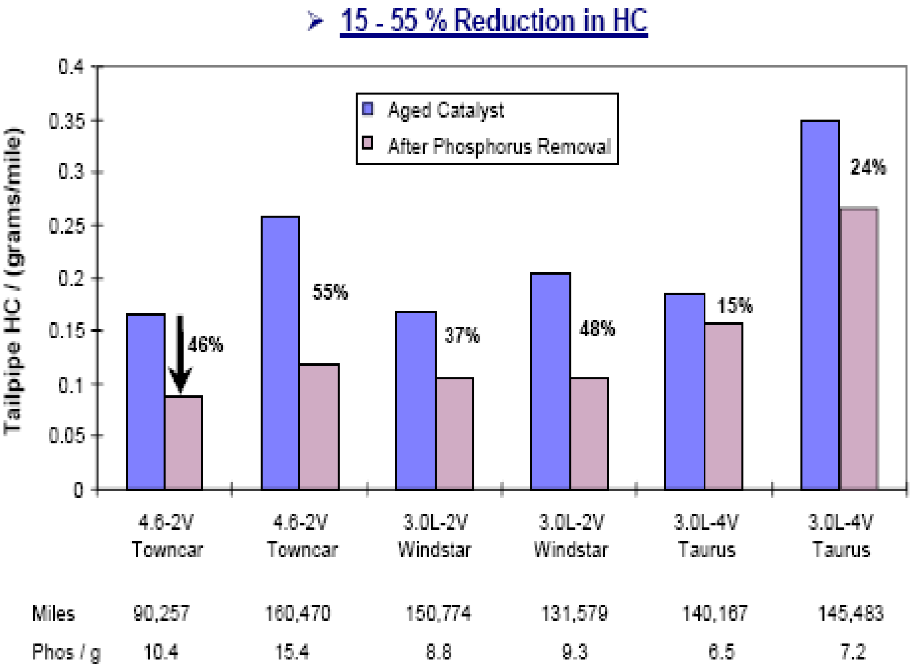

Figure 2.1 Effect of phosphorus removal from catalytic converter on hydrocarbon emissions

Today's new GF-4 oils conforming to environmental regulation limit sulfur to 0.5%, maximum, in 0W- and 5W- engine oils and 0.7%, maximum in 10W- engine oils phosphorus is limited to 0.08% [18]. This restricts the amount of Zinc Dialkyl Dithiophosphate, the workhorse anti-oxidant and anti-wear agent, which can be used in engine oils. So the question is how can less wear and less emission be achieved at the same time.

2.2.2 Wear vs. energy economy

When viscosity of oil selected is too high it may offer more protection for more severe operations such as driving through mountains, high rpm, overloading, overheating [20]. Thicker oil films can also accommodate larger contaminants. So wear is reduced at the expense of greater energy consumption. To the other extreme, exceedingly low viscosity can periodically bring surfaces into boundary conditions (mechanical rubbing) and sharply increased sensitivity to particle contamination thus causing wear [21]. However since thinner oils have less drag save fuel and thus consume less power but as wear increases, the efficiency of an engine declines [20].

2.2.3 A challenge

The convergence of these trends reflects the need for engine lubricants that deliver improved fuel economy at a lower level of Phosphorus and Sulphur (lower emissions) and good level of wear performance. Fuel economy (thin oils) trends generally increase the levels of phosphorus- and sulphur-containing compounds to help reduce friction in the engine and increase wear protection. Emission trends are driving down the levels of phosphorous and sulphur for after treatment system compatibility. This constitutes a challenge.

The enormous economic and environmental damage due to uncontrolled friction and wear as seen in Table 2.2, the desire to understand the relevant wear processes and the need to develop balanced lubricants that satisfy the above conflicting factors have spurred interdisciplinary research activity even on nanometer scale [4].

2.3.Different types of wear

'**Wear** can be defined as damage to a solid surface generally involving progressive loss of material, due to relative motion between that surface and a contacting substance or substances [16].' Wear resistance is not a materials property and that the mechanism of wear of a particular material and the associated rate of wear depend critically on the precise conditions to which it is subjected (by Hutchings 1992).

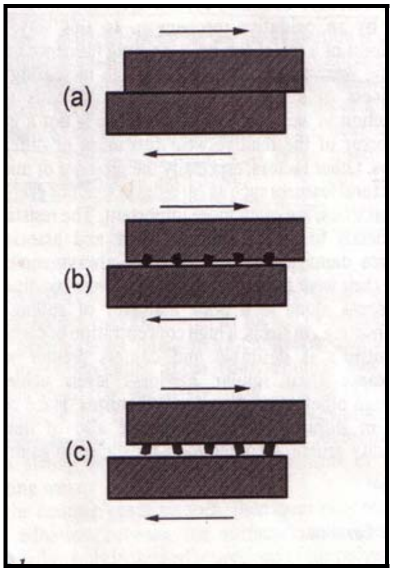

Figure 2.2 Different types of wear (a) sliding wear (b) two-body abrasion (c) three body abrasion

Sliding wear: Two surfaces slide against each other with either continuous or discontinuous relative motion. Often there is a lubricant film present. When sliding occurs unlubricated in air it simulates a worst case in which any lubrication initially present has broken down. Sliding wear is also known as adhesive wear (fig 2.2 a) [16].

Abrasive wear: A third body is present in the form of discrete hard particles which are dragged across the surface by a counter body. These particles may either be fixed to the counter body (2 body abrasion, fig 2.2 b) or be loose and free to slide and roll between the 2 surfaces in 3 body abrasion (fig 2.2c) [16]. The conditions in abrasive wear are either low stress in which abrasive particles are relatively undamaged in wear process or high stress when the particles experience extensive fracture.

The cause of ***friction***, on the other hand, is the resistance between two moving objects in contact. There are two types of friction-surface-to-surface friction and fluid friction. Surface-to-surface friction occurs when there is physical contact between two solid bodies moving relative to each other [17]. The type of motion determines whether it is rolling friction or sliding friction. Fluid friction is the friction between a fluid and two solid bodies which are in relative motion, separated by that fluid and is caused by the resistance to motion between the molecules of the fluid [17]. Friction and wear can be combated primarily by means of either of the two.

1) Lubrication

2) Coatings or Surface modification.

The entire research work is confined to lubrication only.

2.4 Lubrication system

Scientific definition of Lubrication: *Lubrication essentially involves introducing a layer of material with low shear strength between the two surfaces. It is one of the most powerful methods of reducing sliding wear as well as reducing friction*

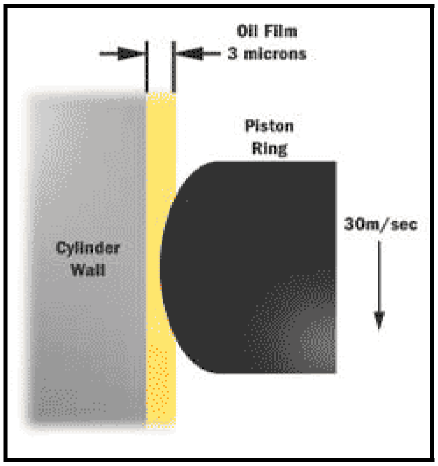

Figure 2.3 A lubricant film sandwiched between moving metal components

In fig 2.3 [6] the film is sandwiched between piston ring of an internal combustion engine moving against the cylinder walls. The oil film is approximately 3 micron thick and prevents the metal to metal contact in other words prevents wear.

2.4.1 Various diverse areas of lubrication and automotive lubrication

These include automotive lubrication, aviation, aerospace lubrication, food and Beverage lubrication, industrial lubrication [22]. For Automotive lubrication components are body Components - Door Systems, Sun Roof Systems, Airbags, Mirrors, Lock Systems, Control Cables, Interior Components, Seating Systems, and Bolts & Fasteners; Chassis and Brake Systems - Chassis and Brake Systems; Electrical Components - Connectors, Relay Switches, Accessories, Ignition Systems, and Lighting; Fuel and Air Systems - Fuel and Air Systems and Power train Components - Assembly Aids, Cooling and Climate Control Systems, Engine Coatings, Clutch, Head Gaskets, and Transmission & Gearboxes [22].

2.4.2 Lubrication in engine and its components

The lubrication system makes sure that every moving part in engine gets oil so that it can move easily. The two main parts in engine needing oil are the pistons (so they can slide easily in their cylinders) and any bearings that allow things like the crankshaft and camshafts to rotate freely. In most cars, oil is sucked out of the oil pan by the oil pump, run through the oil filter to remove any grit, and then squirted under high pressure onto bearings and the cylinder walls. The oil then trickles down into the sump, where it is collected again and the cycle repeats.

2.4.2.1 Lubrication is critical during 'start up'

During those brief moments from starter engagement, engine firing and up to oil pressure rise, the engine runs without sufficient lubrication. Depending on frequency and duration of operation, very significant wear is attributed to this short interval. If the engine is run frequently - every day - less wear occurs during start because oil is retained on critical surfaces. However, if the engine sits for long periods - days, weeks or months - then the oil will evaporate and drain from critical parts, and they will run without lubrication until oil flows sufficiently to pressurize the entire system. Some technical studies have shown as much as 70% of total engine wear to this starting interval [23]. If this interval is eliminated with oil, the engine should last much longer.

Gears, bearings, cam lobes and lifters need oil to prevent distress. When lubricated last nearly indefinite. Plain bearings - mains and rods - need oil at the onset of motion to prevent contact between the crank journals and the bearings. Cylinder walls need oil to lubricate the pistons and piston rings. Without lubrication, the pistons and rings wear quickly and oil consumption increases rapidly. *Hydraulic valve lifters* [23] need oil under pressure to operate properly. Without a constant flow of pressurized oil, lifters collapse and take a pounding as the valve system operates with excess clearance. With lubrication, the lifters extend properly and valves operate with correct timing and little undue distress. *Turbochargers* [23] require special attention during start to avoid bearing and shaft wear. If there is no lubrication for the turbo's shaft, it will wear quickly and will require a premature overhaul.

In brief, all engine parts need lubrication at the first onset of motion to keep wear to a minimum. Pre-oiling the engine by pressurizing the lubricating system and pumping oil through it before starting will eliminate that high wear interval usually experienced during start [23].

2.4.3 Primary functions of lubricant

Friction Reduction Friction is reduced by maintaining a film of lubricant between surfaces that are moving with respect to each other, thereby preventing the surfaces from coming into contact and subsequently causing surface damage. The amount of frictional resistance to motion can be expressed in terms of the coefficient of friction. It is the frictional force opposing motion divided by load @ right angles to surface. For non-lubricated metal of ordinary surface finish and cleanliness, exposed to the atmosphere, the value may be about 1. For the same metal contaminated by handling, the value will drop to about 0.3 to 0.1 [24].

Surface damage is almost always a more important factor than the size of the coefficient of friction. Whilst a good boundary lubricant, in comparison with a poor one, may reduce the coefficient of friction several fold, it is much more significant that interfacial damage may be reduced a thousand fold and similarly a several fold difference in damage may be accompanied by an imperceptible change in friction [25].

Heat Removal To act as a coolant, removing heat generated by either friction or other sources such as combustion or contact with high-temperature substances. In performing this function, the lubricant must remain relatively unchanged. Changes in thermal and oxidative stability will materially decrease a lubricant's efficiency in this regard [24].

Suspension of Contaminants The ability of a lubricant to remain effective in the presence of outside contaminants is quite important. Among these contaminants are water, acidic combustion products, and particulate matter. Abrasive wear may be reduced by filtering intake air and corrosive wear caused by acidic materials may be reduced by adding alkaline detergents [24].

2.4.4 Different types of lubricant

The fluid film lubrication types would include - Oils (mineral, synthetic), Grease and Solid lubricants.

Oils are the most common lubricants. Natural mineral oils contain several different hydrocarbon species with mean molecular hydrocarbon species with mean molecular masses between about 300 and 600 of which predominant are saturated long chain hydrocarbon (paraffin's) with straight or branched chains containing 20-30 carbon atoms and saturated 5 or 6 membered rings with attached side chains up to 20 carbon atoms long (napthenes) [16]. Aromatic components are also present in small proportions. Mineral oils may be broadly classified as paraffinic in which the napthenes have long paraffinic side chains and most of the carbon atoms are present in paraffin chains, naphthenic in which the naphthenic side chains are short and the proportion of carbon atoms in the rings is slightly less than that in the side chains or mixed [16]. Synthetic oils include synthetic hydrocarbons where closer control over chemical and physical properties is required; organic esters; polyglycols; and silicones. For some purposes grease is preferable to oil. It's a semisolid mixture of oil and a thickening agent often soap (metallic salt of carboxylic acid) or a clay mineral (e.g., bentonite).

Solid Lubricants: Thin films of solid materials with low shear strength can also be sued as lubricants. These solid lubricants are particularly useful where supply or replenishment of a liquid lubricant is a problem at high temperature or in vacuum. Some solids with lamellar structure graphite, MoS_2, PTFE can provide low friction. All these materials can be applied as coatings on one of the sliding surfaces or incorporated into composite bearing materials even dispersed in oils [16].

2.4.5 Lubrication regimes

In fluid film lubrication the sliding surfaces are separated by a thin film of lubricant, and both the frictional force and the resulting wear rate depend on the thickness of this film. The minimum film thickness in a lubricated contact, h_{min} , is conveniently described by the dimensionless quantity λ.

$\lambda = h_{min} / \sigma^*$ where σ^* is the root mean square roughness of the two surfaces, defined by $\sigma^{*2} = R^2_{q1} + R^2_{q2}$ where R_{q1} , R_{q2} are the r.m.s roughness values for each surface [16]. The value of λ provides a measure of the extent of asperity interactions during lubricated sliding. (Mean bearing pressure = Normal load/area).

Based on values of λ the lubrication regime can be divided into 3 types in fig 2.4

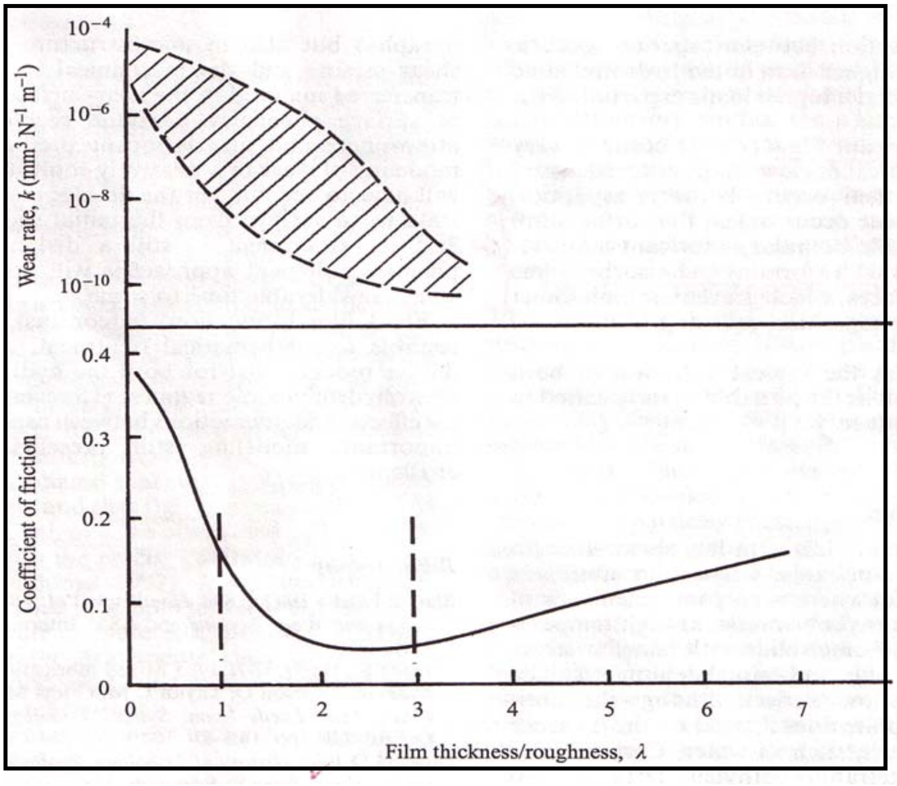

Figure 2.4 Regimes of lubrication and wear in the lubricated sliding of metals as a function of λ, the ratio of oil film thickness to surface roughness

Hydrodynamic condition

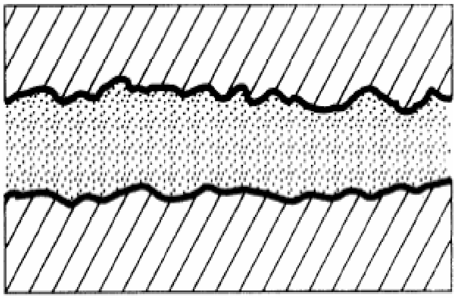

Figure 2.5 Hydrodynamic lubrication

In this situation λ > ~ 5, physical features are

- Full fluid film separates the surfaces at all times
- Asperity contact negligible
- Both friction and wear very low
- Lubricant Flow assumed to be laminar and dominated by linear viscosity.

Oil lubricated hydrodynamic bearings running under steady load are usually < 2 MPa although pressures can reach a transient maximum of ~ 50 Mpa with local maxima in the oil film perhaps five times greater still. The theory assumes that under these conditions, friction occurs only within the fluid film, and is a function of fluid viscosity [16, 17]. The equilibrium thickness of the oil film can be altered by [24]:

- Increasing load, this squeezes out oil.
- Increasing temperature, causing more oil leakage.
- Changing to lower viscosity oil, which also causes more oil leakage.
- Reducing journal speed, which generates a thinner oil film.

Elasto-hydrodynamic condition

As pressure or load increases, viscosity of the oil also increases. As the lubricant is carried into the convergent zone approaching the contact area, the two surfaces deform elastically due to lubricant pressure. In the contact zone, the hydrodynamic pressure developed in the lubricant causes a further increase in viscosity that is sufficient to separate the surfaces at the leading edge of the contact area. Because of this high viscosity and the short time required to carry the lubricant through the contact area, the lubricant cannot escape, and the surfaces will remain separated. The main effect of a load increase is to deform the metal surfaces and increase the contact area, rather than decrease the film thickness as seen in fig 2.6 [24].

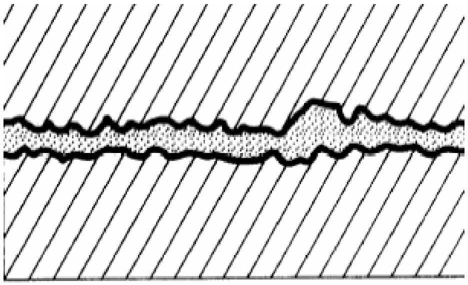

Figure 2.6 Elasto-Hydrodynamic lubrication

In this situation $\lambda < \sim 5$, physical features [17] are

- Contacting surfaces counter formal (i.e., nonconforming) involving nominally line or point contact as a result much greater local pressure ~ atmospheric pressure.
- Both elastic deformation of bearing surface and pressure dependence of the viscosity of oil become important.
- Film thickness > 1 µm.

Boundary condition – the critical regime

Whenever a fluid film is not maintained between sliding surfaces the contacting “boundaries” of the bodies in relative motion suffer wear, usually including some transfer of material of each to the other as seen in fig 2.7. Boundary lubrication controls this damage by interposing a solid barrier.

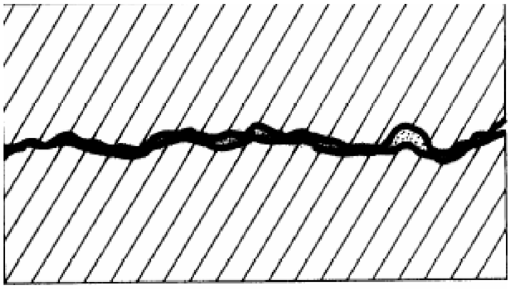

Figure 2.7 Boundary lubrication

In this situation λ < 1, physical features [16, 17] are

- Thinner lubricant films
- Very high contact pressure & low sliding speeds
- Significant contact between asperities
- Thickness of film ~ as same order of size as lubricant molecules
- Under certain conditions -- such as shock loading, steady heavy load, high temperature, slow speed, and critically low viscosity -- the lubricant system no longer remains in the hydrodynamic regime resulting in a significant rise in temperature and subsequent destruction of the contacting surfaces.

Under these circumstances, the fluid film is no longer capable of adequately protecting the surfaces, and physico-chemical properties of lubricant gain importance. This formed the basis for the need of additives in oil [26].

2.5 Role of 'additives or additive package' in lubricant

Oil serves the basic vital function of lubrication. The major causes of engine malfunction due to lubricant quality are deposit formation, contamination, oil thickening, oil consumption, ring sticking, corrosion, and wear [27]. The performance of engine lubricants is judged on their ability to reduce friction, resist oxidation, minimize deposit formation, and prevent corrosion and wear. To meet these functional requirements, engine lubricants must be supplemented with additives. Diverse important functions required in engine are provided by incorporating different types of additives. These are provided in appendix A. So *additives can be classified as materials that impart new properties to or enhance existing properties of the lubricant or fuel into which they are incorporated.* *Lubricant System = Base Oil + Additive package*. A typical recipe for a passenger car lubricant looks somewhat as given below [19].

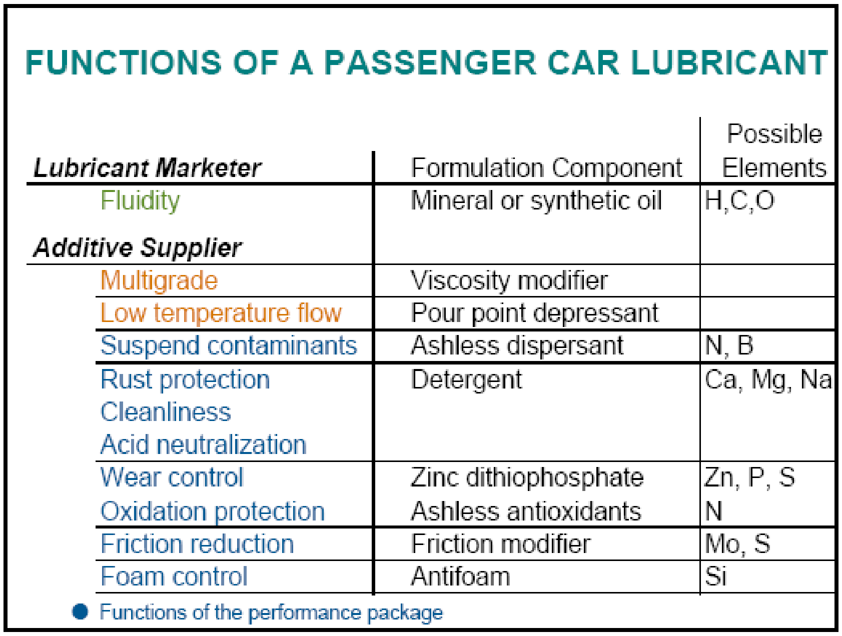

FUNCTIONS OF A PASSENGER CAR LUBRICANT

Lubricant Marketer	Formulation Component	Possible Elements
Fluidity	Mineral or synthetic oil	H,C,O
Additive Supplier		
Multigrade	Viscosity modifier	
Low temperature flow	Pour point depressant	
Suspend contaminants	Ashless dispersant	N, B
Rust protection Cleanliness Acid neutralization	Detergent	Ca, Mg, Na
Wear control	Zinc dithiophosphate	Zn, P, S
Oxidation protection	Ashless antioxidants	N
Friction reduction	Friction modifier	Mo, S
Foam control	Antifoam	Si

● Functions of the performance package

Figure 2.8 A typical recipe for a passenger car showing the additive package added to lubricant

2.6 Antiwear additives

As we have seen earlier that prevention of wear is a prime requirement of a lubricant, several antiwear agents will be discussed. Commonly used antiwear additives include phosphate esters, sulfurized olefins, sulfurized sperm oil, metal dithiophosphates, borates and phosphites. Brief comparison of their advantages and disadvantages has been included in table 2.4 [17]. Brief comparison between few dithiophosphates is given in Table 2.3 [17]. AW = antiwear, AO= anti oxidant, EP =extreme pressure and FR= friction reducer. Of all antiwear agents Zinc Dialkyl Dithio phosphate has been the most cost effective antiwear additive and has enjoyed 60 years in the industry.

Table 2.3 Comparison of wear reducing properties of various dithiophosphates as antiwear agents

Type/ structure	Coefficient of friction (FR)	Wear Scar (AW)	Comments
Molybdenum Dithio phosphate MoDTP	0.045 Best FR Fuel consumption reduced by 2-5%	0.28 (with 0.04% Mo, o.5 wt% oil, 60 min)	Wearing away of asperity tips and formation of micro terraces. Also MoS_2 deposited on valleys, surface layer thin and uniform have Mo, S,P
Zinc Dialkyl Dithio Phosphate ZDDP	0.11	0.80 (1% ZDDP at 40Kg in 60 min) ASTM D 2783	Not so good as compared to MoDTP but very cost effective.
Tri Cresyl Phosphate TCP	0.09, Good FR	0.55 (1% TCP at 40Kg, 60 min) ASTM D 2783	Not thermally stable Toxic, carcinogenic when arsenic is present upto 1ppm.

Table 2.4 Brief comparison of various antiwear additives

Type/ structure	Advantages	Disadvantages	Comments
Phosphate esters, $P(OR)_3$ R = alkyl/aryl 4-20 carbon atoms E.g. , MoDTP, TCP, ZDDP etc	Discussed in table 2.3		
Sulfurized olefins	EP, AW, AO	High friction coefficient Free sulfur problematic with Cu and similar metals	Formation of sulfide films on metal surface
Sulfurized sperm oil	FR, antiscuff agent	Have to be added with iron corrosive chemicals like Cl, S compounds HCl, H_2S corrosive and unsafe	Film of FeS (solid lubricant)
Borates Borates of mixed alcohols, amides, hydroxyl esters etc $K_2OyB_2O_{3x}H_2O$ Y =2.5-4.5 general hydrated formula,	EP, AW (non Phosphorus type)	In presence of water boron crystallizes out of the oil and forms hard granules which cause sever noise and can damage gears/bearings by deposit formation. Compatibility problems with phenates, sulfurized fats	
Phosphite	AW		Not firmly established
Metal Dithiocarbamate $(R_2NSC_2)_xM$ M= Mo, Zn, Sb R= 1-22 C atoms X= 1,2,3 depends on M	FR (non phosphorus) AW viscosity stability copper corrosion inhibitor		Surface film of MoS_2

.

2.7 Boundary lubrication by Zinc Dialkyl Dithiophosphate (ZDDP)

2.7.1 Boundary lubrication films

Under boundary conditions any action to prevent wear must involve means of keeping the two sliding bodies apart other than a continuous oil film. As has been put so rightly by Kapsa and Martin [26] that any wear, degradation or indeed dissipation of energy occurs in a material other than the sliding members themselves provided an interface material can be constantly maintained. This appears in the form of reaction film so called because it is formed at contact positions by chemical reactions involving the additive incorporated in the lubricant base. Thus it could be said that the incidence if wear of mating materials is prevented and replaced by consumption of additive in the oil. They identified two kinds of effect and classified them depending on the chemical nature of the additive [26].

1. Tribo-chemical reaction or tribo films which include all lubricant antiwear additives acting by *chemical reaction processes* involving an *active participation* of both the *friction surfaces material* and *environmental factors* (atmosphere, water etc).

a. Additives reacting by direct chemical reaction with the surface e.g. sulfur and chlorine chemical compounds, fatty acids, fluorinated compounds

b. Additives acting through thermal and/or oxidative degradation process e.g. Metal Dithiophosphate and phosphorus containing organic compounds.

2. Polymeric and non sacrificial films in which *surface plays no direct part* in its formation, although it may catalyze the process. This process also involves formation of high molecular weight compounds through polymerization process e.g. complex esters,

solid lubricant additive like oil soluble molybdenum compounds, borate additives, double bond containing molecules etc. In spite of several advantages like noncorrosive inert low toxic products and friction reduction none were really effective in practical situations.

2.7.2 Lubrication mechanisms of films

Hsu and Gates described several ways in which the boundary films once formed, deliver the lubricant action [28]. Sometimes the unreacted additive molecules form an ordered structure at the metal interface. The result is that sliding is accomplished between the two weakly bonded adsorbed layers in the ordered structure. This is how the friction modifiers like fatty acids work (friction modifying layer) [28, 29]. Alternatively a strongly adhered bonded layer which is shear resistant by itself can provide lubricant action (shear resistant layer). In some cases a lubricant layer behaves as a solid lubricant exhibiting limiting shear and shear band fracture. Another way is when the boundary film composed of reaction products serves as an easily removable low shear interfacial layer against the rubbing that wears instead of metal surface. Because the layer tends to protect the metal by itself being removed, its termed the sacrificial layer. The sacrificial layer then needs to be restored or formed at a rate that is higher than the rate at which it is destroyed to protect the surface e.g. oxide film layer in case of mild wear of steels under dry sliding.

The last mechanism is perhaps the most important one by which the commercially used antiwear agent ZDDP works. The environmental restrictions on phosphorus in engine oils have placed direct constraints on the concentration of ZDDP generally regarded as the only source of phosphorus. Consequently this has created great pressures in replacing ZDDP partially or totally. According to Spikes [3] this has been one of the reasons for a huge increase in the level of research on ZDDP, besides the slow pace of reduction of phosphorus levels (Table 1) reflects the remarkable effectiveness of ZDDP as an antiwear additive and the great difficulty the additive companies have had in finding replacement with comparable performance.

2.7.3 Structure and properties of Zinc Dialkyl Dithio Phosphate

The main functions of ZDDP are wear prevention, antioxidancy and copper-lead bearing corrosion inhibition [17]. Structural formula of ZDDP [3, 30] can be written as

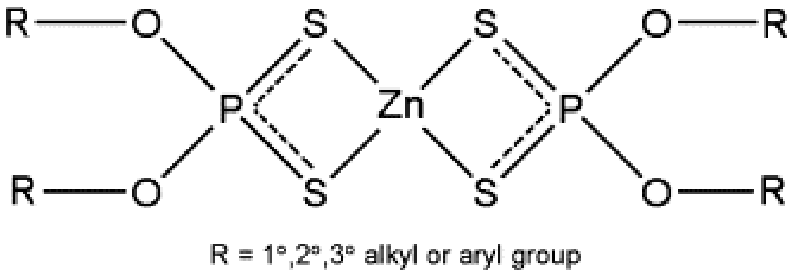

Figure 2.9 Structural formula of ZDDP

In fig 2.9 ‘R’ stands for alkyl or aryl groups. In case of alkyl ZDDP ‘R’ can be primary, secondary or tertiary alkyl chain. The activity and thus properties of ZDDP depend on the R group seen in table 2.5 [31]. Besides the classification based on the alkyl groups of ZDDP, it is available in two different types [17]

Neutral ZDDP, $[(RO)_2PS_2]_2Zn$

Basic ZDDP, $[(RO)_2PS_2]_6Zn_4O$

Table 2.5 Properties of three basic ZDDP derivatives used in hydraulic fluids and other lubricants (aryl, primary alkyl and secondary alkyl)

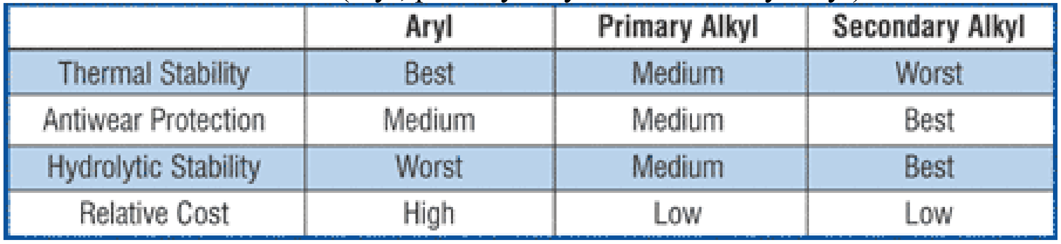

	Aryl	Primary Alkyl	Secondary Alkyl
Thermal Stability	Best	Medium	Worst
Antiwear Protection	Medium	Medium	Best
Hydrolytic Stability	Worst	Medium	Best
Relative Cost	High	Low	Low

2.7.3.1 Neutral ZDDP

In general ZDDP's consist of a core structure. Earlier solid state structural data [32] for two types of ZDDP (ethyl and isopropyl alkyl groups) exhibited a one dimensional polymeric structure for isopropyl ZDDP in which each zinc is chelated by one $S_2P(OPr^i)_2$ ligand and the two zinc atoms of the dimer unit bridged by $S_2P(OPr^i)_2$ groups. Ethyl ZDDP has a one dimensional polymeric structure but with the same chelation and bridging. Recently the molecule of neutral butyl ZDDP investigated revealed a central 8 membered $Zn_2S_4P_2$ core (two bridging DDP ligands) spiro to two four membered ZnS_2P ring systems by X-ray analysis as shown in fig 2.10 [33]. Only the first carbon atom (white) of each alkyl group, R is shown for clarity.

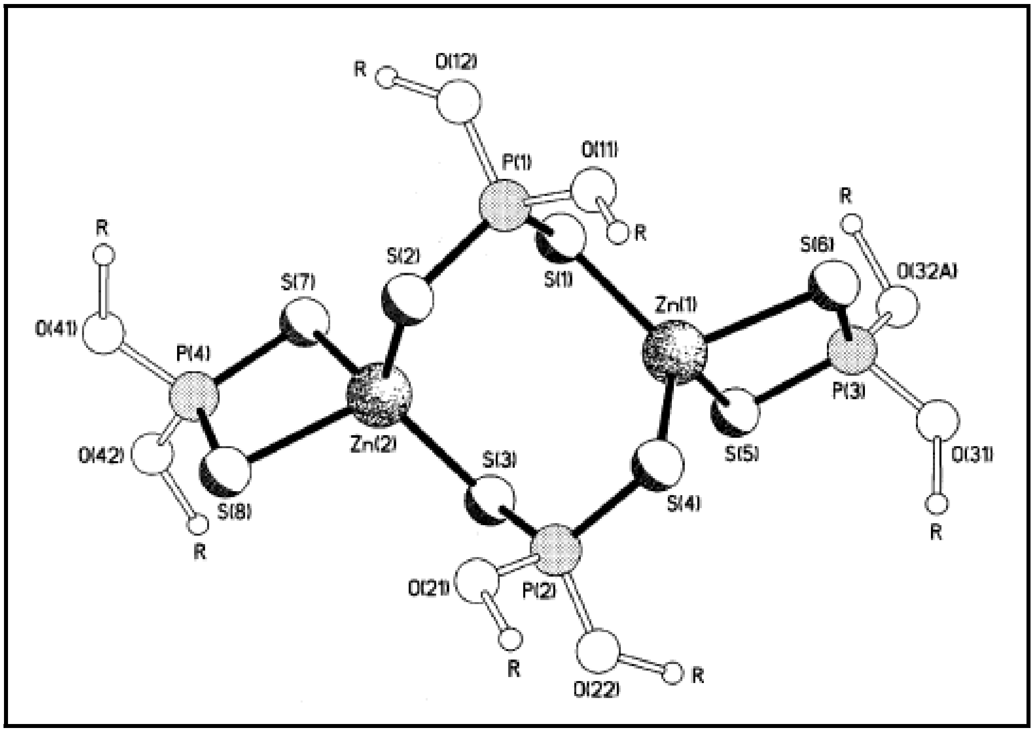

Figure 2.10 The crystal structure of neutral ZDDP $Zn_2[S_2P(OBu^i)_2]_4$.

The molecular structure of ZDDP is rather more complex in solution [3]. Neutral ZDDP exists as an equilibrium between monomer and dimer in solution as seen from fig 2.11 [3].

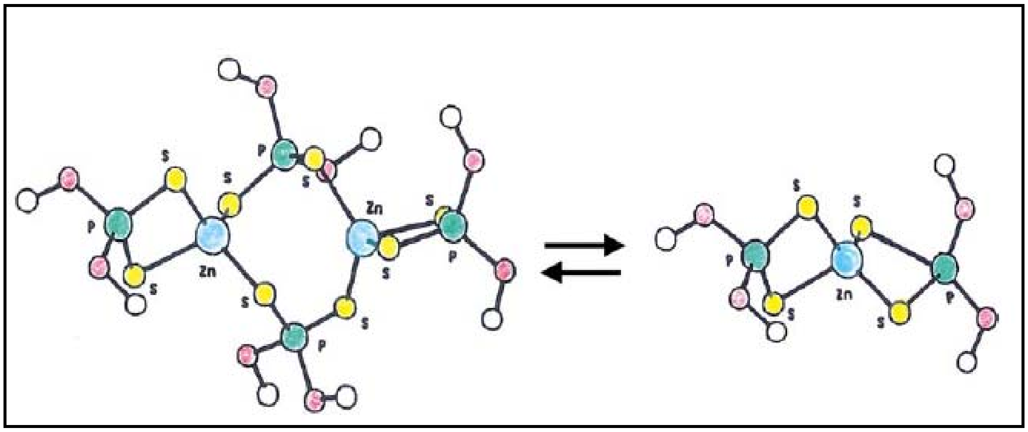

Fig 2.11 Equilibrium between dimeric and monomeric neutral ZDDP forms

2.7.3.2 Basic ZDDP

The crystal structure of basic ZDDP has remained a matter of speculation since a long time however a good quality data was obtained from a single crystal at -100C for Butyl ZDDP, $Zn_4O[S_2P(OBu)_2]_6$ [33] . It revealed a Zn_4O core with four Zinc atoms in an almost prefect tetrahedral arrangement about central oxygen as seen in fig 2.12 [3, 33].

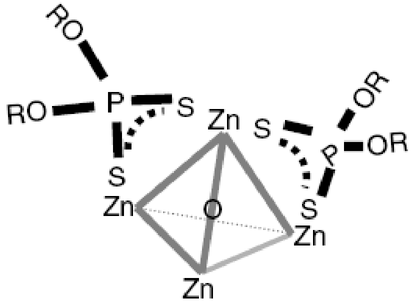

basic-ZnDTP, $(DTP)_6Zn_4O$
(two of four DDP ligands shown)

Figure 2.12 The structure of basic ZDDP

2.7.3.3 Interconversion of normal and basic ZDDP in solution

Detailed studies about the solution behavior of basic and neutral ZDDP were obtained from ^1H and ^{31}P NMR by Harrison and Kikabhai [32]. According to them, the ^{31}P chemical shift is dependent on the nature of the alkyl group, solvent and concentration. In non donor solvents $CDCl_3$ and toluene the ^{31}P chemical shifts of both the Et and Pr^i derivatives decrease steadily and smoothly with decreasing concentration. The authors have also reported that there exists an interconversion between basic and neutral ZDDP in solution according to the equilibrium reaction.

$$Zn_4[S_2P(OR)_2]_6O \rightleftharpoons 3\ Zn[S_2P(OR)_2]_2 + ZnO$$

This was observed when basic ZDDP (on left side of equilibrium reaction) dissolved in $CDCl_3$ exhibited a ^1H NMR spectra of both basic and neutral compound. Significant quantities of normal ZDDP compounds (right side of equilibrium) are present at room temperature immediately upon dissolution, with the amount increasing steadily over a period of 8hrs to 40% conversion. In temperature vs. concentration experiments for the same, the intensity of normal compounds increased from 293K to 353K. ZnO precipitated from the solution. The authors also noticed a third weak resonance in ^{31}P NMR at 108.2 ppm (with $T > 343K$) and attributed it to an intermediate compound in the rupture of basic ZDDP cage to afford the normal ZDDP and ZnO [32]. However on standing at room temperature dissociation reaction was reversed with a very small amount of normal compound after 21 days and disappearance of the intermediate compound.

2.7.4 Antiwear mechanism of ZDDP

Although a large amount of research has been undertaken to resolve the mechanism of ZDDP, no single complete mechanism has been agreed upon so far. Spedding and Watkins have quoted two main reasons for the same [2]. Firstly the antiwear process itself is multidisciplinary requiring the knowledge of metallurgy, metrology and mechanical design. Secondly the antiwear agent ZDDP itself undergoes complex reactions that involve knowledge of the organic, inorganic chemistry and surface adsorption types of fields. All of the cited fields are vast in them and require a combine expertise before elucidating the entire antiwear mechanism of ZDDP in tribological conditions.

ZDDP functions as an antiwear agent, antioxidant and a corrosion inhibitor [3]. It becomes difficult to resolve all 3 mechanisms operating simultaneously in real time conditions. Whether the reaction product in each case acts as a precursor for the other thus intertwining all mechanisms definitely complicates the task. Impurities present in most commercial ZDDP's and existence of both neutral and basic forms in the same make matters worse. Thus it is not surprising that there exists a controversy in so many facts observed by researchers. Nevertheless a summary of how ZDDP functions as an antiwear agent has been discussed briefly.

2.7.4.1 Antiwear mechanism of ZDDP- I

The surface of any metal after polishing and machining shows the presence of asperities that are like 'small hills'. When two surfaces rub against each other, some of these hills come into physical contact with one another and result in friction and heat. According to Hsu and Gates [28], the freshly abraded surface also possesses very high surface energy or active sites and the local temperatures (or flash temperature) can be very high but last only for a microsecond or less. Both flash temperature and nascent surfaces can induce chemical reaction between the lubricant molecules including ZDDP and the surface. In fact Rounds in his work on ZDDP reaction films on heated metal surfaces concluded that temperature is the key driving form in forming ZDDP tribofilms, with boundary films being rapidly formed at contact sites due to flash temperatures [34].

ZDDP decomposes in oil due to high temperature reactions to give a wide variety of products [2]. An outcome of the great deal of research on thermal decomposition and antiwear activity of ZDDP in 1950's and 1960's have been compiled by Spikes in his review [3, 35] has been outlined here.

(i) Depending on the alkyl group structure the antiwear effectiveness of ZDDP can be quoted as secondary alkyl > primary alkyl > aryl .

(ii) ZDDP's in hydrocarbon solution undergo an autocatalytic, thermally activated decomposition reaction which becomes significant above about 150 _C and rapid above about 180 C. This is illustrated in figure 2.13(a) taken from Luther, *et al.*

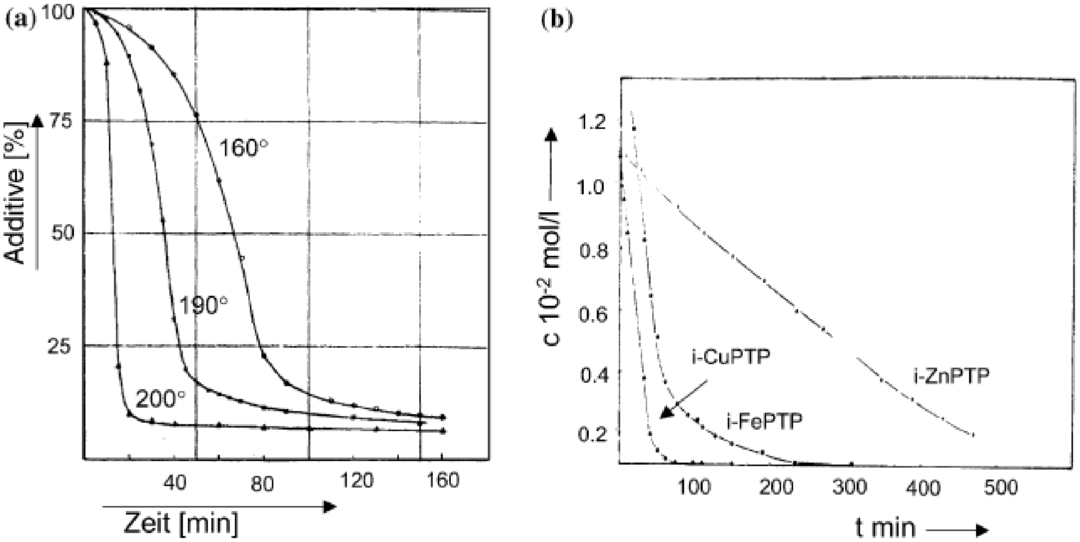

Figure 2.13 Thermal degradation of metal dithiophosphates. (a) Influence of temperature on thermal degradation rate of zinc dithiophosphate (b) Thermal degradation rates of three metal dithiophosphates

(ii) The main volatile products generated are mercaptides, alkyl sulphides, H_2S and olefins. The mercaptides and sulphides are formed directly and not from subsequent reaction between H_2S and olefins. No olefins of higher molecular weight than the original alkyl chain on the ZDDP are produced.

(iii) The other main product is glassy and insoluble and contains phosphorus, oxygen, and zinc with possibly some sulphur.

(iv) ZDDP thermal decomposition is acid-catalyzed but not accelerated by the presence of oxygen.

However it was the outcome of the work through phosphorus NMR by Coy and Jones that the mechanism of thermal degradation of ZDDP came into light. They used ^{1}H and ^{31}P NMR to identify the thermal degradation products of ZDDP and identified a wide range of species formed during thermal decomposition of normal butyl, iso-butyl and s-butyl ZDDP [36]. The final degradation products in each case was $SP(SR)_3$ with the intermediate degradation products being $SP(OR)_2(OR)$ and $SP(SR)(OR)_2$. Through their valuable findings they synthesized each product identified by NMR and compared its performance with the parent ZDDP. The comparable performance demonstrated the fact that parent ZDDP indeed followed a route that consisted of the identified degradation products during the antiwear process.

Based on the products identified stepwise in 1hr, 4hrs, 8hrs and 16hrs by NMR they were able to propose a mechanism for the thermal degradation of ZDDP. The mechanism involves the following major points [37].

1. The decomposition is initiated by a general migration of alkyl groups from oxygen atoms to sulfur atoms.

2. Olefin elimination successfully competes with substitution where the alkyl group structure is favorable leading to phosphorus acids.

3. Nucleophillic substitution of one phosphorus species by another leads to formation of P-O-P type structures and of zinc mercaptides $Zn(SR)_2$ as reaction intermediate. Reaction of mercaptides with dithiophosphate leads to formation of trithiphosphate and eventually tetrathiophosphates.

4. The oil insoluble deposit in a major case is a mixture of zinc thiophosphates and zinc pyro and poly pyro thiophosphates.

Spikes agreed that organothiophosphates are very strong alkylating agents. The initial reaction being with a Nucleophile Nu^- of the form in equation 1. The main points of the chemical mechanism for thermal degradation proposed by Coy and Jones [37] and later summarized by Spikes in his comprehensive review [3] are outlined here.

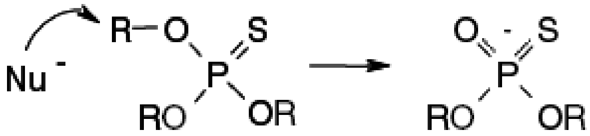

Equation 1: Nucleophilic attack

This is followed by autocatalytic realkylation given by equation 2

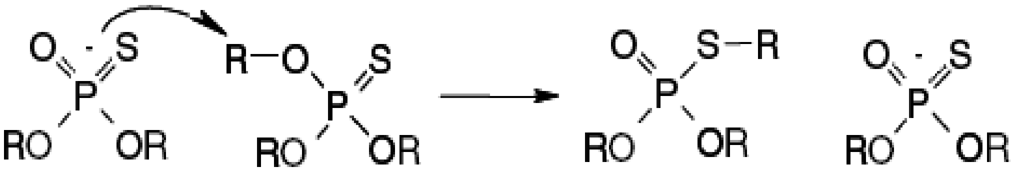

Equation 2: Realkylation

Autocatalytic realkylation is accomplished by dithiophosphates, thiophosphates and even mercaptides (nucleophiles) necessary for self alkylation. Isomerisation to form thionyl species occurs by equation 3 to give the O/S exchange isomer, $(RS)_2POO^-$ [3, 37].

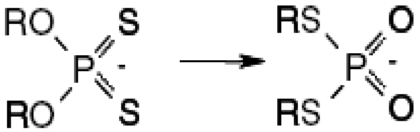

Equation 3: O/S exchange isomer, $(RS)_2POO^-$.

This alkylation reaction has two consequences in that it leads to easy transalkylation and displacement of RS groups formed in thionyl and dithionyl phosphates subsequently by attack of phosphoryl group from a neighboring molecule to give a polyphosphate equation 4

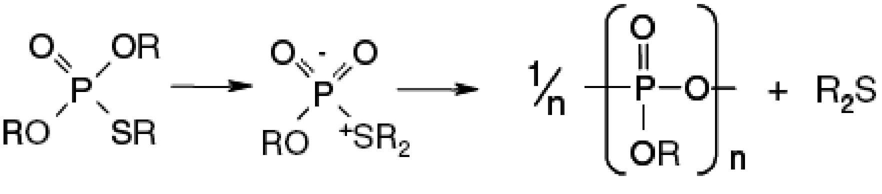

Equation 4: Formation of Polythiophosphate

They accounted the disappearance of sulfur in final polyphosphates formed through the appearance of dithionylphosphorodithionate identified by NMR. They suggested that the dithionylphosphate ion disproportionates to form dithionylphosphorodithionate and the monothionyl species and the latter oligomerises to form poly phosphate glass.

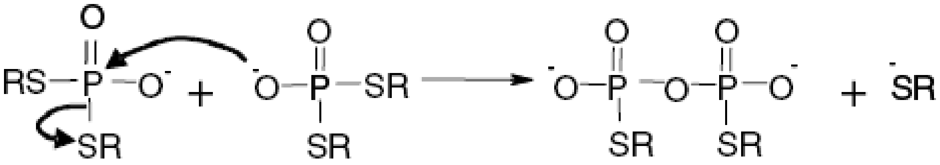

Equation 5

Several intermediates like $(RS)PS(OR)_2$, $(RS)_2PS(OR)$, $(RS)_3PO$ and $(RS)_3PS$ were identified by NMR and supported the mechanism postulated by Coy and Jones [37].

The fate of $(RS)_2PS(OR)$ when formed is probably P-OR to P-SR rearrangement via delkylation and realkylation to give $(RS)_3PO$ and subsequent conversion into $(RS)_3PS$ which is the final end product. The stability of latter is a consequence of it having no Nucleophillic character (i.e $P\text{-}S^-$, $P\text{-}O^-$, or P=O) that can lead to chemical modification and no electrophillic character (P-O-R).

Summary [37]:

1. The accumulation of sulfur and oxygen atoms on different phosphorus atoms is a consequence of attack by nucleophillic Phosphoryl oxygen P=O on another phosphorus atom leading to a $P\text{-}O\text{-}P^+$ system.

2. Nucleophillic attack on the phosphonium species by mercaptans (RS-) leads to cleavage of the original P-O bond and thereby net exchange of one atom of oxygen and one atom of sulfur between the two phosphorus atoms.

3. The reaction continues until no Nucleophillic Phosphoryl oxygen remains. The overall stoichiometry of the reactions followed by the formation of $(RS)_2POO^-$ exchange isomer stand as given in equation 6

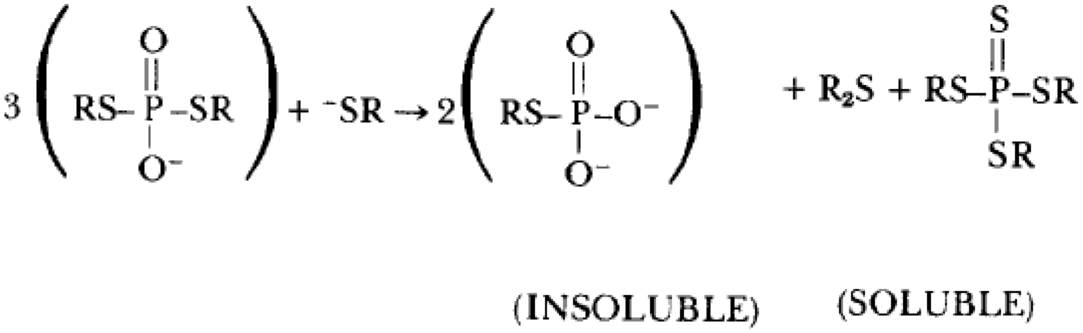

Equation 6: Overall chemical reaction

Thus the chemical literature confirms and explains what is seen when ZDDP's are heated in mineral oil at temperatures over 150C, the formation of insoluble polyphosphates and organic soluble sulfides [3].

The valuable findings of Spedding and Watkins [2] support those of Coy and Jones [36] in that the decomposition products of ZDDP in oil solution upon degradation primarily consist of Zinc polyphosphates and a mixture of alkyl sulfides [2]. Their work primarily consisted of thermal bulk and solution decomposition of ZDDP at 160C and 200C under nitrogen and used NMR, FT-IR, Mass Spectroscopy and elemental analysis to identify the final products. The contribution of NMR was evident once again as the authors quote 'Each of these contributed to the overall picture but ^{31}P NMR was by far the most useful since it is capable of distinguishing all the phosphorus acids'.

The mechanism proposed by them was however a ‘hydrolytic one’ different from the ‘thermal’ one proposed by Coy and Jones for the same final products obtained. This was done on the basis that water accelerated the decomposition of ZDDP. However Willermet disagreed with the same saying that the decomposition of ZDDP occurs by hydro-peroxides and free radicals by which it can also occur at low temperatures than those required for hydrolysis to proceed [38]. According to Willermet decomposition of ZDDP does proceed by thermal and hydrolytic pathways but the key film forming reactions are dependent on ZDDP oxidation. Thus the antiwear film formation may be closely linked to the antioxidant chemistry of ZDDP.

Thus different mechanisms have been proposed for the same end products identified by different authors. Summarized by Kasrai and others in their recent review include several mechanisms proposed by different authors. These include thermal degradation, surface adsorption, oxidation by hydroperoxide, radical reactions, hydrolysis, chemical reaction with FeO and oxygen in the air, or a combination of the above [30].

2.7.4.2 Antiwear Mechanism of ZDDP - II

At this point the question that arises is the mechanism by which tribofilms are formed on metal surfaces during real conditions. As Spikes put forward ‘Is it the same thermal degradation process as found at high temperatures in bulk solution, but driven to taken place at much lower temperatures by cation exchange, frictional heating due to sliding and/or pressure in the rubbing contact? Or is it driven by the rubbing process itself like molecular strain, particle emission or free surface catalysis?’

There seems to be no definite answer for the same at the moment because of no direct evidence. Fujita concluded after several tests that is seems both thermal action and rubbing invoke the antiwear mechanism of ZDDP [3, 39].

There are several interesting mechanisms proposed on the basis of their findings by different authors. Each is elaborate in itself and the best way to review them would be through the review of Kasrai and his coworkers who compiled them. Spedding and Watkins through their work showed that ZDDP is not substantially chemically adsorbed on the metal surface but its 'hydrolytic' decompositions products are. Watkins further demonstrated that these serve as the precursors of antiwear action of ZDDP by interacting with metal surface to form fusible glassy compounds, phosphorus as polyphosphate and iron sulfide as a ternary eutectic with iron oxide provide the antiwear function of ZDDP [40]. Willermet who disagreed with the idea of entire thermal or hydrolytic modes of mechanism proposed a four step process [3, 38].

1. Adsorption of ZDDP on metallic surfaces.
2. Reaction of ZDDP with the metallic surface to form species of phosphates and phosphothionic moieties bound to the metal surface.
3. Formation of phosphate film precursors from antioxidant reactions of ZDDP.
4. Condensation of the phosphates/phosphothionates species occur and are then terminated by zinc-containing compounds or other metal ions in solution (such as from detergents).

Yin modified Willermet's mechanism slightly and proposed a thermo-oxidative process which was later remodified by Fuller that can be stated in 5 steps [30, 41].

1. ZDDP is adsorbed onto the metal surface.

2. ZDDP (in solution) is converted to phosphate intermediate termed Linkage Isomer (in solution).

3. LI (in solution) is adsorbed to the metal surface.

4. Thermal-oxidation of adsorbed LI and ZDDP occurs by either O_2 or ROOH to form long-chain polyphosphates $Zn(PO_3)_2$.

5. With continued rubbing, in the presence of water from the base oil, hydrolysis of polyphosphates occurs, creating short-chain polyphosphates.

These mechanisms explain the formation of protective polyphosphates on steel from ZDDP. Whatever be the exact mechanism Kasrai and his coworkers believe that two combined mechanisms thermal decomposition of ZDDP and chemical reaction of degradation products seem to be most appropriate [30]. At this stage Spike also quotes that 'probably the only way to resolve this question is to carry out in contact analysis, and thus observe the chemical intermediates present within the rubbing contact' [3].

Through the various mechanisms proposed for how ZDDP delivers the antiwear function and prevents metal-metal contact, a definite mechanism may not exist at the moment but some idea can be obtained regarding the process and the extensive research ongoing in this area.

2.7.5 ZDDP-additive interactions

Over the years, although a wide variety of chemical compounds have been introduced as additives to improve the performance of the oil; sufficient efforts have not been made to understand the mutual interactions of these additives when blended in a formulation. Thus understanding and making due allowance for interactions of additives when assessing the overall performance of an oil form the vital step of the balancing act [12].

When the combined effects of two or more additives are higher than could be expected from simple additivity principle, the phenomenon is called synergism. The action opposite to synergism when one additive suppresses the activity of another is called antagonism. In fig Interactions can occur between the additives of the same class e.g. between two extreme pressure additives or between additives with different functions such as between an antiwear and a dispersant additive. Spikes had nicely described the types of interactions with real examples in one of his works [9] (i) Direct interaction in the liquid phase (ii) Direct interactions on the surface (iii) Complementary/exclusory effects and (iv) Graded response

It is evident from table 2.5 [9] that ZDDP undergoes interactions with detergent and dispersant employed in engine oils. (+) indicates synergism and (-) indicates antagonism.

Table 2.6 Summary of main interactions for various groups of additives

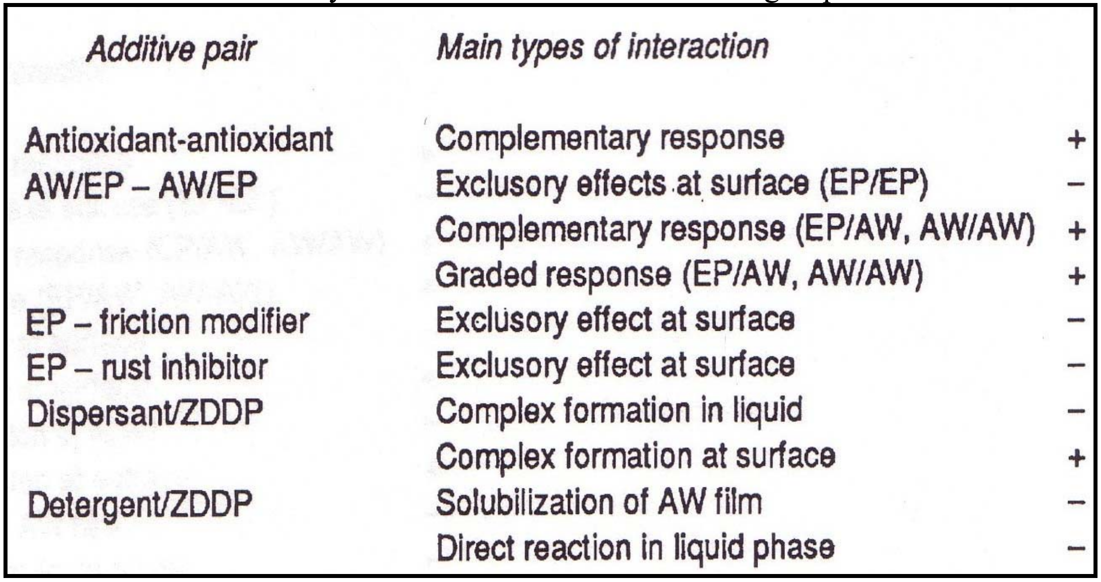

Additive pair	*Main types of interaction*	
Antioxidant-antioxidant	Complementary response	+
AW/EP – AW/EP	Exclusory effects at surface (EP/EP)	–
	Complementary response (EP/AW, AW/AW)	+
	Graded response (EP/AW, AW/AW)	+
EP – friction modifier	Exclusory effect at surface	–
EP – rust inhibitor	Exclusory effect at surface	–
Dispersant/ZDDP	Complex formation in liquid	–
	Complex formation at surface	+
Detergent/ZDDP	Solubilization of AW film	–
	Direct reaction in liquid phase	–

2.8 Introduction of fluorinated species FeF_3 along with ZDDP

The idea has its origin that can be traced back to polytetrafluoroethylene (PTFE) Platinum Research Organization (PRO), Dallas TX along with UTA made efforts to introduce environmentally friendly oils that could deliver high performance in terms of wear performance, friction and fuel economy keeping with the limits of phosphorus level regulations. The first approach was to obtain PTFE-chemically modified metal surfaces to significantly improve wear protection on metal. This chemisorption process was significant only at high temperatures. It was discovered that the introduction of FeF_3 into the system catalyzed the conversion i.e. PTFE could be delivered on the metal surfaces at much lower temperatures (at normal operating temperatures of engine, 100C) [42]. This technology has been patented (patent #5,877,128) by PRO and involves fluorinating metal surfaces from dilute PTFE dispersions in oil at normal engine operating temperatures and the mechanism can be found in references [13, 42]

2.8.1 Synergy between FeF_3 and ZDDP

FeF_3 which was used for catalyzing metal surface with PTFE was found to work in synergy with ZDDP fig 2.15. DSC studies by Dr. Huq revealed lowering of decomposition temperature of ZDDP in presence of FeF_3 [15]. Thus the protective antiwear films would be formed at lower temperatures and earlier in the wear process resulting in high wear performance observed for the ZDDP-FeF_3 system. In fact extensive research has been done in these areas where iron (III) fluoride is found to significantly improve the antiwear performance of ZDDP even at very low levels of phosphorus [13].

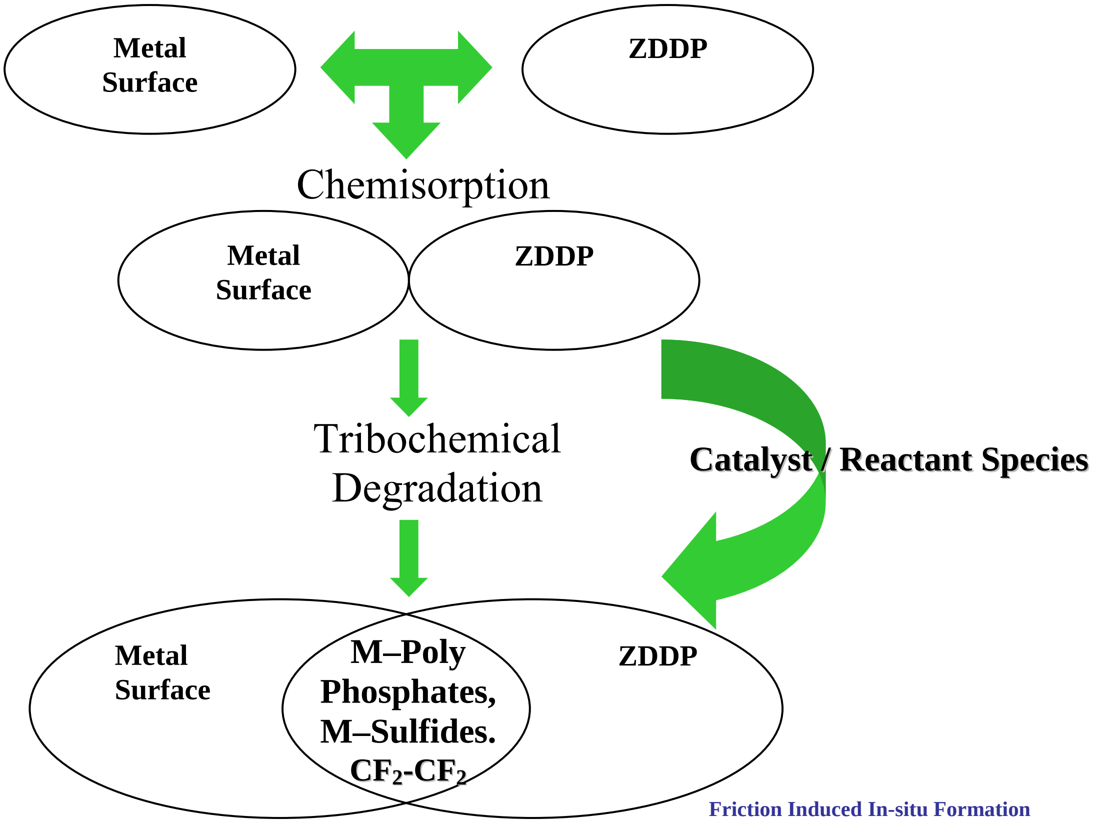

Friction Induced In-situ Formation Of Organo-Fluorides
Md. Zahedul Huq, Pranesh Aswath
Ronald L. Elsenbaumer, F. Conrad Greer
U.S. Patent Application No. 10/944,452
Filed: Sept. 17, 2004

Engine Oil Additive
Hal Shaub, Pranesh Aswath and
Md. Zahedul Huq
U.S. Patent Application No 10/965,686
Filed: Oct. 14, 2004

Low Phosphorus Lubricant Additive
Kajal Parekh, Pranesh Aswath,
Harold Shaub and Ronald Elsenbaumer
U.S Patent Application No.50715/P006CP1
Filed: Sept 2005

Figure 2.14 Synergy of FeF_3 with ZDDP

It results in the formation of fluorocarbons (XPS work) as one of the end products in the tribofilm on metal surface thus providing enhanced wear protection.

CHAPTER 3

APPROACH AND OUTLINE OF RESEARCH

To determine the interactions between ZDDP and FeF_3 it was necessary to find a suitable approach. Based on the literature survey included in section 2.6 the options consisted of addressing the interactions either under

i) Thermal conditions in which products of chemical interaction between ZDDP and FeF_3 would be investigated in solution in 'test tubes' at high temperatures, or

ii) Tribological conditions in which tribo films formed on the surface involving ZDDP-FeF_3 system would be investigated.

The first study would involve identifying products in strictly thermal conditions and then assume that similar reactions take place in real or tribological conditions. This assumption is based on scientific literature.

According to literature, thermal decomposition end products of ZDDP investigated consist of polyphosphates and organic sulfides by Coy and Jones [36], Spedding and Watkins [2, 40] and several others. These indeed have been found in the tribofilms on the surface in real tribological tests. Comparisons made between thermal films (by immersing metal coupons in heated ZDDP solutions) and tribofilms (formed during rubbing) concluded that chemistry of the two were similar [43, 3]. This was established through XANES work recently that strongly confirmed that films formed on rubbed surfaces have similar compositions to thermal films [3] however thermal film lack a layer structure observed in tribofilms [30].

Good antiwear performance is associated with the formation of sacrificial stable films for which rate of film formation must be higher than the rate of scraping the films [44, 45]. Lin and So investigated extensively the effect of different factors affecting the rate of growth of films under tribological conditions. Their results indicate that if the rates of recovery and growth exceed that of scraping the films off the rubbing surfaces antiwear performance is evident. Under severe conditions like high pressure (over 90MPa), high temperature (over 200C) with an insufficient concentration of ZDDP and the rubbing of a rough and harder surface on a softer surface, the antiwear performance of ZDDP's is negligible [44, 45]. Compositions of tribofilms formed depend on the oil temperature and condition of surface finish [45].

Thus there seem to be a number of variables that control the wear process and dictate the antiwear performance of ZDDP. This must also be true for ZDDP-FeF_3 system. A complete control may not be achieved on some conditions like surface roughness of mating surfaces (variations of Ra between 0.2-0.4 micron), contact temperature, hertzian contact loads that may change during the actual test. For these reasons the first approach consisting of the thermal degradation of ZDDP-FeF_3 system was chosen to investigate the underlying chemical interactions.

3.1 Approach

The approach adopted involves thermal degradation of ZDDP in which temperature solely triggers chemical reactions and this route as opposed to tribological one helps in understanding the underlying mechanism in terms of the products that are formed in presence and absence of FeF_3. This is evident in the flowchart below.

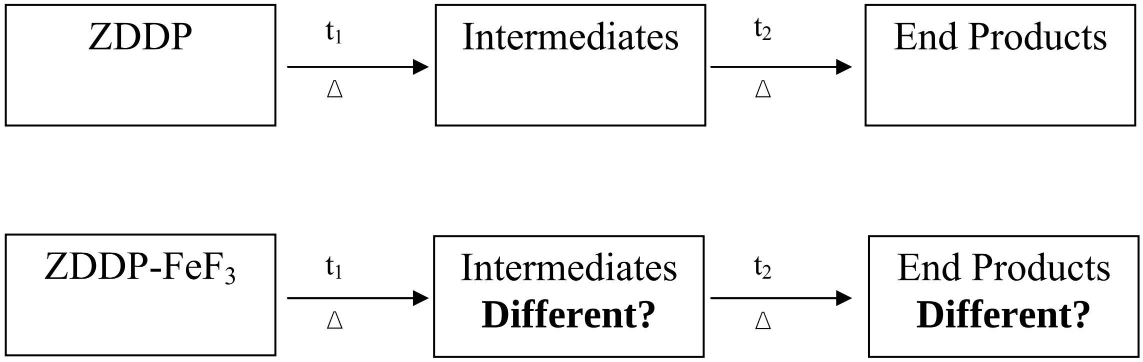

Figure 3.1 Approach of thermal degradation for ZDDP and ZDDP – FeF_3

ZDDP is heated at a certain temperature for a span of time to give ‘intermediate products’ and for longer times to give ‘end products’. The temperature of reaction can vary from room temperature to 150C; t = time, $t_1 < t_2$. The same reaction when carried out in presence of FeF_3 may give rise to intermediates and end products that are different. The products formed at each stage can be characterized by NMR and IR. The use of NMR in determining the products has already been described in section 2.4 through the work of Coy and Jones, Spedding and Watkins.

It was observed that temperature and time were inter-related in the above reactions i.e. at 150C the intermediate products appeared in 20 min, however at room temperature the same intermediates were obtained in less than 1 month. Thus when one parameter is fixed say temperature, time becomes a dependent variable. When the reactions are carried out in presence of Nitrogen they are termed thermal degradation experiments and the same in air comprise Oxidative degradation experiments.

3.2 Outline of entire work

The whole work attempting to study the interactions of ZDDP and Iron Fluoride has been roughly divided into 4 parts. Fate of new fluorinated compounds is a sub-addition to thermal degradation study. Optimization of fluorine has been treated separately in details with its established protocols.

The characterization techniques employed for each part have been stated in the flowchart in fig 3.2 and have been dealt in more details in experimental procedure chapter 4.

ZDDP-FeF_3 interactions in Nitrogen (Thermal Degradation)

This would suppress the antioxidant behavior of ZDDP, focusing more on its antiwear characteristics and the manner in which FeF_3 assists the process. The study was carried out at a fixed chosen temperature of 150 C for 20 min. ^{31}P NMR and ^{19}F NMR have been principally used to identify these products. The chemical differences observed were related to the improved tribological behavior of the fluorinated ZDDP.

Fate of 'early intermediate' compounds (a subset of thermal degradation)

Once the new fluorinated compounds were found to form in the early stages of reaction between ZDDP and FeF_3, it was important to know the fate of these compounds when heated for longer times. Do they continue to exist or breakdown? If they do then which form do they exist in? With this in mind the studies were carried out for longer times, 2 hours at 150 C.

ZDDP- FeF_3 interactions in air (oxidative degradation)

In tribological situations O_2 from environment invokes the antioxidant nature of multifunctional ZDDP additive, besides its antiwear property. The goal is to examine how different are the products from non-O_2 environment at same temperature and for same periods of time.

Optimization of Fluorine

Once new chemical species formed in presence of FeF_3 were established in degradation process of ZDDP, optimization of the fluorine level was desired with good antiwear performance. The study was carried out at a temperature preferred by industry (~80 C) and varying times in two different conditions air and nitrogen.

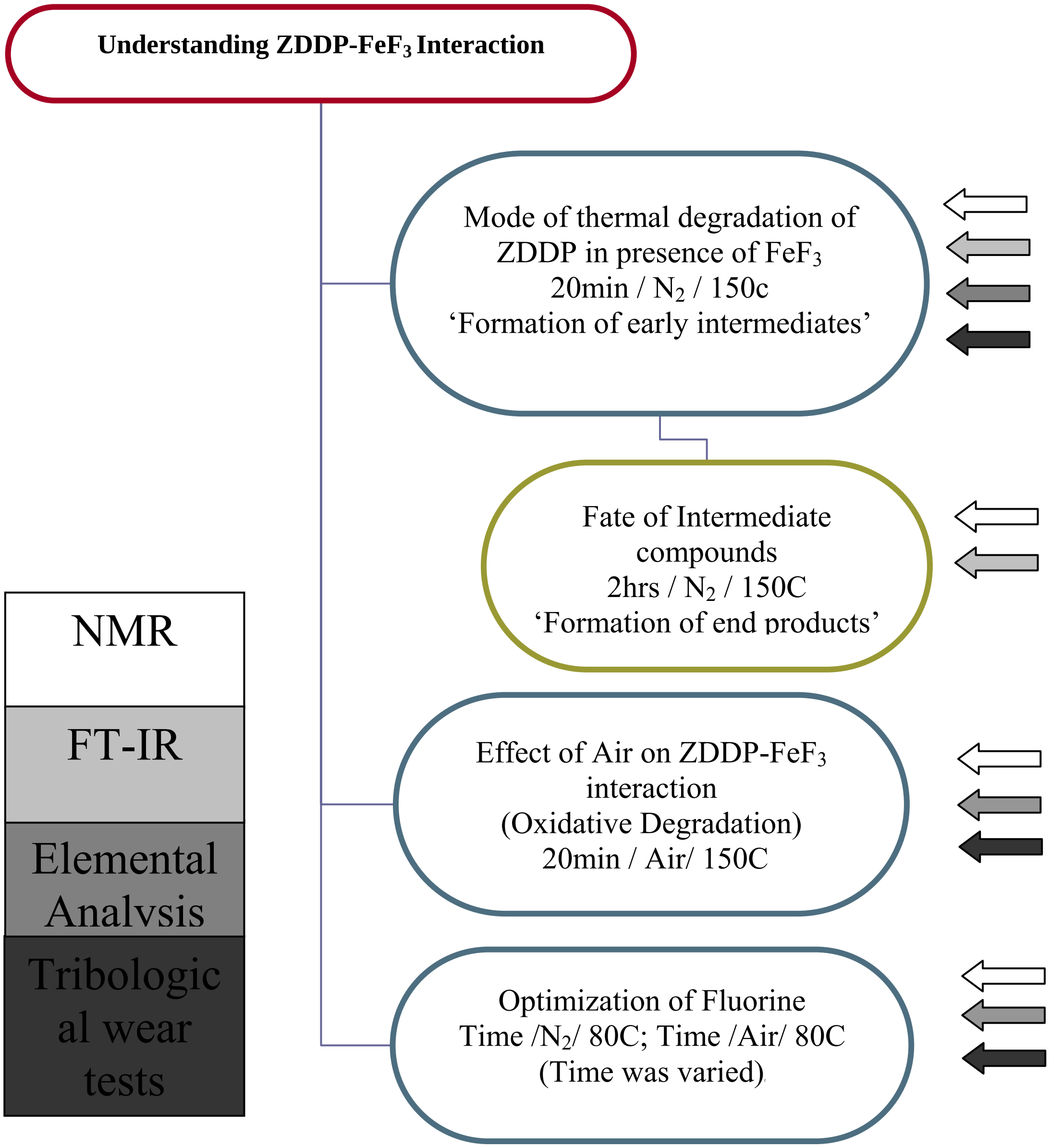

Figure 3.2 Outline of entire research work in a flowchart form

CHAPTER 4

EXPERIMENTAL PROCEDURE

A secondary ZDDP research sample (7.2%P, S, Zn) was obtained from Chevron Oronite, CA, USA. In order to better understand the thermal degradation process of ZDDP and resolve all the degradation products formed, a higher concentration of ZDDP was used while retaining the ratio of ZDDP and FeF_3 at 1:0.4.

4.1 Thermal decomposition experiments

The decomposition of ZDDP is known to commence around 80°C slowly and rapidly at higher temperatures for a given ZDDP [38]. The temperatures reached in an engine are usually in the range of 130-200 C [3]. In addition the DSC data indicated that both in the case of plain ZDDP as well as in a mixture of ZDDP and FeF3 decomposition commences at a temperature of between 160 and 170 C at lower heating rates of 0.5°C/minutes. A temperature of 150 C was chosen for all the degradation experiments. ZDDP is well known for its antiwear and antioxidant property, the latter is called into action in presence of air or oxygen. Thus both mechanisms simultaneously operating in presence of air would complicate the objective of this research. Therefore thermal degradation experiments were carried out under N_2. The primary objective of selecting the time for thermal degradation was to capture the early decomposition products and hence the degradation was conducted over a period of 20 minutes. In addition, thermal degradation over longer times can result in some precipitation and evaluation of the wear performance of only the decant may not reveal the true performance of the decomposed products.

About 20 g of sample was taken in test tube the mouth of which was covered with a silicon rubber cork. Two long silicon hoses were allowed to pass through the tube. Vacuum was applied through one and contents stirred simultaneously to allow the entrapped air bubbles to escape and nitrogen applied through other hose subsequently. This process of ‘vacuum-nitrogen’ was repeated several times to ensure complete removal of entrapped air. Nitrogen was allowed to continuously flow for the rest of the experiment at a flow rate of 5 psi. The test tube was then introduced (from the top opening of oven) in a silicon oil bath placed inside the oven, set at 150°C. A hood was connected to the second outlet hose for removal of gases. At the end of the experiment, the contents were poured in small vials and refrigerated during storage to prevent any further reactions.

There was no precipitation in case of ZDDP baked for 20 min. On the contrary ZDDP-FeF_3 sample required centrifugation followed by decantation. This decant was a dark green solution as opposed to a pale yellow color of baked ZDDP. All subsequent tests were carried out with this ‘decant’. Both the unbaked and baked samples with and without ZDDP were analyzed by ICP.

4.1.1 Characterization of samples (NMR, FT-IR, Tribological wear test, TEM of wear debris)

The four samples that were characterized in detail include the following **(**a). 50 wt% of ZDDP in mineral oil (b) ZDDP (50wt %): FeF_3 (1:0.4) in mineral oil (c) 50 wt% of ZDDP in mineral oil baked in a nitrogen environment as described earlier for 20 minutes and (d) ZDDP (50wt %): FeF_3 (1:0.4) in mineral oil baked in a nitrogen environment for 20 minutes.

4.1.1.1 Nuclear Magnetic Resonance Spectroscopy

A JEOL 300MHz NMR Instrument was used to obtain ^{31}P and ^{19}F qualitative NMR spectrums. ^{31}P NMR decoupled with proton were obtained at operating frequency of 121.66 MHz , relaxation delay of 6[s], sweep of 30.488 [KHz] and 2000 scans. 85% Phosphoric acid was used as an external reference.

^{31}P NMR decoupled with fluorine was also obtained where required at the same operating parameters. ^{19}F NMR at 282.78 MHz, delay of 5[s], 300 or 600 scans was found to be satisfactory. All chemical shifts in the low field direction are defined positive. Approximately 0.3grams of sample in 1.5 ml of $CDCl_3$ (lock solvent) was found to give good shimming and good intensity signals, using 5mm OD tubes. Theory and working principle of NMR have been dealt in a separate chapter.

4.1.1.2 Fourier Transform-Infrared Spectroscopy

Transmission FT-IR spectrums were recorded using NaCl windows using a Brucker FTIR Spectrometer. In addition to cases (a, b and d) FTIR spectra was also obtained for a different type of ZDDP (oil free Ethyl Hexyl ZDDP) both in presence and absence of FeF_3 at room temperature but for different lengths of time.

4.1.1.3 Tribological wear test

The tribological performance was evaluated by a home built ball on cylinder Lubricity evaluator (BOCLE) with well-defined protocols and good reproducibility. All tests were conducted under boundary conditions as detailed in reference [46].

i) All samples were diluted to 0.1wt % Phosphorus and 50 micro liters of base oil was used in each test. Wear tests were carried out at 24kg load, 700rpm, 25,000 cycles using 0.25'' WC ball (78 HRc hardness) on Timken 50'' diameter hardened steel rings (62 HRc hardness) surface roughness (Ra) between 0.088 to 0.12 micron meter as measured by profilometer. The real time data acquired consisted of Temperature and Coefficient of Friction vs. No of rotations. Wear profile was measured at 6 locations on the ring 60° apart using a Mahr Perthometer M1. The wear volume was calculated by measuring the area under the wear track and multiplying it with the circumference of the ring.

4.1.1.4 Transmission Electron Microscopy Analysis of Wear Debris

After the boundary condition tribological wear test, a small stiff piece of plastic was used to collect the used oil on the ring surface. This oil would contain wear debris generated during the test and would reasonably differ with type of test and formulation chemistry. Bright field Transmission Electron Microscopy coupled with Energy Dispersive Spectroscopy (TEM and EDS) were conducted on this wear debris using a JEOL 1200 EX STEM.

4.2 Fate of 'early intermediate compounds'

These experiments were carried out in the same way as thermal degradation experiments except for the fact that the baking times were increased to 2 hours instead of 20 min with temperatures being maintained at 150C. At the end of the experiment the samples were refrigerated in the same fashion listed in section 4.1 and decanted the next day (after 20-24 hrs). The large amount of precipitates were formed at 2 hrs and the quantity of liquid in the precipitates (or decant) was small. Even after centrifugation, the ‘decant’ had a foul smell (H_2S). These were few reasons for which the sample could not be sent out for phosphorus or fluorine elemental analysis. Evaluation of the wear performance of the decant may not reveal the true performance of the decomposed products. For these reasons wear performance tests were not conducted on these samples. Only NMR was carried out and details as listed section 4.1.1.1 apply.

4.3 Oxidative degradation experiments

These experiments were carried out in the same way as thermal degradation experiments except for the fact that instead of Nitrogen (and no vacuum), house-air was allowed to flow through the samples at 5 psi pressure with temperatures being maintained at 150C for 20 min. At the end of the experiment the samples were refrigerated in the same fashion listed in section 4.1 and decanted the next day (after 20-24 hrs). The sample containing only ZDDP had turned orange. However the sample containing ZDDP-FeF_3 had turned greenish but greenish tinge being paler as compared to Nitrogen samples. Both baked samples with and without FeF_3 were analyzed by ICP. Both ^{31}P and ^{19}F NMR were carried out as listed in section 4.1.1.1.The phosphorus levels reported in the analysis were used for preparing samples of 0.1% Phosphorus concentration for subsequent wear tests that were carried out in base stock and tested in the same way as listed in 4.1.1.3. Only wear performance and NMR spectroscopy were carried out on these oxidation degradation samples.

4.4 Optimization of fluorine

The intensity of the green color attributed due to presence of fluorine varied as observed in different samples. To obtain fluorine content with good wear performance at economically feasible temperatures and times would be the optimum amount of fluorine desired.

Once the fluorinated phosphorus compounds were discovered to form and exist, attempts were made to reproduce the same compounds to achieve better control over the process. However some observations in the process lead to the fact that these compounds were formed provided certain temperature and or time conditions were satisfied. In the same event they led to the possible mode of mechanism of action.

4.4.1 Achieving process control

Since P-F bonds were discovered, the formation of the same was found to be preceded by complexation between the same. This was attributed to some observations and facts.

a. A ZDDP-FeF_3 mixture formulated in a big surface area vessel (e.g. a beaker or a conical flask) was baked immediately (without ultrasonication or keeping overnight).

b. Another formulated mixture in a big surface area vessel was kept overnight and baked the next day.

c. Again another ZDDP-FeF_3 mixture formulated (as in the protocol) was emptied out in a long vial with a very small surface area and stored overnight, baked the next day.

d. A ZDDP-FeF_3 mixture was formulated (in a beaker) but ultrasonicated for few hours before baking next day.

e. A similar formulation ultrasonicated and baked immediately.

Only 1b showed immediate fluorination upon baking. This suggests the essence of complexation preceding actual reactions that occur when formulated mixes are left undisturbed for overnight. When sufficient complexation is not allowed to occur reactions are very slow ultimately not resulting in any fluorinated compounds within the estimated temperature- time ranges.

However the unused portion of formulated mixtures from a to e showed signs of room temperature fluorination when stored for a long time at least 1 month (confirmed through ^{19}F NMR) further supporting the case.

These observations lead to the fact that the reaction between ZDDP and FeF_3 is preceded by a complexation process. Any factor that hinders this process would either prevent the formation of these compounds or higher temperatures and/or times (unscaled depending on intensity of complexation) would be then necessary.

In an unstirred or undisturbed mixture, iron fluoride is found to settle in less than an hour. ZDDP with dissolved iron fluoride complexes and forms a distinct layer separated from settled iron fluoride. With higher surface area available, more iron fluoride is solubilized (till solubility limit) and complexes together with ZDDP in a favorable orientation with minimum steric hindrance and maximum vanderwaals attraction. At this stage any factor like ultrasonication would obviously disturb the process besides the heat generated facilitates oil molecules to travel in between them. Again a low concentration of ZDDP and FeF_3 would be unfavorable for the same reasons as observed in 0.1P solution with 1:0.4 ZDDP: FeF_3 kept for several days with no signs of color as opposed to room temperature samples of the same at 50% ZDDP concentration stored for the same periods of time.

4.4.2 Protocols for the optimized process

Thus a series of experiments were devised. Reactions of ZDDP and FeF_3 were allowed to occur at 80C for different spans of time varying from 1hr to 14 hrs. The following process and protocols were used for the optimization of fluorine.

1. Formulation of ZDDP: FeF_3 (1:0.4) mix

- To a weighed amount of FeF_3 powder, appropriate amount of ZDDP was added and mixed vigorously with spatula and contents shaken thoroughly. Balance base oil was not added at this stage.
- This was carried out in a container with huge surface area, preferably this container should be the same one in which baking needs to be carried out (eg conical flask)
- No ultrasonication or any mechanical agitation, hand mixing just once (thoroughly) should be sufficient.
- Storing at room temperature. No continuous shaking necessary.
- Sample allowed to stand overnight (~ 18-24 hours or more before baking)
- 5 min before baking any balance base oil is mixed, and shaken thoroughly.

2. Baking at 80 C for desired time in air next day.

As the flask is introduced it acts as a heat sink, time of start should be when temperature of oil bath reaches 80 C again.

3. After baking is complete, cooling to room temperature for 10-15 min is desired. At this stage (after 10 min in ambient air) the flask is shaken thoroughly to mix all the contents (including precipitate).

4. Sample refrigerated overnight (~ 24 hrs).

5. Contents centrifuged (no need to disturb supernatant or natural settling in the baked container, top fluid poured out in centrifuging tubes). Centrifuging twice would ensure better separation. However once is also fine.

6. The centrifuged sample is decanted and stored in containers at room temperature. It can be used immediately or even later.

CHAPTER 5

NUCLEAR MAGNETIC RESONANCE SPECTROSCOPY (NMR)

Over the past fifty years nuclear magnetic resonance spectroscopy, commonly referred to as NMR, has become the preeminent technique for determining the structure of organic compounds. Of all the spectroscopic methods, it is the only one for which a complete analysis and interpretation of the entire spectrum is normally expected. Although larger amounts of sample are needed than for mass spectroscopy, NMR is rapid, non-destructive, and with modern instruments good data may be obtained from samples weighing less than a milligram. Its uses include [47]:

- Structural elucidation
- Qualitative analysis and quantitative analysis of pure compounds and of mixtures
- Reaction rate measurements
- Detection of more subtle interactions between molecules and their environments

To be successful in using NMR as an analytical tool, it is necessary to understand the physical principles on which the methods are based.

5.1 Physical principle of NMR

The nuclei of many elemental isotopes may be assumed to rotate about an axis and thus have a characteristic spin (**I**). Some nuclei have integral spins (e.g. I = 1, 2, 3 ....), some have fractional spins (e.g., I = 1/2, 3/2, 5/2 ....), and a few have no spin, I = 0 (e.g. ^{12}C, ^{16}O, ^{32}S, ...). Isotopes of particular interest and use to organic chemists are ^{1}H,

^{13}C, ^{19}F and ^{31}P, all of which have I = ½ and magntic properties of same are listed in table 5.1 [48].

Table 5.1 Magnetic properties of four important nuclei having spin quantum numbers ½

Nucleus	Magnetogyric Ratio $T^{-1}\ s^{-1}$	Isotopic abundance, %	Relative Sensitivity	Absorption frequency, MHz
1H	2.68×10^{8}	99.98	1.00	200
13C	6.73×10^{7}	1.11	0.016	50.2
19F	2.52×10^{8}	100.00	0.83	188
31P	1.08×10^{8}	100.00	0.066	81.0

The following features lead to the NMR phenomenon. Both quantum mechanics and classical mechanics have been used to explain the same.

1. Because a nucleus bears a charge and has the property of spin, a spinning charge generates a magnetic field fig 5.1 [49]. The resulting spin-magnet has a magnetic moment (**μ**) proportional to the spin [48, 49].

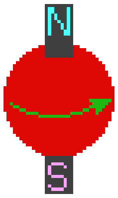

Figure 5.1 Magnetic nucleus or a spin magnet

2. In the absence of a magnetic field, the energies of magnetic quantum states are identical. When placed in a strong homogenous magnetic field (B_0), the nucleus tends to align in one of the two theoretically permissible directions with respect to the field that correspond to two spin states +1/2 and -1/2 in fig 5.2 [49]. The magnetic moment of the lower energy +1/2 state is aligned with the external field, but that of the higher energy -1/2 spin state is opposed to the external field. Note that the arrow representing the external field points north [47, 48, 49].

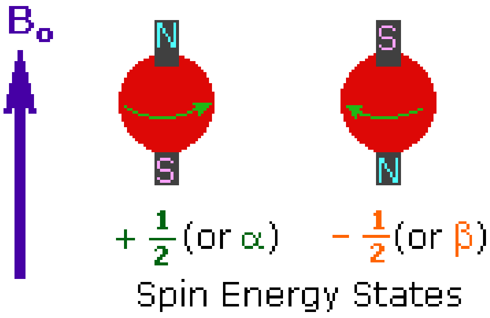

Figure 5.2 Nuclei aligning parallel or antiparallel with the applied magnetic field

3. The difference in energy between the two orientations, is given by ∆E fig 5.3 [49]

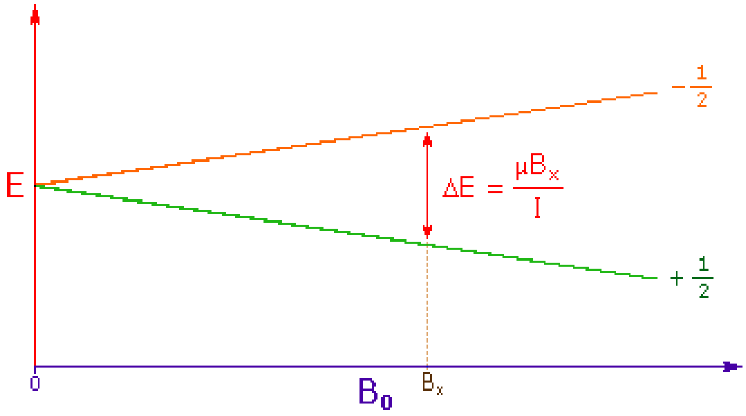

Figure 5.3 Difference in energy between two orientations of a nucleus in presence of a magnetic field

The difference in energy between the two spin states is dependent on the external magnetic field strength, and is always very small. Diagram 5.4 [49] illustrates that the two spin states have the same energy when the external field is zero, but diverge as the field increases.

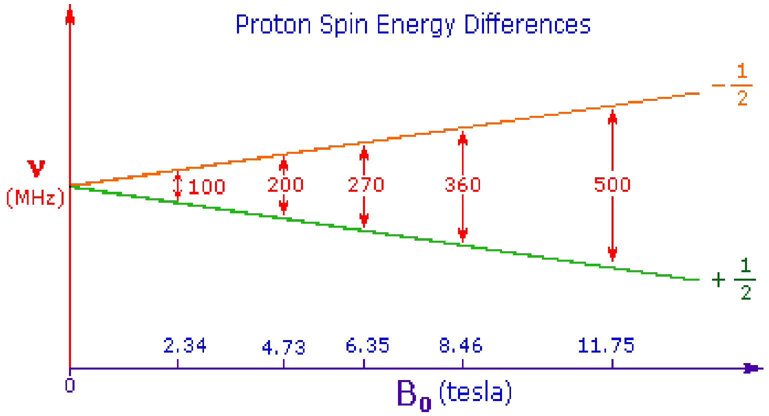

Figure 5.4 Two spin states have same energy when magnetic field B_0 is zero but diverge as field increases

Strong magnetic fields are necessary for NMR spectroscopy. The international unit for magnetic flux is the tesla (**T**). For NMR purposes, this small energy difference (ΔE) is usually given as a frequency in units of MHz (10^6 Hz), ranging from 20 to 900 Mz, depending on the magnetic field strength and the specific nucleus being studied.

4. Transition between these states can be produced by perturbing the nuclei with a second, much weaker magnetic field oscillating at right angles to the strong field called radio frequency (rf) energy. Irradiation of a sample with rf energy corresponding exactly to the spin state separation of a specific set of nuclei will cause excitation of those nuclei in the +1/2 state to the higher -1/2 spin state. Because the lower energy state has a slightly higher population of nuclei (lower energy) there results a net

absorption of rf energy. This absorption is detected electronically by a coil wound around the sample and the resulting signal is amplified and displayed or recorded [47,48,49].

Classical Picture of NMR*:* When a magnetic nucleus is subjected to a strong magnetic field, the effect may be visualized as force applied by the field to the axis of rotation of nuclei (spinning rapidly). This causes movement in the plane that is perpendicular to the field direction; the axis of rotating particle therefore moves in a circular path (or precesses) around the magnetic field. The angular frequency of this motion ω can be converted to precessional frequency called Larmor frequency by the relation,

$\omega = \gamma H$ where γ = magnetogyric ratio and H = strength of field

The rf energy or the frequency of weak oscillating magnetic field must be chosen to match the angular Larmor precessional frequency. This is the condition for Nuclear Magnetic Resonance [48, 49].

5.1.1 Chemical shift

Since the entire research is focuses on phosphorus and its related compounds, applications of NMR have been discusses in context with ^{31}P NMR. If the observed ^{31}P nuclei are present in chemically different environments, then separate absorption peaks are generally recorded in the high resolution NMR spectrum for each kind of ^{31}P environment. Each nucleus is partly shielded from the full strength of the applied field H_0 by the action of the rapidly moving electrons which generate small local magnetic fields of their own, partly canceling the main field. The resonance condition given by equation can be reexpressed as [47]

$$\omega = 2\Pi\nu = \gamma H_0(1 - \sigma)$$

Where σ is a screening constant, characteristic of a particular chemical environment and H_0 is the externally applied magnetic field. Different values of σ attributed to changes in the shielding by the valence electrons from one compound to another, cause the resonance peaks for nuclei in different environments to be shifted in the NMR spectrum. Because it is not possible to measure σ directly, the resonance of the ^{31}P nucleus in some arbitrary standard substance (traditionally 85% Phosphoric acid) is assigned the value of zero and the ^{31}P chemical shifts of other phosphorus compounds are then reported relative to this reference compound in terms of the parts per million (ppm) change in the magnetic field H_0 between the two resonances. The chemical shift δ, with respect to H_3PO_4 is defined by the equation [47]

$$\delta = ((H_{obs} - H_{H3PO4}) / H_{H3PO4}) \times 10^6$$

H_{obs} = strength of the external field at the observed resonance

H_{H3PO4} = strength of the field at the resonance of H_3PO_4. By this condition positive chemical shifts indicate greater shielding than in H_3PO_4 while negative shifts indicate lesser shielding. Since $H \infty \nu$, it's also true that

$-\delta = ((\nu_{obs} - \nu_{H3PO4)} / \nu_{H3PO4}) \times 10^6$ where ν is frequency in cycles per second. Experimentally it is easier to measure frequencies so chemical shifts are calculated by equation. This is because the frequency difference falls in the convenient audio range and can be directly determined. When expressed in parts per million, ppm the chemical shift is independent of the particular magnetic field strength H which is used for the measurement.

5.1.2 Spin-Spin splitting

The chemically shifted peaks in a ^{31}P NMR spectrum can also show fine structure due to the ^{31}P nucleus associated with a given resonance interacting through the electronic structure with other magnetically active in the same molecule. The effect is to split the individual peaks of the ^{31}P NMR spectrum into smaller multiplet peaks of the same total intensity. This is called spin-spin splitting. The strength of the coupling between the magnetically active nuclei is measured in terms of the coupling constant J which is expressed in cycles per second (cps). Spectra's exhibiting these ca be divided into two limiting categories

a. *First Order Splitting*: Simple first order splitting occurs when a ^{31}P nucleus is coupled by a chemical bond or a sequence of bonded atoms to n magnetic nuclei which are different from the ^{31}P nucleus being observed but equivalent to each other – with a coupling constant which is small compared to the relative chemical shift between the ^{31}P nucleus and n nuclei. This will always be the case when the n nuclei are not phosphorus. It can be the case for the different nuclei being phosphorus atoms situated in locations which are not equivalent to that of the particular phosphorus if the coupling constants are sufficiently small or the chemical shifts sufficiently large. The spectra corresponding to the latter case are sometimes called pseudo first order spectra. The multiplicity or the splitting pattern of a given nucleus (or set of equivalent nuclei) can be predicted by the **n+1 rule**, where n is the number of neighboring spin-coupled nuclei with the same (or very similar) Js. If there are 2 neighboring, spin-coupled, nuclei the observed signal is a triplet (2+1=3); if there are three spin-coupled neighbors the signal is a quartet (3+1=4). In all cases the central line(s) of the splitting pattern are stronger than those on the periphery.

b. *Second Order splitting*: when the coupling constants between nonequivalent phosphorus atoms in the same molecule are of a size comparable to are larger than their relative chemical shifts (with both being measured in the same units e.g. cps) then the simple rules for the limiting case of first order spectra no longer hold. Additional peaks appear in the spectrum. Computer programming is generally recommended. Few illustrations can clarify the concept of chemical shifts and Splitting.

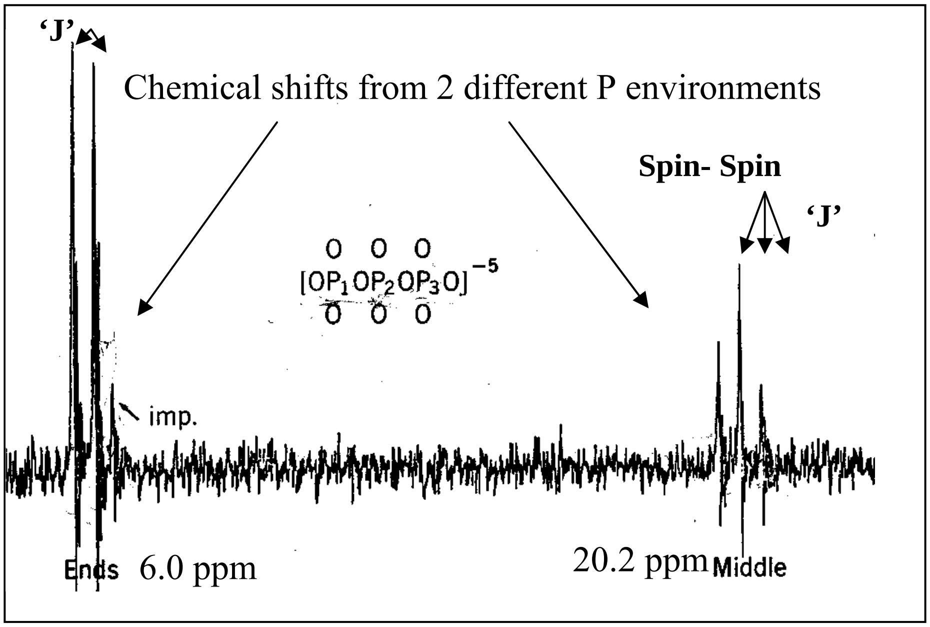

Figure 5.5 Phosphorus NMR of sodium tripolyphosphate in aqueous solution

In the above fig 5.5 [47] the middle phosphorus $P_{2,}$ is attached to two chemically different phosphorus atoms P_1, P_3 (ends), spin-spin splitting into a 1:2:1 triplet is to be expected. Likewise attachment of the two end group phosphorus atoms to the lone middle group phosphorus gives spin-spin splitting into a 1:1 doublet. So the end- and middle group phosphorus atoms interact with each other to give a doublet and a triplet, respectively with $J_{p1p2} = J_{p2p3} = 19.3$cps, $P_1 = P_3 = +6.0$ ppm, and $P_2 = +20.2$ ppm. The intensity of the doublet is twice that of the triplet since it represents twice the number of nuclei. The small singlet just up field of the doublet arises from the presence of a small amount of pyrophosphate impurity [47].

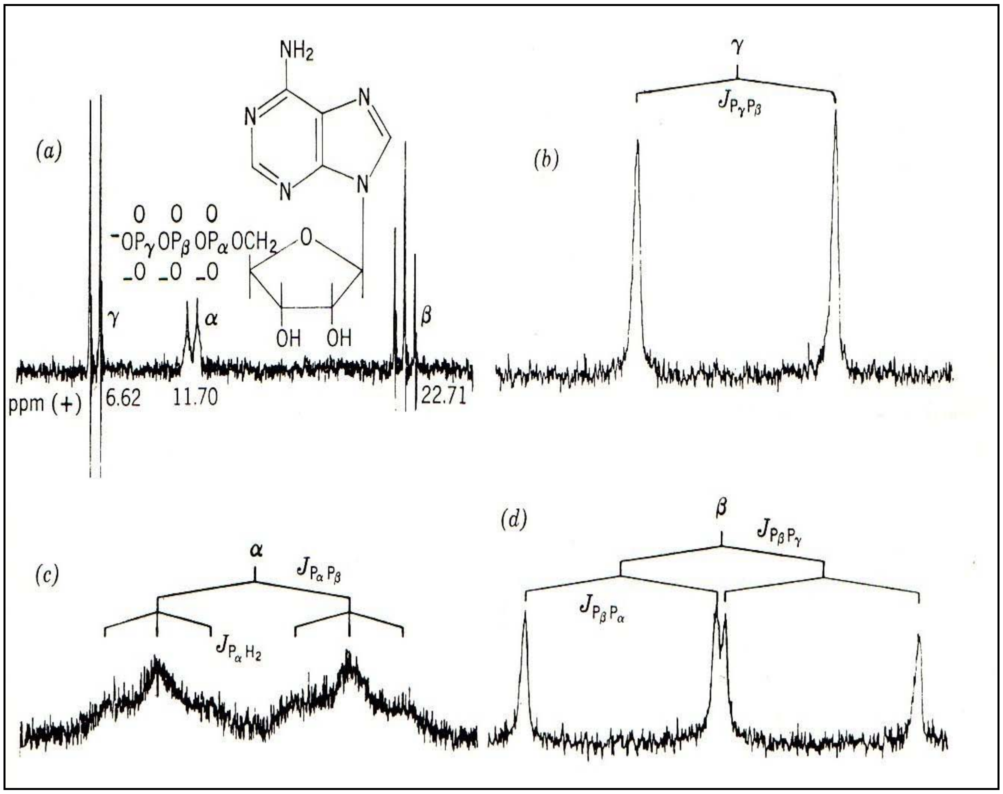

Figure 5.6 A high resolution phosphorus NMR spectrum of tetra methyl ammonium adenosine triphosphate at pH 10

In the above figure 5.6 the phosphorus atoms at each end of the P-O-P-O-P part of this molecule are chemically different unlike in fig 5.5 and accordingly appear in the spectrum as separate multiplets. The α and γ resonances are split into 1:1 doublet by the β phosphorus. This β or middle phosphorus atom is in turn split into a double-doublet. By virtue of the αα and ββ P-O-P couplings. The expanded spectrum in fig 5.6 shows that the α phosphorus is split not only by the middle group ^{31}P atom but also by the adjacent –CH_2O- hydrogen's of the ribose moiety. This results in a mutiplet having 2 x 3 = 6 peaks. Fig 5.6 a shows the complete ^{31}P spectrum of this compound showing the relative positions of the α, β and γ phosphorus resonances. Fig 5.6 b is a slow scan of the γ doublet. The splitting (21.3 cps) results from the interaction of the β phosphorus. 5.6 c shows a 'Double triplet' representing the α phosphorus atoms where the splitting by both the β phosphorus atom ($J_{P\alpha P\beta}$ =20.6 cps) and the adjacent methylene hydrogen's of the R group (5.7 cps) can be seen. 5.6 d shows a 'Double doublet' representing the middle group or β phosphorus atom. Unequal splitting by the other two phosphorus atoms is apparent with $J_{P\alpha P\beta}$ =20.6 cps and $J_{P\beta P\gamma}$ = 21.3 cps [47].

5.1.3 Heteronuclear decoupling

Essentially the decoupling experiment involves the observation of a resonance mutiplet form a given phosphorus nucleus, while simultaneously exciting the resonance of other magnetically active nuclei to which it is spin coupled. The other nuclei are usually excited at high rf power level. The result is that nuclear spin coupling is obliterated by the rapid nuclear transitions at the other nuclei and the original mutiplet in the phosphorus NMR spectrum collapses to a single peak. Depending on whether or not the decoupled nuclei are also ^{31}P the terms homonuclear and heteronuclear decoupling are used.

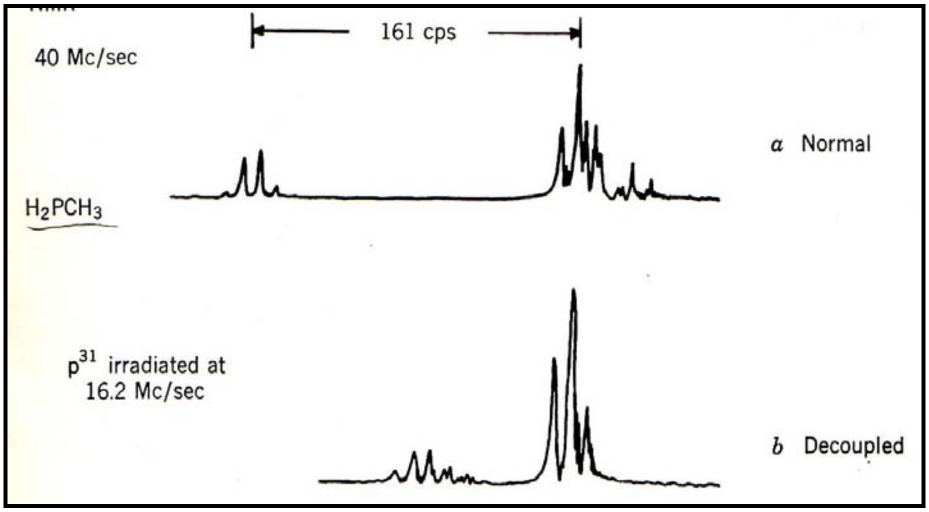

Figure 5.7 Heteronuclear phosphorus spin decoupling

Fig 5.7 (a) [47] shows the normal 40.0 Mc/sec ^1H spectrum of monomethyl phosphine 5.7 (b) shows the 40.0 Mc/sec spectrum of the same compound in which the ^{31}P nucleus was simultaneously irradiated at a radiofrequency of 16.2 Mc/sec to give a quartet for the two hydrogen's directly bonded to the phosphorus and a triplet for the three hydrogen's directly bonded to the phosphorus and a triplet for the three hydrogen's of the methyl group. This fine structure results from the HPCH coupling.

CHAPTER 6

RESULTS AND DISCUSSION

The entire work has been divided into 4 parts. Results of each part have been discussed separately under each section in this chapter (sections 6.1-6.4).

- ZDDP-FeF_3 interactions in nitrogen - Thermal degradation studies
- Fate of ‘early intermediate compounds’
- Effect of air on ZDDP-FeF_3 interactions - Oxidative degradation studies
- Optimization of wear performance of ‘fluorinated ZDDP’ with reaction conditions

The last section (6.5) deals with different possible conditions that are favorable for the formation of the new fluorinated products.

6.1 Thermal degradation studies

The four samples that were characterized in detail include the following (a) 50 wt% of ZDDP in mineral oil (b) ZDDP (50wt %): FeF_3 (1:0.4) in mineral oil (c) 50 wt% of ZDDP in mineral oil baked in a nitrogen environment for 20 minutes and (d) ZDDP (50wt %): FeF_3 (1:0.4) in mineral oil baked in a nitrogen environment for 20 minutes. Results obtained by test procedures described in chapter 4 include

- Phosphorus and fluorine NMR spectrums
- Elemental analysis (Phosphorus, Sulfur, Iron, Zinc, Fluorine)
- Wear performance in terms of wear volume
- TEM-EDS of wear debris post wear tests

- FT-IR spectrums

6.1.1 Nuclear Magnetic Resonance Spectroscopy

A first guess about the type of phosphorus compound can be made from the general chemical shifts for different phosphorus valence state compounds ranging from -250 ppm to + 300 ppm [47].

Table 6.1 Chemical shifts for different phosphorus valence state compounds

Group , Structure type	Chemical shifts	Range (ppm)
Phosphine, P<	Highly negative shifts , But entire range possible	
Phosphoryl, OP<	Lower negative to lower positive	-25 to + 50
thiophosphoryl compounds, SP<	Mediocre negative shifts	-100 to 0
Five/six fold Phosphorus	positive chemical shifts	> + 20

Besides chemical shifts, coupling constants are an important feature of spin-spin multiplets and these have been utilized to provide valuable information regarding the structures of new compound.

6.1.1.1 Phosphorus NMR – Original compound ZDDP, baseline

Figure 6.1 is the ^{31}P NMR spectra decoupled with proton for starting material consisting of 50% ZDDP in mineral oil at room temperature indicating at least 6-7 different phosphorus environments. Decoupling phosphorus spectrum with proton (refer heteronuclear decoupling discussed in chapter 5) prevents splitting of phosphorus signals (leading to reduction in signal intensity) by hydrogen's bonded either directly or indirectly to phosphorous. Two of phosphorus environments at ~ 99.9 ppm and ~ 93.8 ppm can be attributed to basic and neutral forms of the parent ZDDP. Thus it is a mixture of neutral and basic forms. It is also a secondary type of ZDDP (secondary alkyl groups) from its chemical shift values for basic and neutral forms in fig 6.1 [50]. The neutral form of ZDDP corresponding to ~93.8 ppm is the dominant peak while the basic form of ZDDP at ~ 99.9 ppm comprises approximately 15% of the mixture.

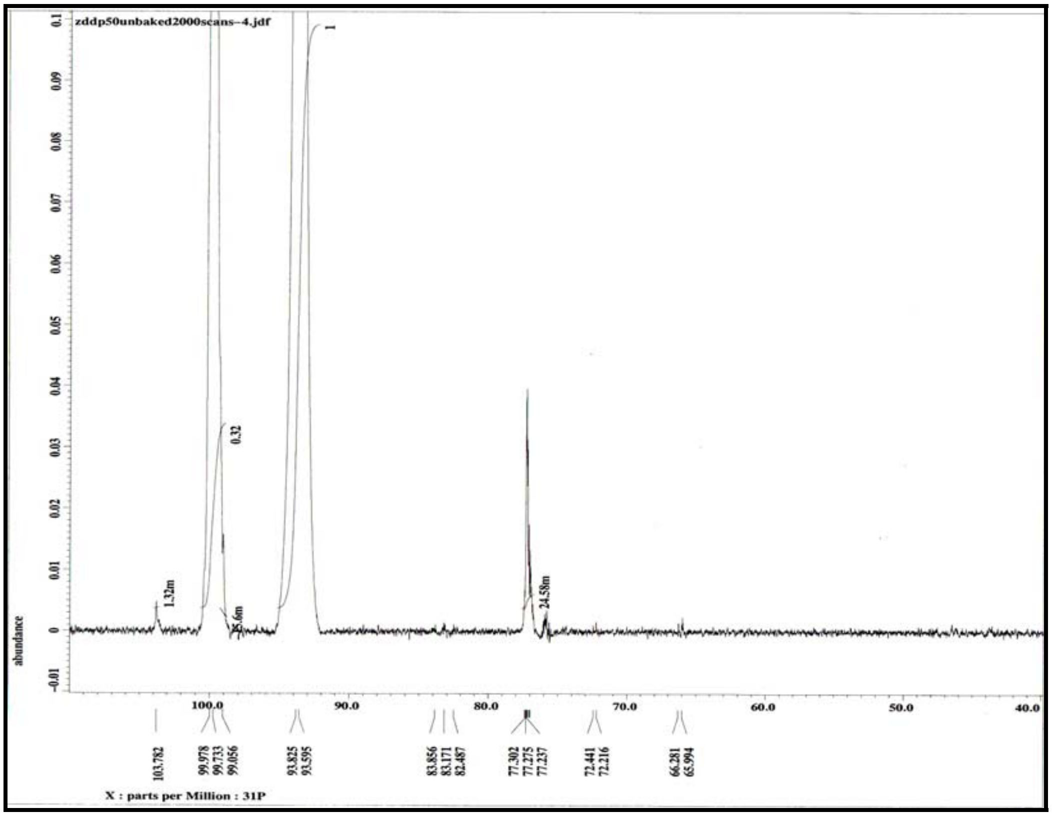

Figure 6.1 Phosphorus NMR of ZDDP (original parent compound) in mineral oil at room temperature

The remaining peaks at 103 ppm, ~82-83 ppm, ~ 77 ppm, ~72 ppm, ~66 ppm and ~43 ppm arise due to impurities and/or minor reaction/degradation products probably during the synthesis of ZDDP. Only the peak at ~77 ppm is a predominant impurity peak. It can be seen from the table that most peaks are in the range of 40-100 ppm (low-field shifts regarded as positive, convention different from that in table 6.1 but essentially same). This implies that are mostly due to thiophosphorus compounds. For the ^{31}P NMR spectrum corresponding to figure 6.1, the chemical shifts corresponding to the peaks have been listed in Table 6.2 and correlated to possible compounds.

Table 6.2 Phosphorus NMR interpretations from chemicals shifts for ZDDP (original parent compound) in mineral oil at room temperature

No	Observed Chemical shift ppm	Possible structures	Theoretical peaks ppm	Ref.
1	93.595-93.825	Neutral ZDDP	94, 102-93, 95.8	[50,47]
2	99.056-99.978	Basic ZDDP	102-110, 100(sec.)	[50]
3	103.782	$(RO)_2P(S)(SR)$	100	
4	82.487-83.856	$\{S_2P(OR)_2\}^-H^+$ $(RO)_2PS\text{-}S_n\text{-}PS\ (RO)_2$	(1°,86 ; 2°, 82.4) (78.4-83.4)	[47]
5	72.216-72.441	R(R'S)2PS, R= CH_3, R' > CH_3 $(RO)_3PS$, R= CH_3 $(RO)(R'S)P(O)SZn^-$	74+-3.0 73, 50-82 68-90	[53] [53,52]
6	65.994-66.281	$(RS)_3PO$	65,55-65	[51,52]
7	77.237-77.302	$(RO)_2(S)PSP(S)(OR)_2$ $(RO)(R'S)P(O)SZn^-$	76-83,78.4-83.4 68-90	[52,47] [52]
8	43.747	$(RS)_2P(O)(OR)$ >P(O)SP(O)<	44 38-42	[53, 52]

The ^{31}P NMR spectrum in fig 6.1 for the original starting compound ZDDP and its peak interpretations table 6.2 serves as a baseline for other modified samples.

6.1.1.2 Phosphorus NMR – ZDDP baked 20min/nitrogen/150C

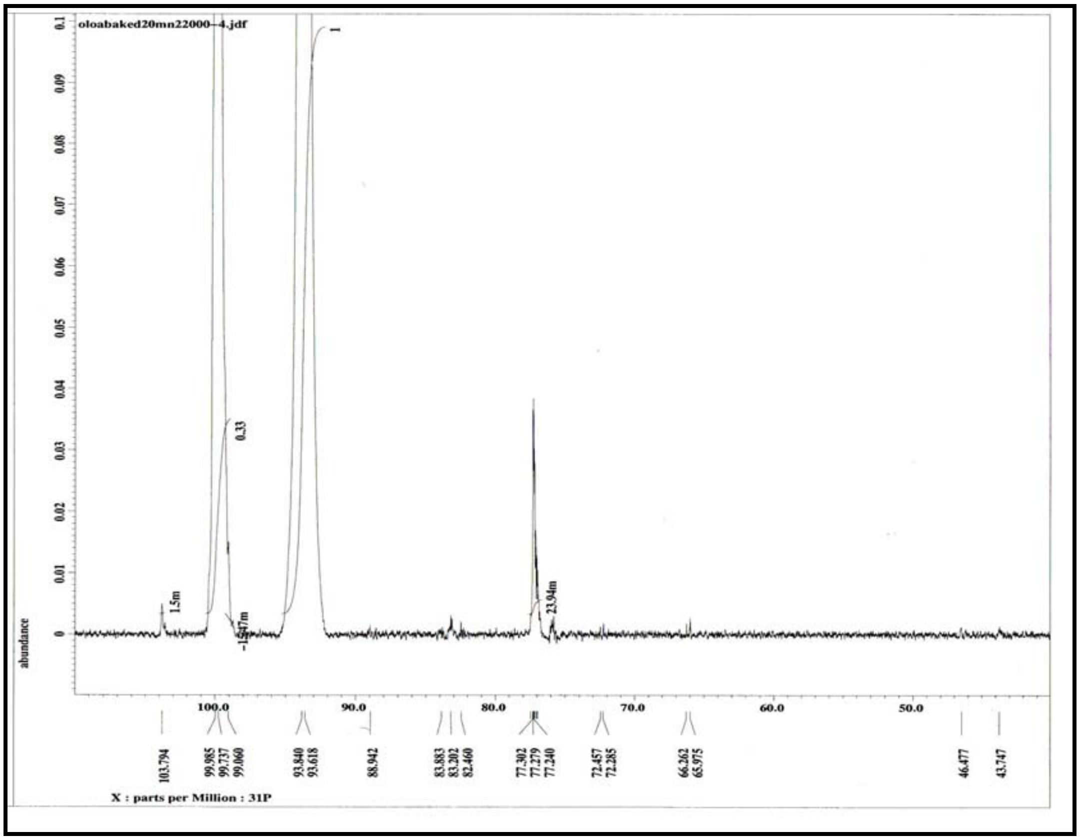

Figure 6.2 Phosphorus NMR of ZDDP baked at 150C for 20 min in nitrogen

Fig 6.2 is a ^{31}P NMR spectra decoupled with proton for 50 % ZDDP solution in mineral oil that was baked at 150C for 20 min in a nitrogen environment. The impurities remain unchanged however small new peaks appear at ~46 and ~88 ppm indicative of the early decomposition products of the ZDDP. These are likely phosphate, thiophosphate and polyphosphate compounds of zinc that form on the decomposition of ZDDP. Peaks at ~82-83 ppm slightly increase in intensity as compared to parent compound signifying the possibility of being decomposition reaction products.

Table 6.3 Phosphorus NMR interpretations from chemical shifts for ZDDP baked at 150C for 20 min in nitrogen

(Peaks in addition to 1-8 in table 6.2)				
S. No	Observed Chemical shift ppm	Possible structures	Theoretical peaks ppm	References
9	88.942	$(RO)_2P(S)(SR)$ $RP(S)(SR)_2$	85-93 90,86,85	[50] [51]
10	46.477	$(RO)_2P(S)O^-$ $R_3P(O)$, $R>CH_3$	55-37, 43-46, 35-55 46+/-2.5	[51],[52],[52] [53]

For the ^{31}P NMR spectrum corresponding to fig 6.2, the chemical shifts corresponding to the peaks have been listed in the Table 6.3 and correlated to possible compounds.

An important point is that the intensity of basic ZDDP in 'baked ZDDP' remains nearly the same as in the original compound. This signifies that there's not much decomposition which is also reflected from 'not many' decomposition products of strong intensity. Not much color change was noticed in the sample.

6.1.1.3 Phosphorus and fluorine NMR – ZDDP:FeF$_3$ baked 20 min/Nitrogen/150C

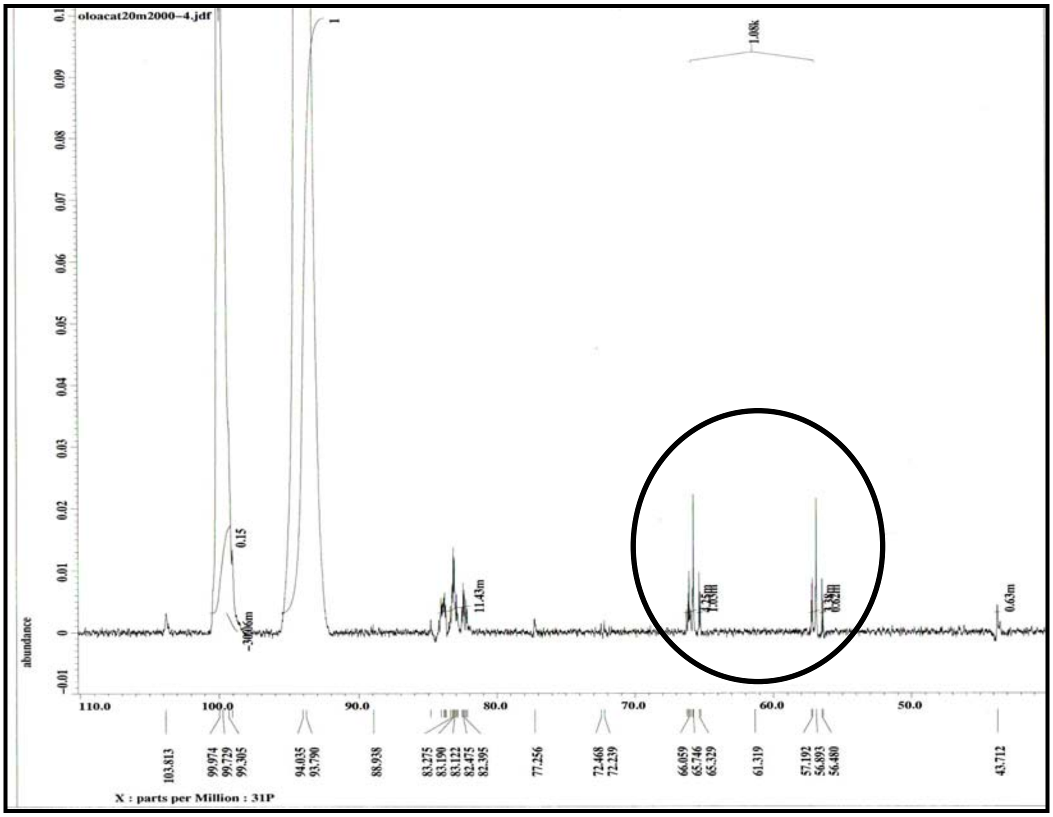

Figure 6.3 Phosphorus NMR of ZDDP - FeF$_3$ baked at 150C for 20 min in nitrogen

Figure 6.3 is a ^{31}P NMR spectra decoupled with proton for the ZDDP baked at 150°C for 20 min in Nitrogen in presence of FeF$_3$ (ZDDP: FeF$_3$ ratio at 1:0.4). The series of peaks at ~82-83 ppm and ~ 43ppm are found to be stronger in intensity in presence of FeF$_3$ than when ZDDP is baked alone indicating that either the decomposition of ZDDP is more rapid in the presence of FeF$_3$ or the products are more favored in presence of FeF$_3$. Earlier DSC studies have shown that the decomposition of

ZDDP is accelerated in presence of FeF_3 by at least 10-15% [15]. Compounds of type $(RO)_2P(S)O^-$ (~46 ppm) are not formed here unlike in case of baked ZDDP.

The other small impurity peaks still remain unchanged. The intensity of basic ZDDP becomes nearly half of that of the starting material ZDDP when ZDDP is baked with FeF_3 unlike when it is heated alone. This strengthens the fact that the decomposition of ZDDP is accelerated in presence of FeF_3. The circled peaks are the ones that are only formed when ZDDP is baked in presence of FeF_3 and the other peaks are formed by the normal decomposition of ZDDP as they are also observed when ZDDP is baked alone. A ^{19}F NMR revealed similar nature of peaks

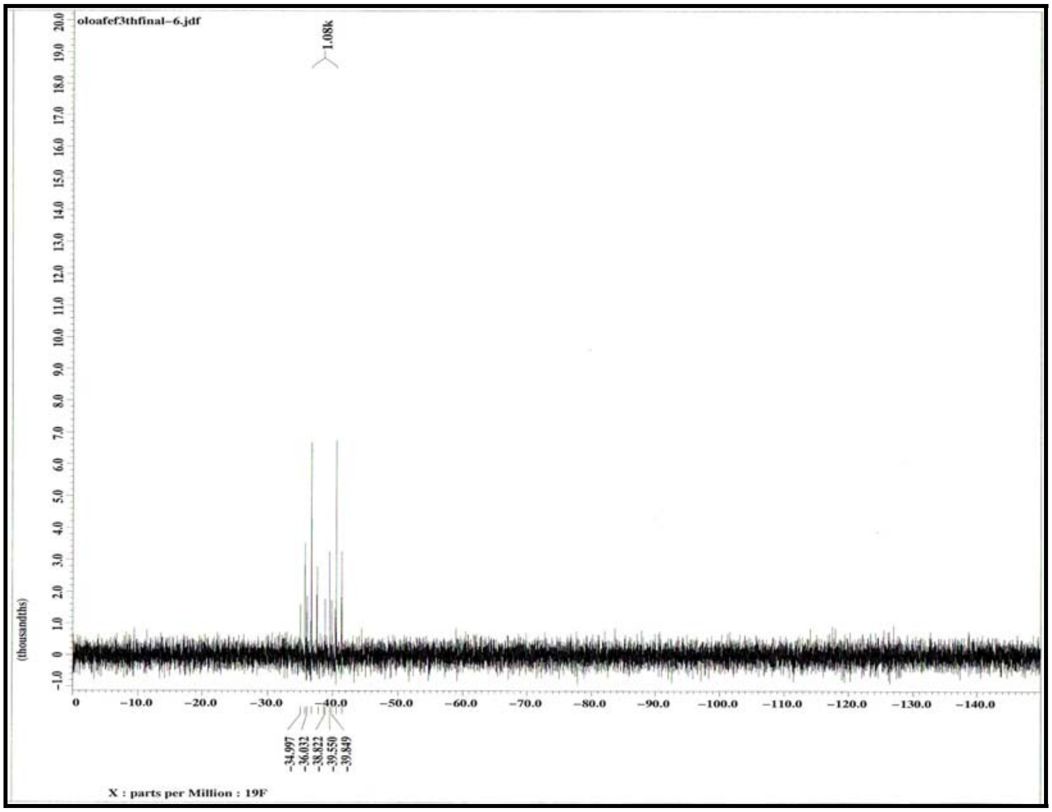

Figure 6.4 Fluorine NMR of ZDDP - FeF_3 baked at 150C for 20 min in nitrogen

6.1.1.4 Elucidation of structure from the new peaks formed with FeF_3 only

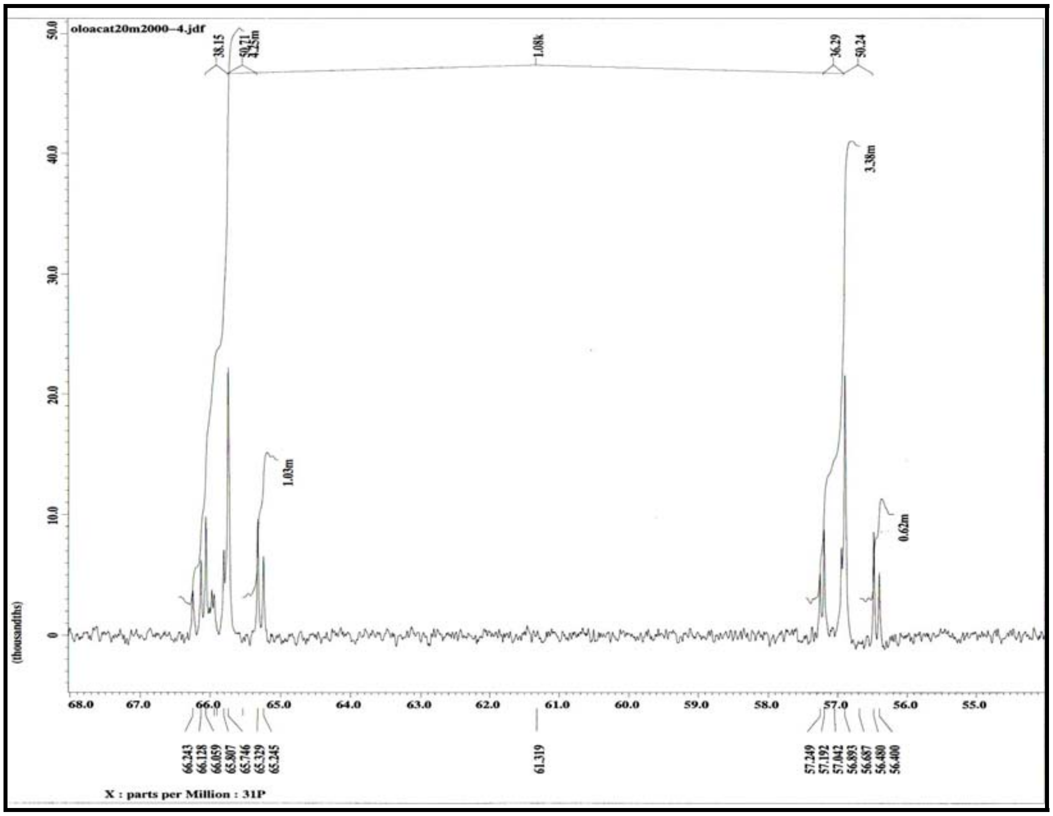

Figure 6.5 A closer view of new peaks in phosphorus NMR of ZDDP - FeF_3 baked at 150C for 20 min in nitrogen

a. The Doublets in ^{31}P decoupled with ^{1}H and ^{19}F NMR

A closer view of the circled peaks in fig. 6.3 arising from new species formed when ZDDP is baked in presence of FeF_3 is shown in fig 6.5. It seems that these are identical replicas arising due to spin-spin splitting. Thus the peaks could be regarded as a doublet with a huge coupling constant, J of 1080 Hz. Each set of the doublet is again a triplet but an unsymmetrical one with J values of approximately 36-38 Hz and 50 Hz. From fig 6.5 the left hand side of the triplet at ~ 66ppm appears to be composed of more finer peaks that seem to be absent in the triplet at ~ 57ppm. This can be accounted to the fine peaks present at ~66.2 and 65.9 ppm as impurity peaks in the original compound. They are absent at ~ 57ppm. Thus it can be safely said that the doublet (~66pm and ~57ppm) arises as a result of reaction products from the interaction of ZDDP and FeF_3. The spin-spin coupling constant J has a high value of 1080 (fig 6.3 and 6.5) and can be correlated to the possible type of phosphorus compound from table 6.4.

Table 6.4 Phosphorus-Phosphorus and Phosphorus-Fluorine coupling constants

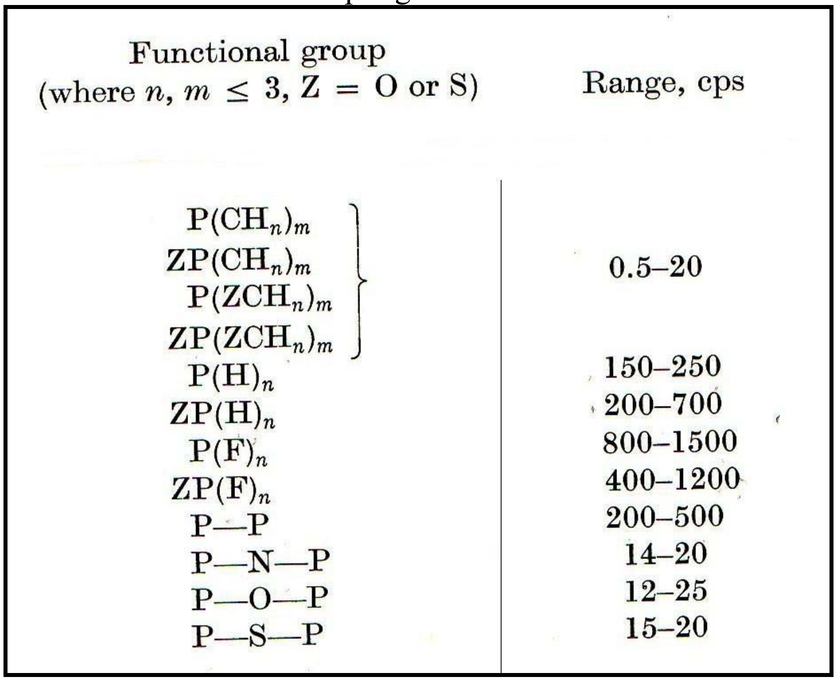

Functional group (where $n, m \leq 3$, Z = O or S)	Range, cps
$P(CH_n)_m$ $ZP(CH_n)_m$ $P(ZCH_n)_m$ $ZP(ZCH_n)_m$	0.5–20
$P(H)_n$	150–250
$ZP(H)_n$	200–700
$P(F)_n$	800–1500
$ZP(F)_n$	400–1200
P—P	200–500
P—N—P	14–20
P—O—P	12–25
P—S—P	15–20

There are two possibilities for these type of P-F compounds as seen in table 6.4. P(F)n (for n=3 signifies a trivalent phosphorus compounds) and ZP(F)n (for n=3 signifies a pentavalent phosphorus compound) structures are attributed to the doublet ~66ppm and ~57ppm. These phosphorus chemical shifts are highly indicative of pentavalent phosphorus type of compound (table 6.1). The splitting of each set of the doublet into more finer peaks (J ~ 37 & 50Hz) cannot be explained by only 3 fluorine subsitituents in PF_3. This leads us to believe that the structure for this type of compounds is ZP(F)n. Fig 6.4, a ^{19}F NMR in is zoomed for a closer view of the peaks shown in fig 6.6

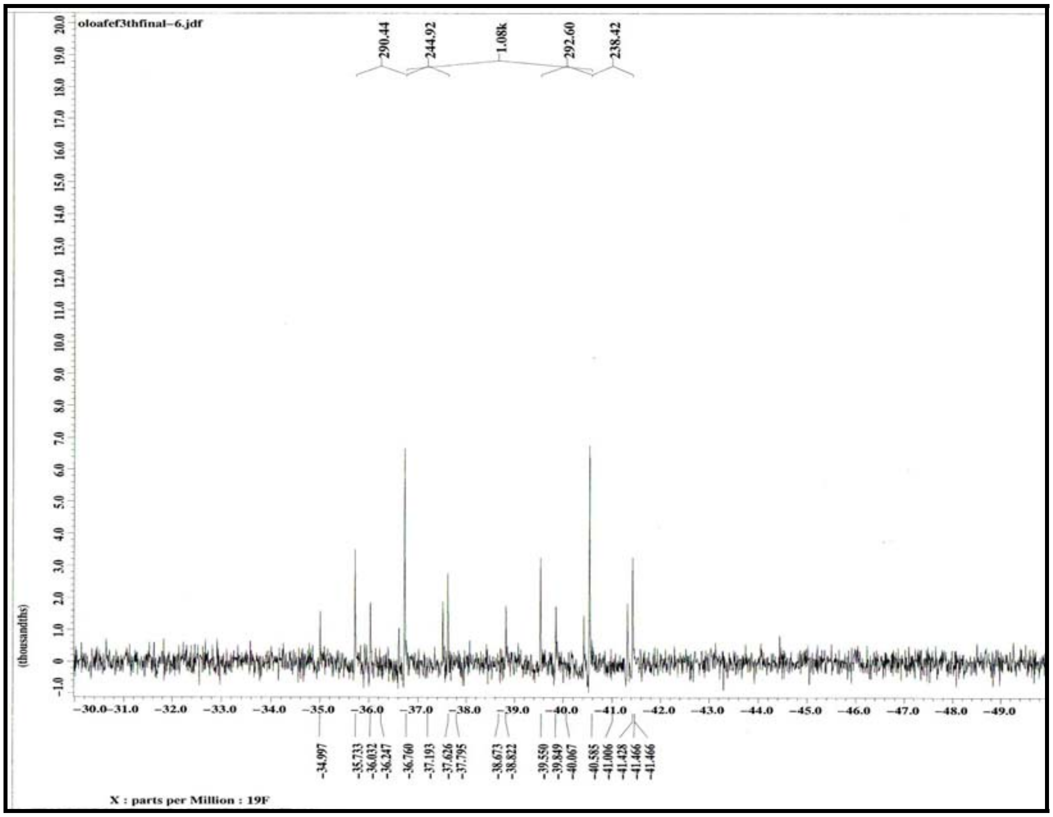

Figure 6.6 A closer view of fluorine NMR of ZDDP -FeF_3 baked at 150C for 20 min in nitrogen

Coupling constant J value for the above splits is 1080. The inner fine structure of doublet in ^{19}F NMR closely resembles that in ^{31}P NMR (compare fig 6.5 and 6.6). *First Proof:* Both ^{31}P NMR (decoupled with ^{1}H) and ^{19}F NMR suggest a direct P-F linkage (from the huge coupling constant value J, 1080 Hz of the spin-spin splits or doublet)

b. Merging of doublets (phosphorus decoupled with fluorine)

In figures 6.3 and 6.5, phosphorus was decoupled with proton; P-H bonding possibility was eliminated from contributing towards this spin-spin splitting of 1080. Further such huge J values can be unmistakably attributed to a direct P-F bonding, table 6.4. This fact can be further proved by decoupling phosphorus with fluorine in a ^{31}P NMR spectrum (fig 6.7). The two replicas of the doublet coalesce into one at ~61.3 ppm with the unsymmetrical triplet, splits maintained at ~37 and ~50 Hz.

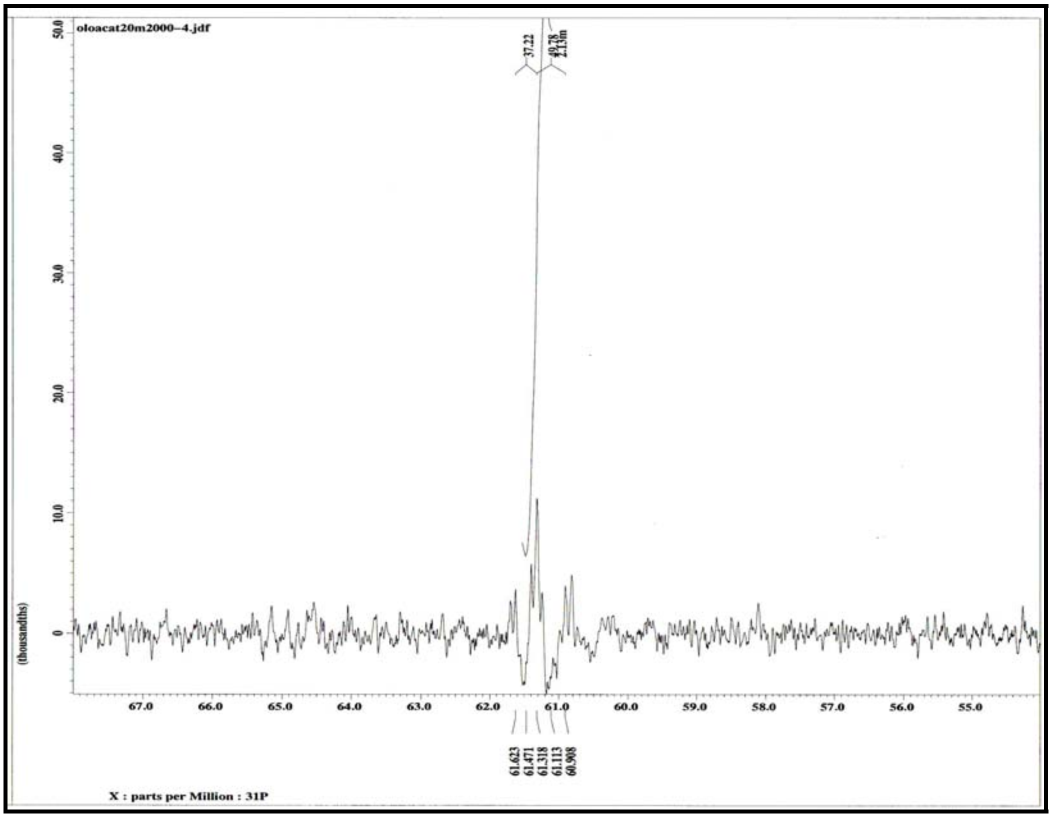

Figure 6.7 A closer view of phosphorus NMR (decoupled with fluorine) of ZDDP - FeF_3 baked at 150C for 20 min in nitrogen

The apparent spin-spin splits or doublets coalesce into one set of peaks (as expected when P-F interaction is suppressed or decoupled) in fig 6.7. They appear at a median value of 57 & 65 ppm approximately. This confirms the presence of P-F bonding. Notice the reduction in intensity of the triplet.

Second Proof: Decoupling phosphorus with fluorine (F perturbed at -38.5ppm) results in doublets merging into one proving the splitting of phosphorus peak into doublet by fluorine. This proves the presence of a direct P-F linkage in a molecule.

c. The unsymmetrical triplet

In fig 6.3, 6.5 where the doublet due to P-F bonding was obtained by decoupling phosphorus P with proton (H), the triplet set of the doublet could be a spin-spin split due to phosphorus coupled with phosphorus or phosphorus coupled with fluorine. Again in a ^{31}P NMR in which P was decoupled with F (fig 6.7) this triplet with the same coupling constants was retained. This eliminates the possibility of splitting due to P-F coupling in this case and signifies that the inner triplet is due to P-P or P-X-P bonding (where X = O, S). The triplet is unsymmetrical pointing to the possibility of separate phosphorus peaks or non-identical phosphorus environments. In latter case, each would give rise to its own chemical shift. Apparently three chemical shifts are not observed for each different phosphorus atom. This can be explained by the fact that the three phosphorus environments are not identical and the spectrum is of second order. This feature can be considered similar to ^{31}P NMR of ATP (pH =10) [chapter 5].

To sum up the doublet arises due to a direct P-F bonding in the structure consisting of at least three non identical phosphorus environments. The latter (P-P) couple together, splitting each doublet into a rough triplet. This is if the spectrum is indeed of second order. The other several structural possibilities for spectra being 1st order and 2nd order have been included in [54].

d. Structure of new fluorinated phosphorus compounds (FPC)

To propose a structure in the light of the above NMR interpretations for this new compound seems a complex task. Phosphorus chemical shift in ^{31}P NMR at ~61-62ppm along with fluorine shifts in ^{19}F NMR at -38.5ppm (figure 6.7, 6.4) for FPC suggests a structure that best fits tetravalent coordinate phosphorus compound of a type listed in table 6.5. The alkyl groups of ZDDP and sulfur are possibly retained in the structure from the nature of shift values. When phosphorus was decoupled with Fluorine in fig 6.7 phosphorus was automatically coupled with proton. Presence of any protons H, on the FPC structure would split the signal intensity of phosphorus in these compounds. Thus the intensity of doublet in fig 6.5 (P decoupled with H) is greater than the intensity of peak in fig 6.7 (P decoupled with F) owing to the presence of H in the structure and thus indicates the presence of alkyl groups. Again shift values between 40-100 indicate thiophosphorus compounds. Unlike the mono-phosphorus compounds of the references, the compound under investigation is a poly-phosphorus one.

Table 6.5 Possible valence states of phosphorus in different phosphorus compounds with their corresponding chemical shifts [54, 55]

1.	Tri-coordinate $(RO)_nPF_{3-n}$	Very Large Negative Shifts
2	Tetra-coordinate R_nPOF_{3-n} , $(RO)_2PSF$	Medium Negative Shifts
3	Penta-coordinate R_nPF_{5-n}	Positive/slightly negative shifts
4	Hexa-coordinate PF_6^{n-}	Largest Positive shifts

Various possibilities of structure that fit both ^{31}P and ^{19}F chemical shifts and spin-spin multiplets are included in the patent [56]. No attempts have been taken to verify the structure.

For the ^{31}P NMR spectrum corresponding to figure 6.3, the chemical shifts corresponding to the peaks have been listed in the Table 6.6 and correlated to possible compounds.

Table 6.6 Phosphorus NMR interpretations from chemical shifts for ZDDP- FeF_3 baked at 150C for 20min in nitrogen

(Peaks in addition to 1-8, 9 in table 6.2 and 6.3)		
S. No	Possible structures	Observed Chemical shift , ppm
1	Fluorinated phosphorus compounds	61.3

6.1.2 Elemental analysis - final evidence for fluorinated phosphorus compounds

The final evidence of fluorine (of iron fluoride) embedded into phosphorus compounds comes from Elemental Analysis of these compounds which reveal iron at 2 ppm as trace impurity and fluorine at 270 ppm (table 6.7). A dark green suspension is obtained when ZDDP is baked with FeF_3 at 150c for 20 min. Upon centrifuging the green decant as termed ZDDP-FeF_3 'decant' is subjected to all subsequent characterizations. NMR on the same revealed presence of fluorinated phosphorus compounds (fig 6.3-6.7) and is finally confirmed by elemental analysis. Absence of iron but presence of fluorine with phosphorus sulfur and zinc (table 6.8) confirms close connection of fluorine to these elements which validate the NMR interpretations that indicate that fluorine is directly connected to phosphorus.

Table 6.7 Elemental analysis of iron and fluorine in 'decant' of ZDDP- FeF_3 baked at 150C for 20 min in nitrogen

	 ZDDP (Baked)	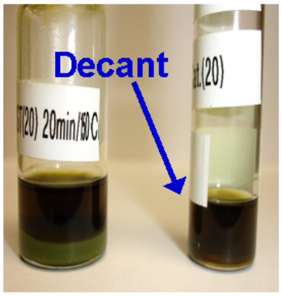 ZDDP + FeF_3 (Baked)
Iron (Fe) (IN DECANT)	0 ppm	2 ppm
Fluorine (F) (IN DECANT)	0 ppm	270 ppm

From table 6.8 it is observed that phosphorus, sulfur and zinc levels do not change much in the baked samples and are within experimental error as compared to that of original starting material ZDDP. It reflects the fact that there was not much precipitation which was apparent for baked ZDDP.

Table 6.8 Elemental analysis for unbaked ZDDP, baked ZDDP and ZDDP-FeF_3 baked at 150C for 20 min in nitrogen

S. No	Elements	ZDDP untreated ppm	ZDDP baked 150C/Nitrogen ppm	ZDDP-FeF_3 baked 150C/Nitrogen ppm
1	Phosphorus	1000	1000	1000
2	Sulfur	1192	1365	1267
3	Zinc	1087	1148	1203
4	Iron	0	0	1-2
5	Fluorine	0	0	163

6.1.3 Wear performance

The wear performance of the four formulations evaluated by the procedure listed in chapter 4 is included here. It can be seen that the wear performance of 'baked ZDDP-FeF_3' formulation surpasses all the other formulations as seen in fig 6.8. There is an improvement over baked ZDDP consistently by ~ 22-30% which signifies that the additional improvement in performance is due to some additional species present evidently FPC. There is also ~ 40% improvement over ZDDP-FeF_3 unbaked formulation. This can be possibly attributed to the availability of the fluorinated phosphorus compounds for protection against metal to metal contact right from the beginning of the boundary condition test.

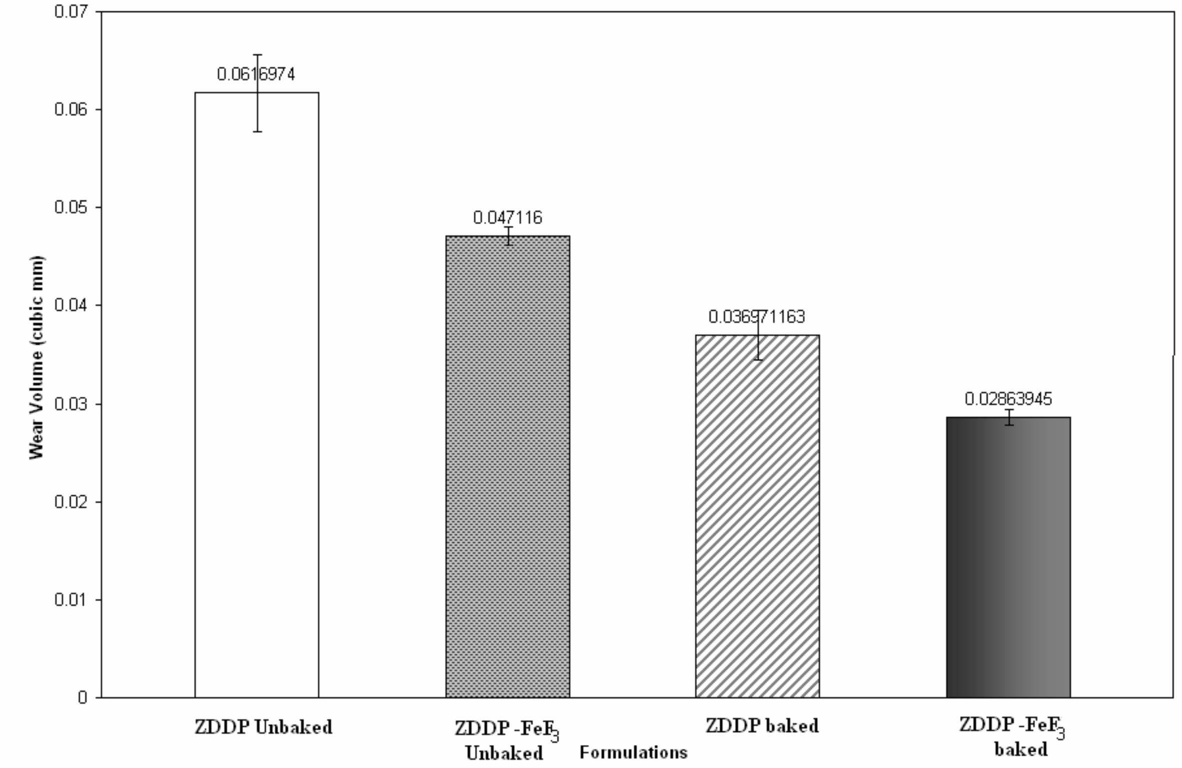

Figure 6.8 Wear volume for formulations at 0.1wt% phosphorus in base stock baked at 150C in nitrogen for 20 min tested at 24Kg load, 25000 cycles and 700 rpm

Above all there is 50% improvement in wear performance of ZDDP-FeF_3 decant over the original baseline ZDDP.

6.1.4 TEM of wear debris

Results obtained by TEM/EDS of the wear debris obtained during the wear test by the procedure listed in section 4 are included here. The wear test conditions include 24Kg Load or 3.54 Hz contact load, 25000 cycles, 700 rpm at 0.1wt% phosphorus.

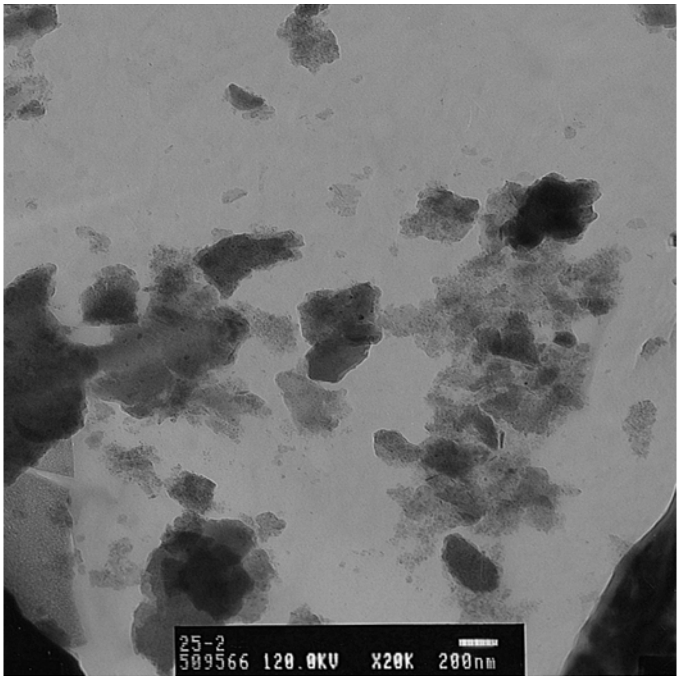

Figure 6.9 TEM of wear debris of unbaked ZDDP

The wear debris of original parent compound is shown in fig 6.9 on a scale of 200 nm. Composition of the same obtained by EDS is shown in fig 6.10. Phosphorus and sulfur are found to be nearly equal in proportion. However wear debris from ZDDP baked for 20min in nitrogen shows a composition in which phosphorus is much higher than sulfur, fig 6.11.

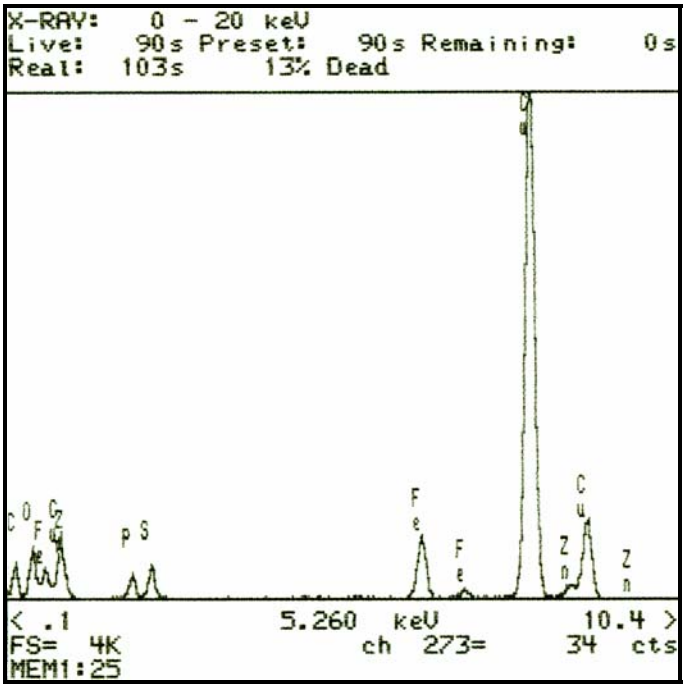

```
X-RAY:    0 - 20 keV
Live:    90s Preset:    90s Remaining:     0s
Real:   103s      13% Dead
< .1               5.260  keV            10.4 >
FS=  4K                ch  273=       34  cts
MEM1:25
```

Figure 6.10 TEM-EDS of wear debris of unbaked ZDDP

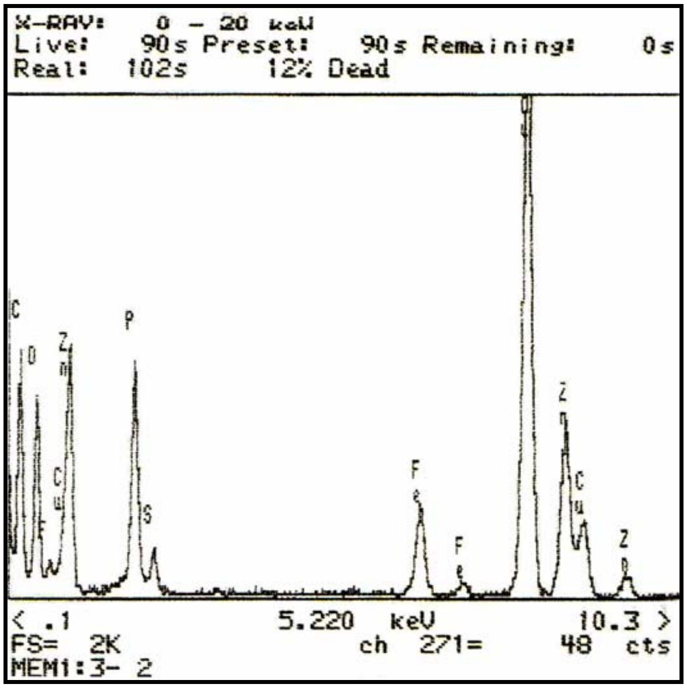

```
X-RAY:    0 - 20 keV
Live:    90s Preset:    90s Remaining:     0s
Real:   102s      12% Dead
< .1               5.220  keV            10.3 >
FS=  2K                ch  271=       48  cts
MEM1:3- 2
```

Figure 6.11 TEM-EDS of wear debris (post wear test) of ZDDP baked at 150C for 20 min in nitrogen

Wear Debris for ZDDP- FeF_3 unbaked sample is shown in fig 6.12. Two kinds of particles light and dark ones were observed. The darker particles showed a crystalline pattern (fig 6.15) unlike the lighter ones signifying the amorphous nature of latter (fig 6.13). Compostion of the two kinds revealed that the darker particles contain no phosphorus and sulfur. Only iron and fluorine signals were observed, (fig 6.14). Clearly this was attributed to FeF_3 particles present in the wear debris. The amorphous particles are attributed to phosphate and polyphosphate glass that has an amorphous nature. Also the concentration of phosphorus was higher than sulfur in these particles.

For 'ZDDP-FeF_3 baked' both light and dark particles are observed in the wear debris as seen in fig 6.16. Both of them showed no crystalline pattern (fig not shown) and thus indicated their amorphous nature. Both of them contained a higher phosphorus content than sulfur fig 6.17, 6.18. NMR results indicated the formation of fluorinated phosphorus compounds in previous section, however no trace of fluorine was observed in the amorphous debris containing phosphorus for ZDDP-FeF_3 baked. Possible reason is that the amount of fluorine ~ 163ppm (for 0.1wt% P in wear tests) was too small for the instrument to capture.

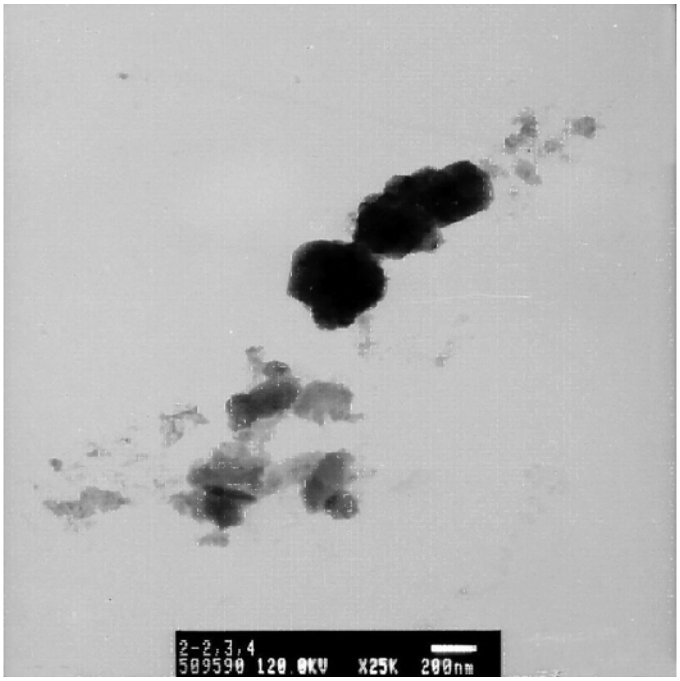

Figure 6.12 TEM of wear debris of unbaked ZDDP-FeF_3

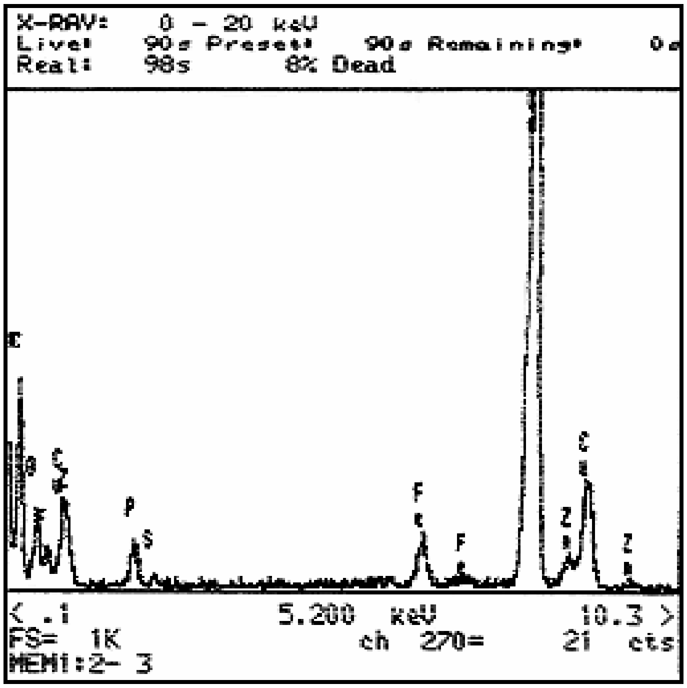

Figure 6.13 TEM-EDS of a light particle in wear debris of unbaked ZDDP-FeF_3

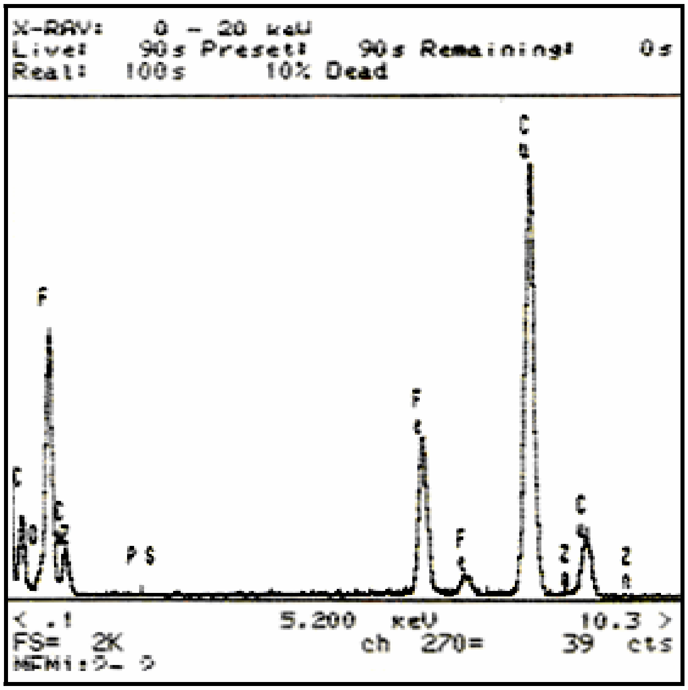

Figure 6.14 TEM-EDS of a dark particle in the wear debris of unbaked ZDDP-FeF_3

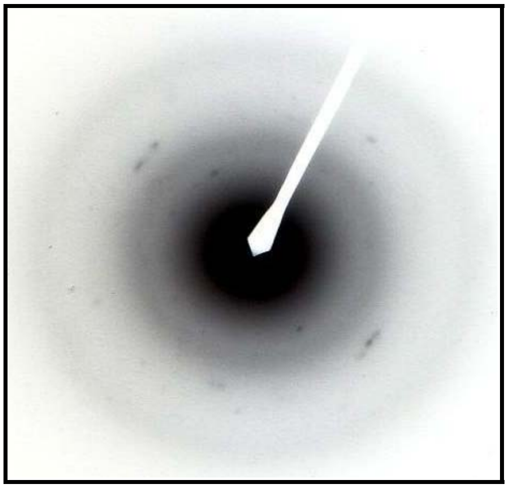

Figure 6.15 A diffraction pattern from dark particle in the wear debris attributed to FeF_3

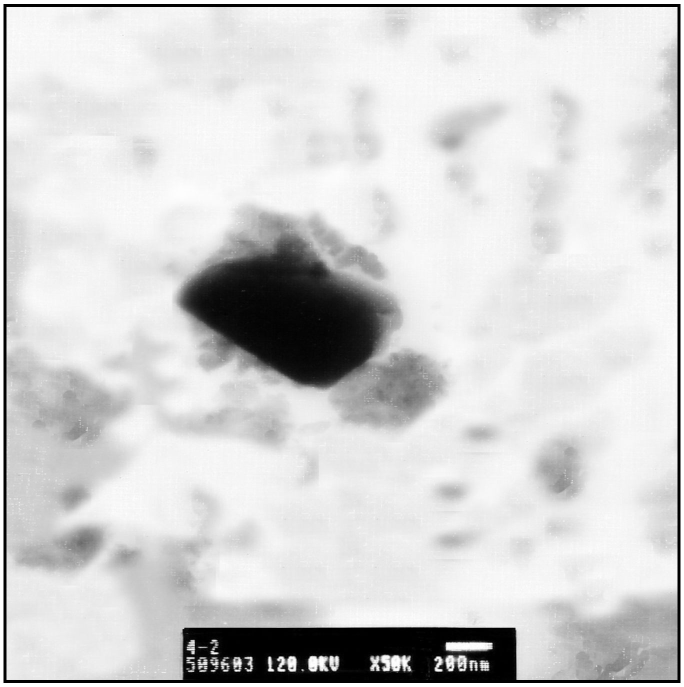

Figure 6.16 TEM of wear debris (post wear test) of ZDDP-FeF_3 baked at 150C for 20 min in nitrogen

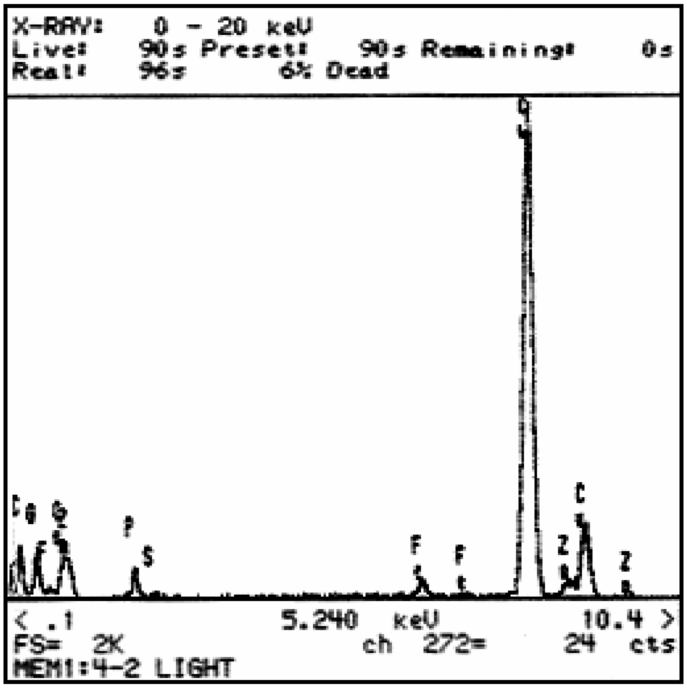

Figure 6.17 TEM-EDS of a light particle in the wear debris (post wear test) of ZDDP-FeF_3 baked at 150C for 20 min in nitrogen

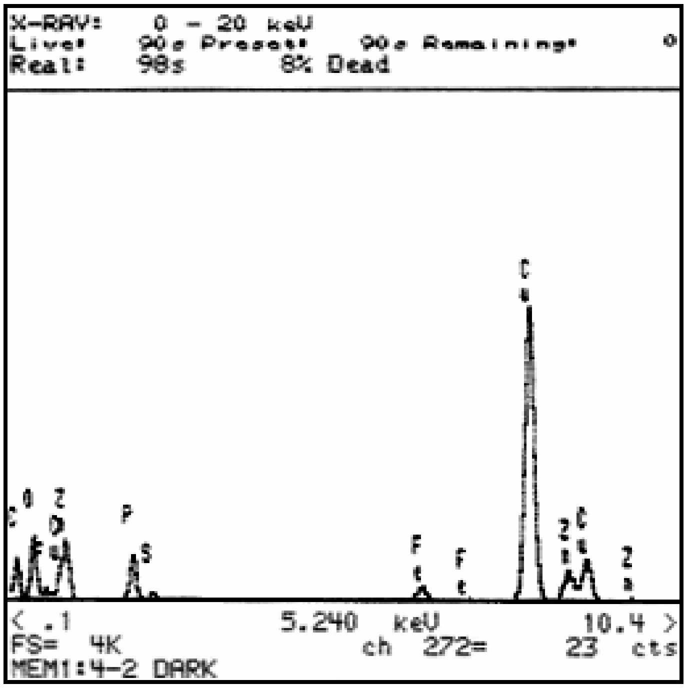

Figure 6.18 TEM-EDS of a dark particle in the wear debris (post wear test) of ZDDP-FeF_3 baked at 150C for 20 min in nitrogen

All formulations except the original compound showed high phosphorus to sulfur ratio. From literature it is well established that the antiwear tribofilms are composed of polyphosphates and sulfides on the metal surface [30, 4, 57]. Higher phosphorus content suggests the film being richer in polyphosphates. Better wear performance for all formulations compared to the original compound can be associated with this polyphosphate film that serves as an amorphous glass.

6.1.5 Fourier Transform Infrared Spectroscopy

If a vibration results in a change of dipole moment of a molecule it will absorb infrared radiation [59]. FT-IR spectra for the formulations have been included here.

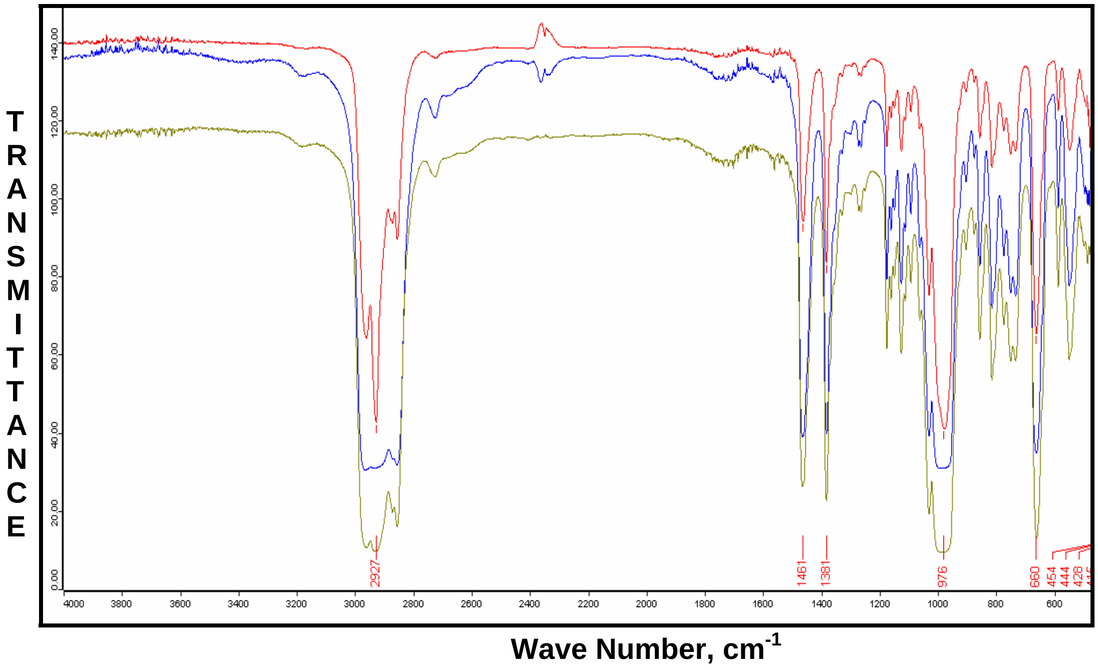

50% ZDDP unbaked	1
50% ZDDP baked 20min/150C/N_2	2
50% ZDDP-FeF_3 baked 20min/150C/N_2	3

Figure 6.19 An FT-IR spectrum of ZDDP - FeF_3 baked at 150C for 20 min in nitrogen (4000-500 cm^{-1})

The entire spectrum from 4000-500 cm-1 could be simplified by diving it into 2 regions each of which is zoomed and discussed separately.

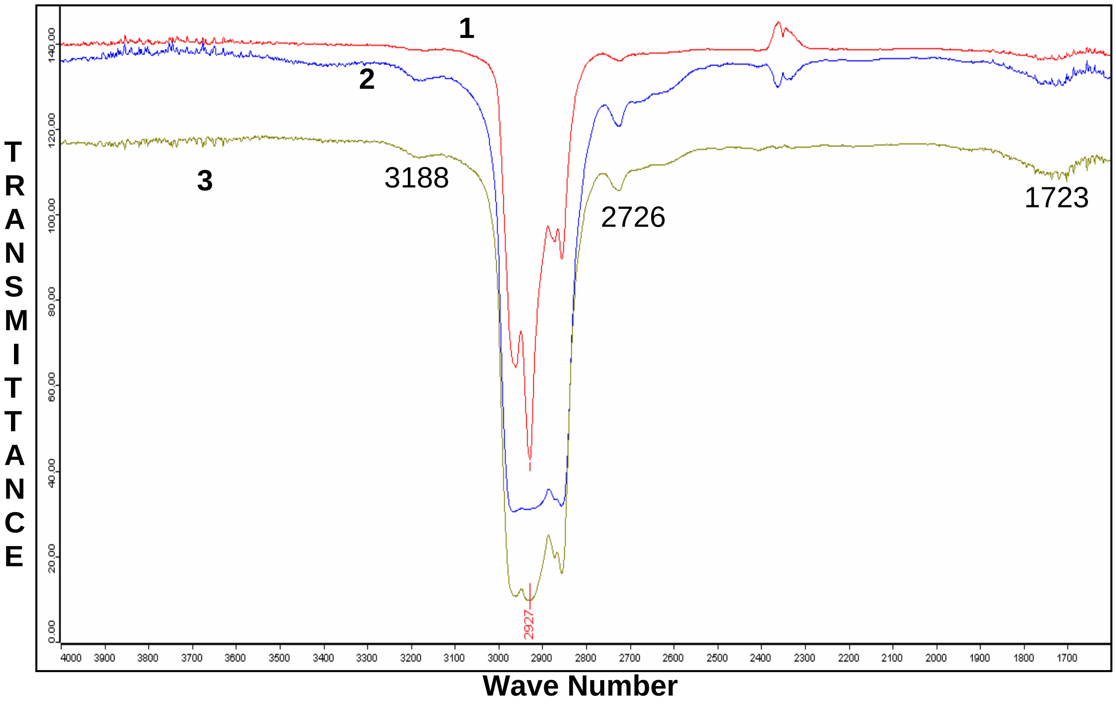

50% ZDDP unbaked	1
50% ZDDP baked 20min/150c/N_2	2
50% ZDDP-FeF_3 baked 20min/150c/N_2	3

Figure 6.20 An FT-IR spectrum of ZDDP - FeF_3 baked at 150C for 20 min in nitrogen (4000-1600 cm^{-1})

The peaks associated with this region have been identified and included in table 6.9, 6.10.

Table 6.9 Peaks identified for unbaked ZDDP, ZDDP and ZDDP- FeF_3 baked at 150C for 20min in nitrogen in FT-IR (4000-1600cm^{-1}) [10, 59,60]

S. No	Observed Peak	Features	Literature Peak value And group	Attributed Functional Group
1	2800-3000	Broad Band	2820-2810 2970-2860 2935-2845 (C-H stretch, bend)	CH_3-O- , -CH_3, -CH_2 CH_3- $(CH_2)_n$ – Hydrocarbon in oil and Alkyl groups of ZDDP CH_3, -CH_2 Indicative of n ≥3 - (CH_2)n – Aldehyde >P(S)OH (reaction product or impurity) Aldehyde Ester Free CO_2H/ Ketone
2	1461	Big, Sharp band	1485-1370 C-H stretch, Bend	
3	1381	Big, very Sharp band	1350-1000 C-C stretch, Bend	
4	771	Small bands	750-720	
5	2726	Small hump	2800-2700	
6	3188	Small hump	3100-3000	
7	1723	Small hump	1740-1725 1750-1725 1725-1700	

It is observed from the FT-IR of Baked samples that minor humps or peaks appear in 20 min as compared to unbaked ZDDP. These consist of 2726, 3188 and 1723 cm^{-1} .

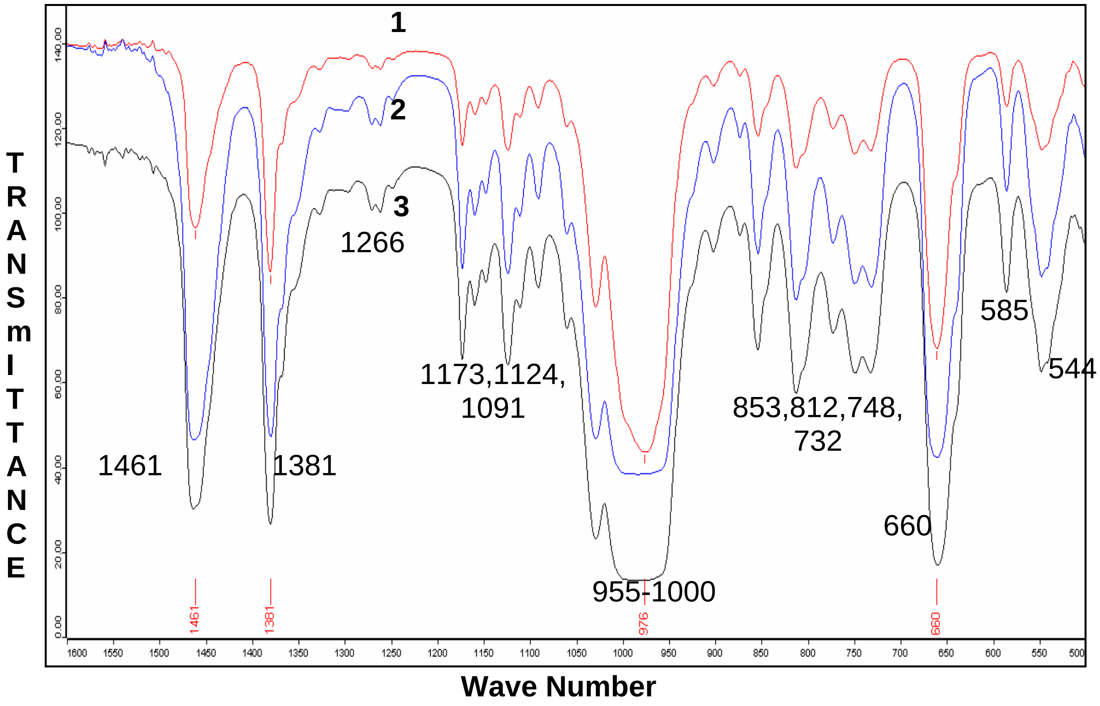

50% ZDDP unbaked	1
50% ZDDP baked 20min/150c/N_2	2
50% ZDDP-FeF_3 baked 20min/150c/N_2	3

Figure 6.21 An FT-IR spectrum of ZDDP - FeF_3 baked at 150C for 20 min in nitrogen (1600-500 cm^{-1})

Table 6.10 Peaks identified for ZDDP, ZDDP and ZDDP- FeF_3 baked at 150C for 20 min in nitrogen in FT-IR (1600-500 cm^{-1}) [10, 59,60]

s.no	Observed Peak	Features	Literature Peak value Cm-1 and group	Attributed Functional Group
8	1266	Small hump	1260-1270, P-S-R	Could be P-S-R
9	1173,1124,1091	Multiple , Medium-sharp peaks	1087-1200, Medium –weak, (general) Band II characteristic of P-O-C 1105-1170, RCH_2-O-P, 1^0 1087-1190, R_2CH-O-P, 2^0 Multiple in character and used to give nature of ester group.	P-O-C of ZDDP Possibility of 20 alkyl
10	955-1000 1029, 1059	Broad band (strong)	950-1088, P-O-C, strong bands, (general) Band I characteristic of P-O-C. 987-1042, P-O-CH2R, 1^0 950-1018, P-O-CHR2 , 2^0 Broad and complex for higher esters	P-O-(C) alkyl of ZDDP

Table 6.11 Peaks identified for unbaked ZDDP, ZDDP and ZDDP- FeF_3 baked at 150C for 20min in nitrogen in FT-IR (1600-500 cm^{-1}) [10, 59,60] (contd.)

s.no	Observed Peak	Features	Literature peak value in Cm-1 and group	Attributed Functional Group
11	853, 812,748,732	Medium-small peaks	685-862 general, band I of P=S	P=S of ZDDP
12	660	Big sharp peak	550-737 general, band II of P=S 652, 635 , P=S 650, 670 P=S 580-690, P=S	P=S or PS^{2-} of ZDDP
13	585	Medium sharp peak		
14	544	Medium sharp peak	556-742 general, Band I Asymmetric frequency of $[(RO)_2PS_2-]_2$ Zn^{+2} 660-665 for 10 and 20 alkyl,	PS^{2-} of ZDDP
			476-570 Band II Symmetric frequency of $[(RO)_2PS_2-]_2$ Zn^{+2} When R= C_nH_{2n+1} , n > 4 550-553, 10 alkyl, 530-540, 20 alkyl	PS^{2-} of ZDDP
			440-613, P-S 460-660, medium intensity P-S , a broad range but 550 for DDP's	PS^{2-} of ZDDP

No significant changes were reflected in FT-IR spectrums upon baking. Probably very low concentrations of new compounds formed in short baking period could not be captured by FT-IR which is sensitive to concentrations. It seems that changes in phosphorus environments due to degradation are better reflected by NMR spectroscopy rather than FT-IR because most phosphorus reaction products have their peaks overlapping in the same wavelength regions in FT-IR. The same has been found by others in that it is well adapted for following the changes in the phosphorus species present [61, 62].

Using oil free ethyl hexyl ZDDP with FeF_3 at room temperature some changes were noticed over a period of time as seen from fig. The FT-IR results for these mark a significant merging of the ZDDP peaks in the region around 550-600 cm-1 (fig 6.22). The peak for FeF_3 is known to be around ~720 cm^{-}1 in the solid state [62]. This merging of the peaks increases with time (spectra 0 hours and 2 weeks). It could be possible that complexation occurs between the PS_2^-ions/P=S and FeF_3 that prevents the unwanted complexation between ZDDP and other additives at ambient temperatures

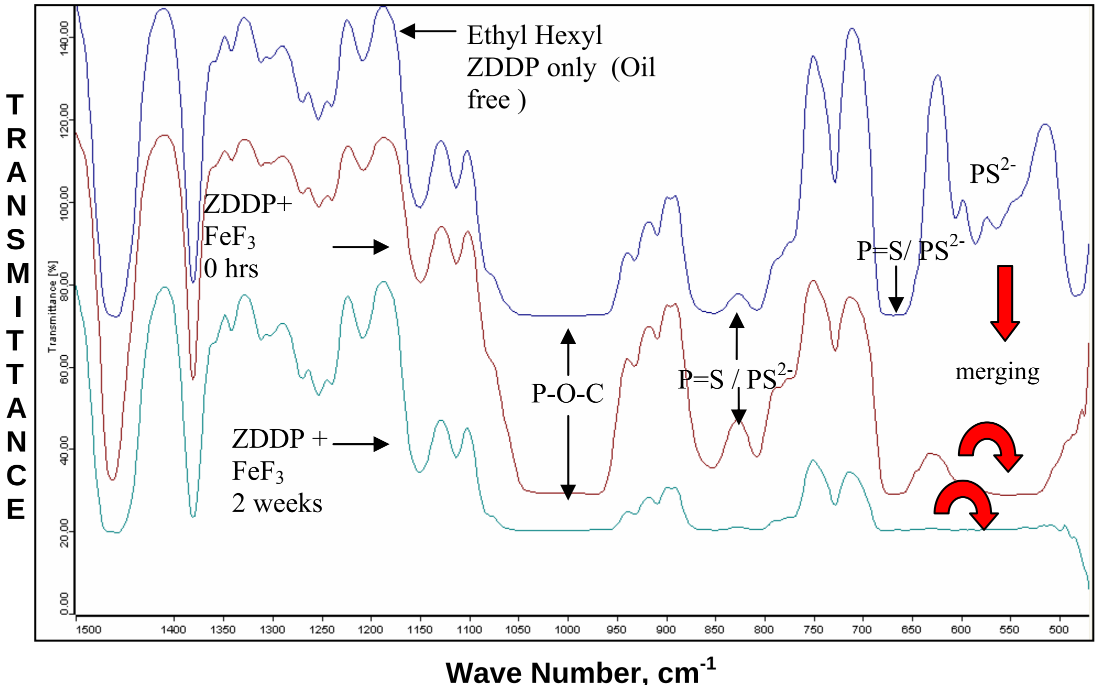

Figure 6.22 An FT-IR spectrum of oil free ethyl-hexyl ZDDP with FeF_3 at room temperature (1500-450 cm^{-1})

6.2 Fate of ‘early intermediate compounds’

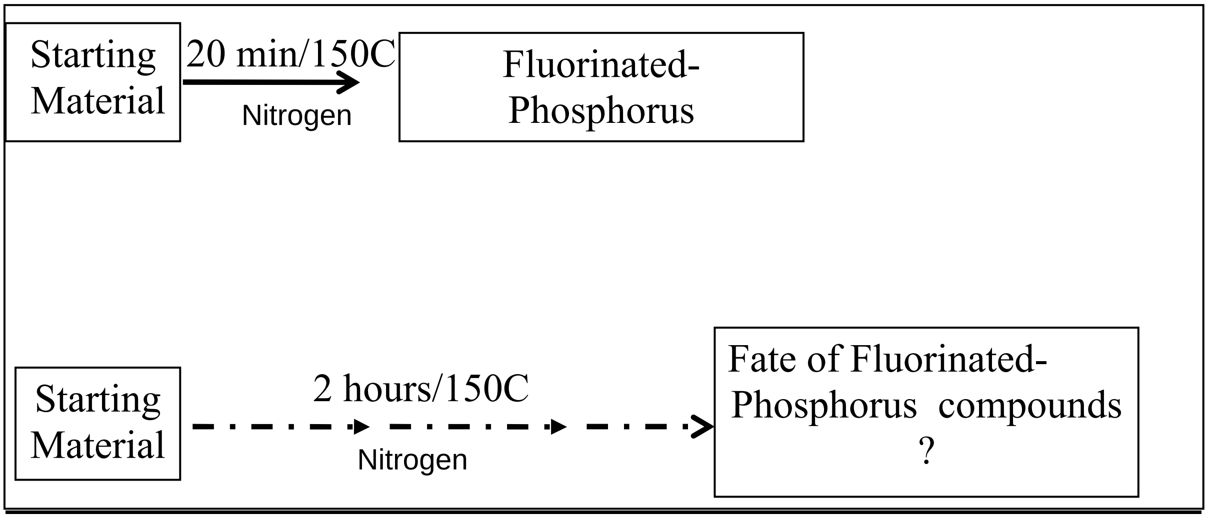

Fig 6.23 At early stages: fluorinated phosphorus compounds; at later stages ?

Results pertain to the samples ‘a’ and ‘b’

(a) 50 wt% of ZDDP in mineral oil baked in a nitrogen environment (as described in section 4) for 2hours and (b) ZDDP (50wt %): FeF_3 (1:0.4) in mineral oil baked in a nitrogen environment for 2 hours. Results include

- Phosphorus and fluorine NMR spectrums
- Elemental analysis (Phosphorus, Sulfur, Iron, Zinc, Fluorine)
- FT-IR spectrums

6.2.1 Nuclear Magnetic Resonance Spectroscopy

6.2.1.1 Phosphorus NMR – ZDDP baked 2hours/150C/nitrogen

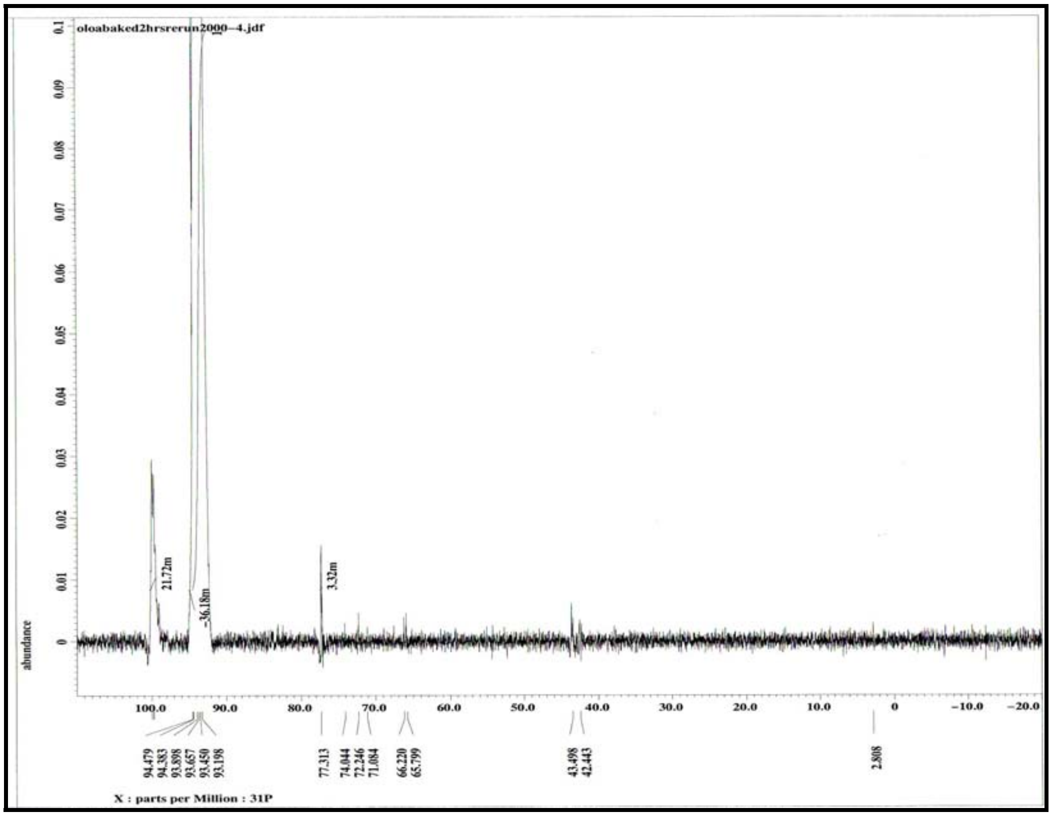

Figure 6.24 Phosphorus NMR of ZDDP baked at 150C for 2 hours in nitrogen

Fig 6.24 shows the appearance of some small peaks or new products resulting from the decomposition of ZDDP. These have been tabulated in table 6.12. The intensity of Basic ZDDP falls significantly. The basic form of ZDDP is the first component to decompose yielding products. This observation agrees with the work of some researchers [50]. It is also observed that there's a little decrease in the intensity of impurity peak at ~77 ppm as compared to earlier 20 min spectra. The peak at 82-83 ppm also observed earlier for ZDDP baked for 20min fig 2 disappears in 2 hours. They seem to be an intermediate compound that later breakdown or transform into other products.

Table 6.12 Phosphorus NMR interpretations from chemical shifts for ZDDP baked at 150C for 2 hours in nitrogen [50,51,52,53,47]

Observed Chemical shifts, ppm	Possible Products	Literature peak values, ppm
93.198-94.479	Neutral ZDDP	(93-94)
99.925	Basic ZDDP	(99-100)
77.313	$(RO)_2(S)PSP(S)(OR)_2$ $(RO)(R'S)P(O)SZn^-$	76-83,78.4-83.4 68-90
71.084, 72.246	R(R'S)2PS, R= CH_3, R' > CH_3	74+-3.0
	$(RO)_3PS$, R= CH_3	73, 50-82
74.04	$(RO)(R'S)P(O)SZn^-$	68-90
	$SPH(OCH_3)_2$	74
65.799-66.22	$(RS)_3PO$	(55-65)
42.443	>P(O)SP(O)<	(38-42)
43.498	$(RS)_2P(O)(OR)$	(44)

6.2.1.2 Phosphorus NMR – ZDDP- FeF_3 baked 2hours/150C/Nitrogen

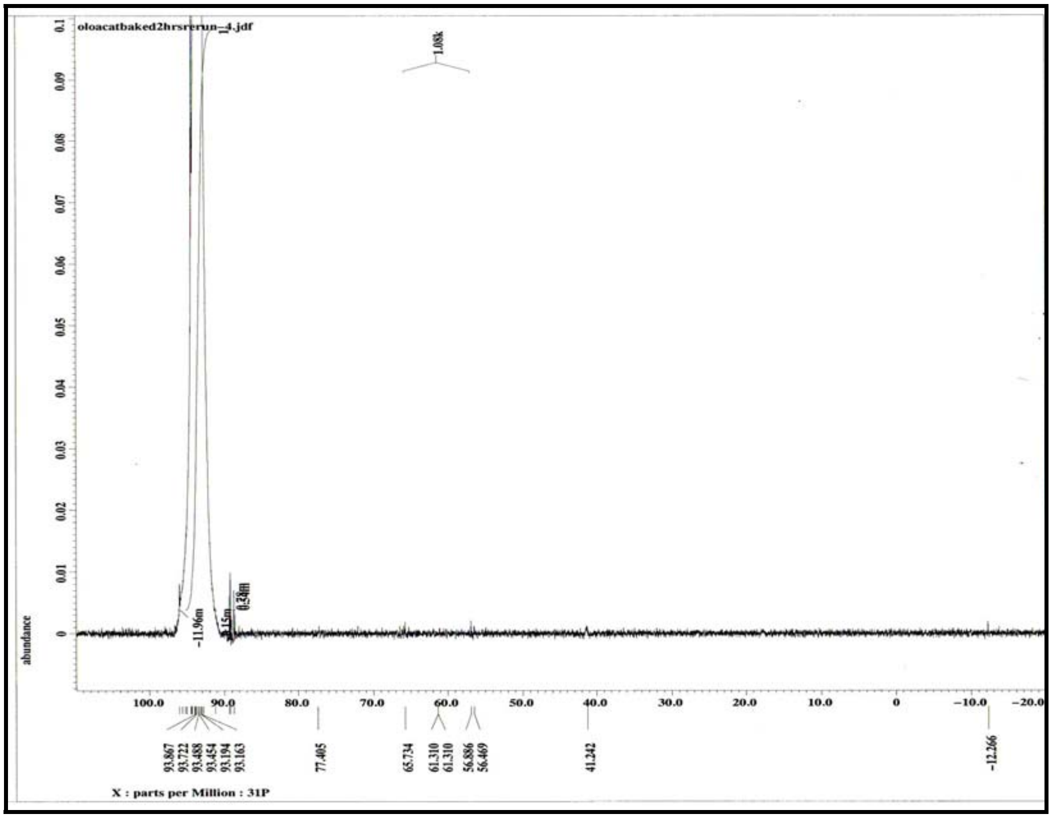

Figure 6.25 Phosphorus NMR of ZDDP- FeF_3 baked at 150C for 2 hours in nitrogen

Figure 6.25 is the NMR spectrum of ZDDP baked with FeF_3 for 2 hours. The disappearance of the peak at 99.9 ppm attributed to basic ZDDP suggests that it has completely reacted in presence of FeF_3 unlike when ZDDP is baked alone, fig 6.24. The impurity peak at ~77ppm greatly reduces in intensity unlike in case of ZDDP baked alone for 2 hours. Most products (peaks) are common with 'baked ZDDP', except for two of them. These include twin sets of peaks at 57 and 65 and other at ~ 89 ppm. The former twin sets of peaks when observed closely resemble the twin sets corresponding to fluorinated phosphorus compounds but significantly reduced in intensity figure 6.26 as compared at 20 min in nitrogen in fig 6.5.

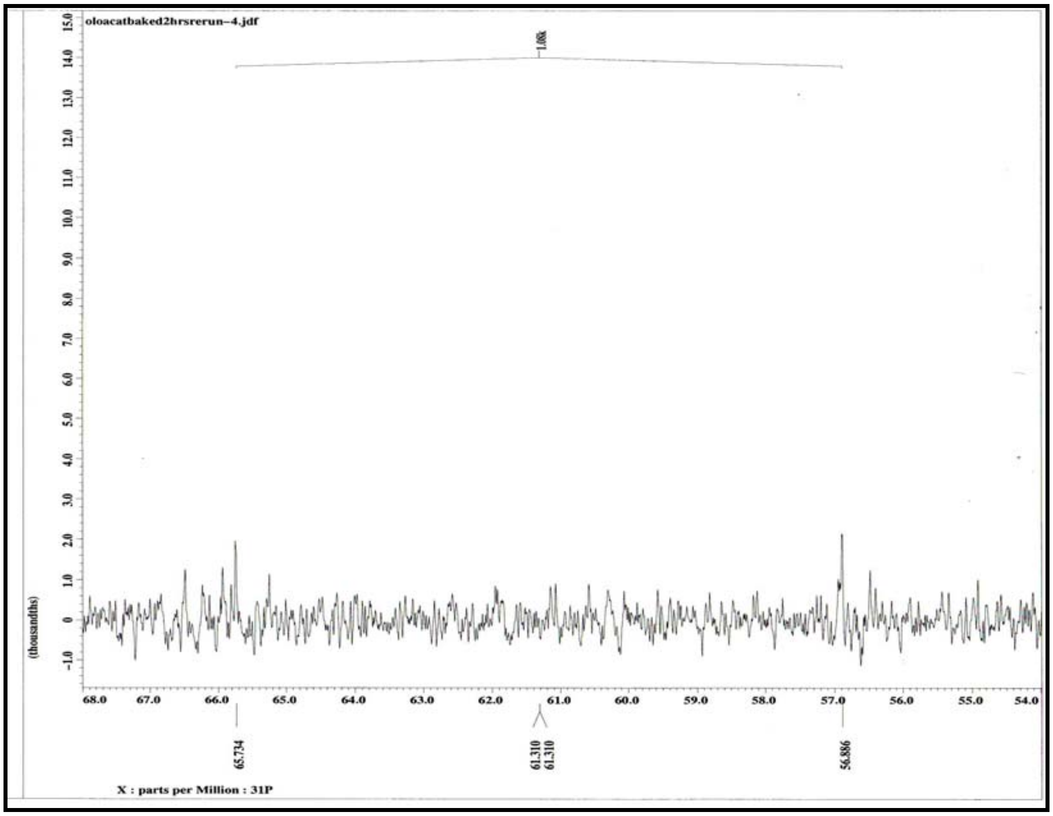

Figure 6.26 A closer view of fluorinated phosphorus compounds in phosphorus NMR of ZDDP- FeF_3 baked at 150C for 2 hours in nitrogen compared at 20 min in nitrogen

The peak at ~89 ppm in a closer view in fig 6.27 is observed to appear only in presence of FeF_3 signifies that it's a product resulting from a direct or indirect interaction between ZDDP and FeF_3. Since the appearance of these compounds occur simultaneously with significant reduction in intensity of FPC, it is possible that FPC may be the source for these compounds.

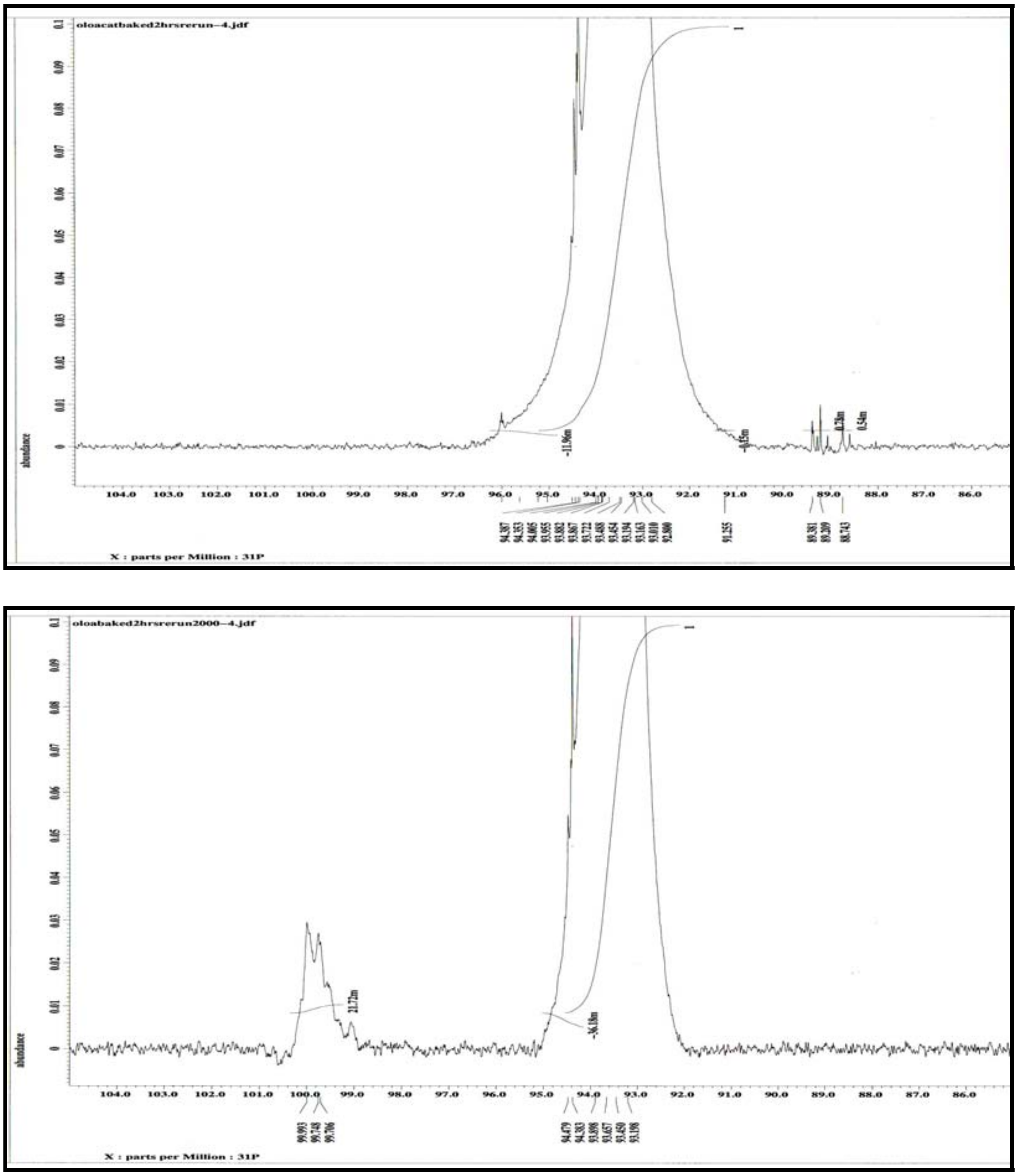

Figure 6.27 A closer view of peak at ~89ppm in phosphorus NMR of ZDDP- FeF_3 baked at 150C for 2 hours in nitrogen (top) compared at ZDDP baked under identical conditions (bottom)

These twin sets of peaks attributed to FPC compounds in fig 6.26 are also observed in the ^{19}F spectrum fig 6.28 at ~ -38 to -39 ppm chemical shifts as originally observed in 20 min compounds figure 5.3 with same J, 1080 Hz. The ^{19}F spectrum shows appearance of few distinct peaks at -14 ppm, ~ -38ppm (regarded to be FPC compounds) and one at -130ppm. The spurious signal at -100 is a result of the offset at -100 ppm. Of these peaks when the peak at -130 ppm is observed closely in figure 6.29, it is split into 5-6 splits.

6.2.1.3 Fluorine NMR – ZDDP baked 2hours/150C/nitrogen

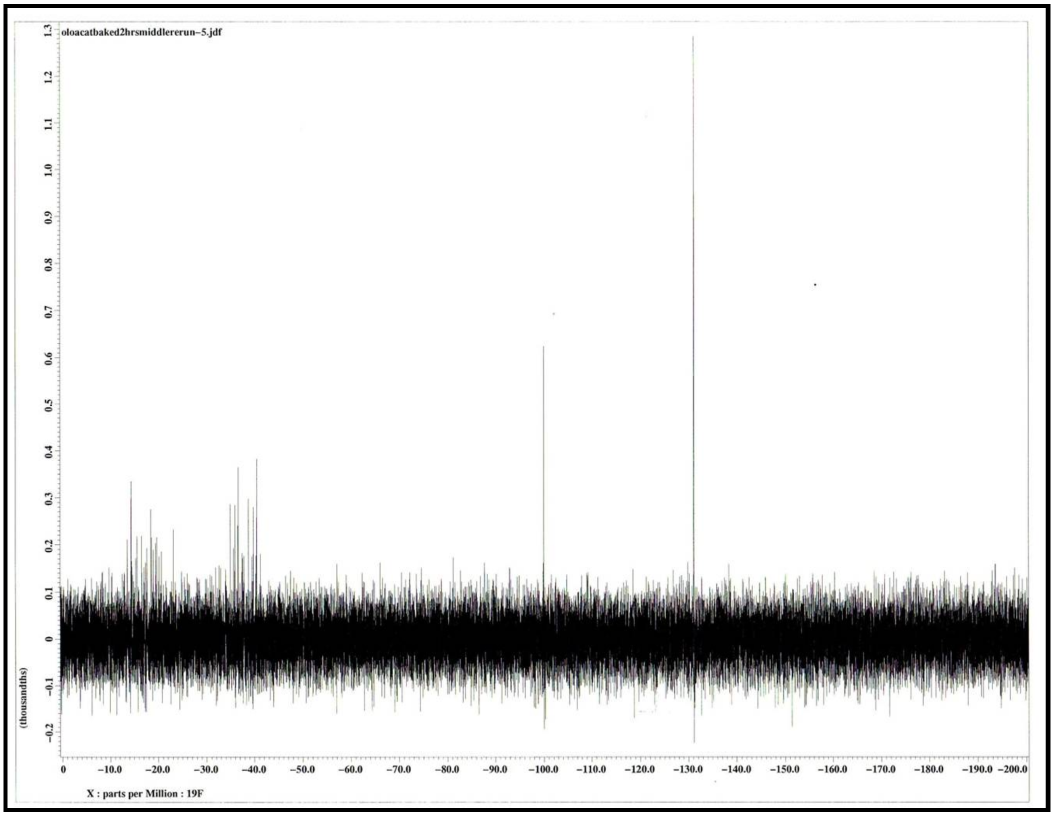

Figure 6.28 Fluorine NMR of ZDDP- FeF_3 baked at 150C for 2 hours in nitrogen

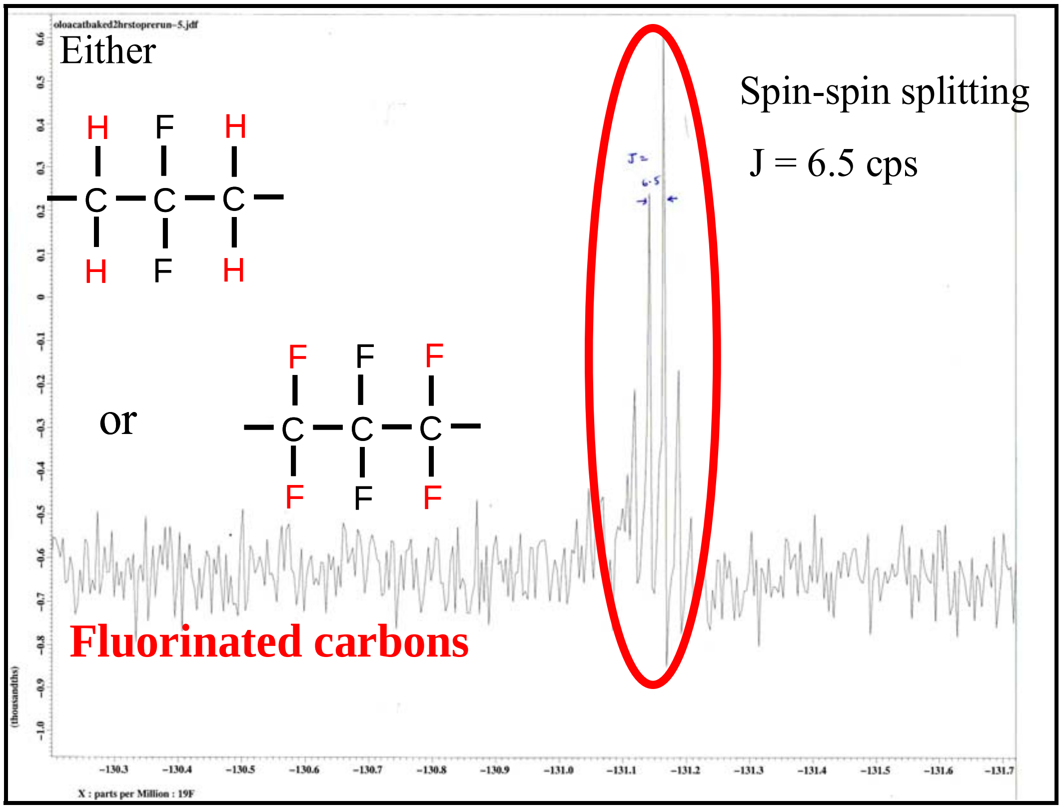

Figure 6.29 A closer view of peak at 130ppm in fluorine NMR of ZDDP- FeF_3 baked at 150C for 2 hours in nitrogen

From literature value for the chemical shifts ~ -130ppm, the best match seems to be as seen from table 6.13.

6.2.1.4 Elucidation of type of compounds with ZDD-FeF$_3$ baked for 2 hours/150C/nitrogen

Table 6.13 Chemical shifts for C-F compounds

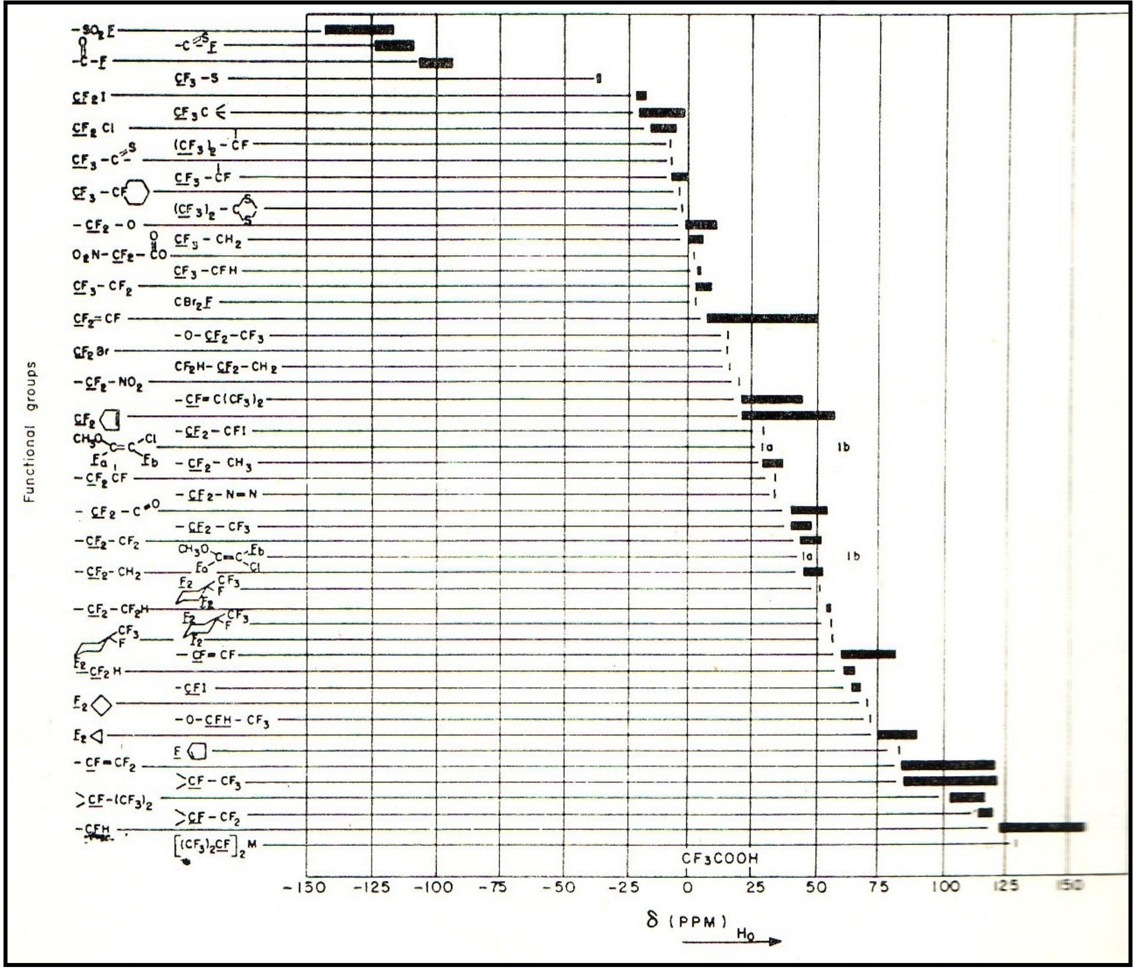

The best fit seems to be >CF-CF$_2$ (125- 150ppm) and [(CF$_3$)$_2$CF]$_2$M ~ 130 ppm. The presence of >CF-CF$_2$ or CF$_2$-CF$_2$-CF$_2$ functional groups is supported by the presence of 5 splits as expected by n+ 1 rule. The adjacent fluorine’s (or hydrogen’s) split the central fluorine being perturbed into 4+1 = 5 peaks or 5+1 =6 peaks.

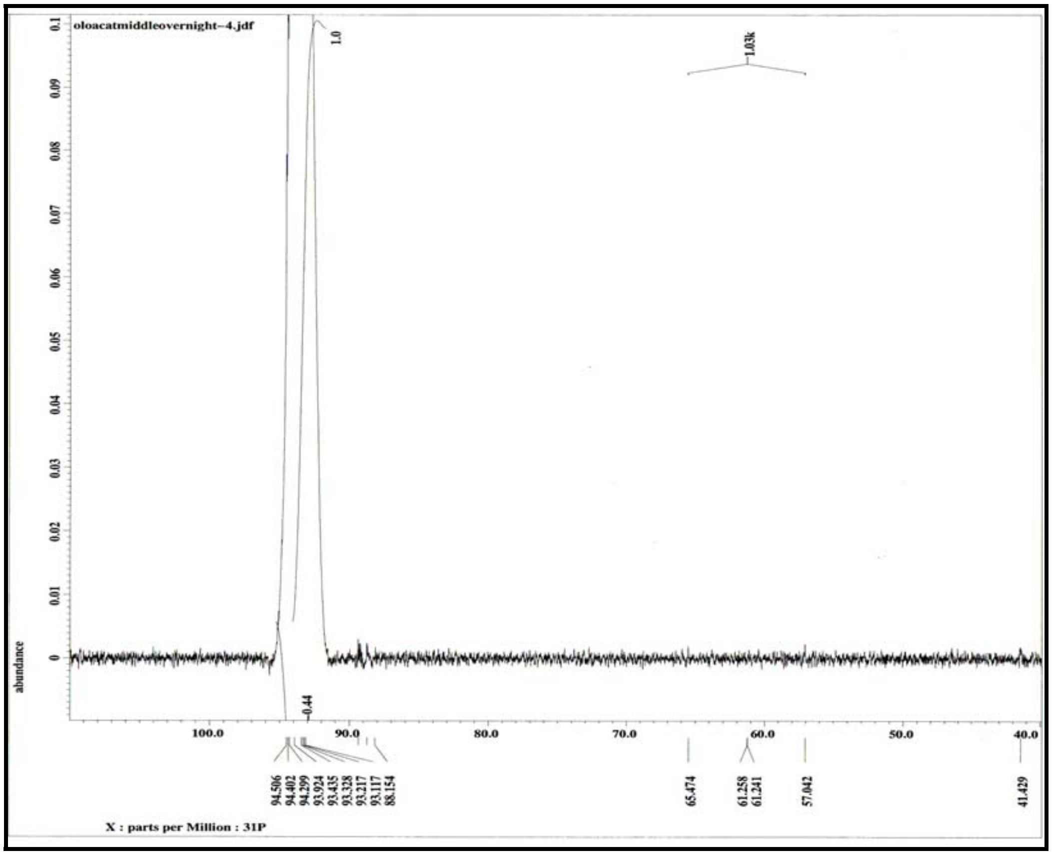

Figure 6.30 Phosphorus NMR of ZDDP- FeF_3 baked at 150C for 2 hours in nitrogen (decoupled with fluorine)

The presence of >CF-CF_2 or CF_2-CF_2-CF_2 functional groups is supported by the presence of 5 splits as expected by n+ 1 rule. The adjacent fluorine's (or hydrogen's) split the central fluorine being perturbed into 4+1 = 5 peaks or 5+1 =6 peaks. This inference has huge implications. The interaction of ZDDP along with FeF_3 results in the formation of fluorinated carbons when heated for long times. It's highly possible the compounds at 89 ppm in phosphorus NMR of the same could be associated with the peak at -14 ppm (that remains unidentified yet) and / or -130 ppm. An attempt to decouple phosphorus with fluorine to give more insight regarding the association of suspected peaks was not successful fig 6.30.

For the ^{31}P NMR spectrum corresponding to figures 6.25, the chemical shifts corresponding to the peaks have been listed in the Table 6.14 and correlated to possible compounds.

An important point to note is that CF-CF_2's were found to form with ZDDP-FeF_3 (unbaked) on the surface during tribological conditions. These were characterized through XPS studies and have been patented. So the thermal degradation study product could be closely correlated to product formed on the surface.

Table 6.14 Phosphorus NMR interpretations from chemical shifts for ZDDP- FeF_3 baked at 150C for 2 hours in nitrogen

Observed chemical shift (ppm)	Possible Products	(Literature peak values)
93.163-93.867	Neutral ZDDP	(93-94)
89.168	New Fluorinated phosphorus compound (No P-F) & Fluorinated Carbons	
77.405	Impurity	
56.469-65.734 (splitting, J=1080)	Original Fluorinated phosphorus compounds (P-F direct bonding)	
41.242	$(RO)_2P(S)O^-$ >P(O)SP(O)<	(37-55), (38-42)
26.742	$(RO)_2PO(SR)$ >P(O)SH	(23-35) (21-30)
17.779	$OPH_2(OR)$ $OPR'(OR)_2$	(51.6-19) (14-31)

6.2.2 Fourier Transform Infrared Spectroscopy

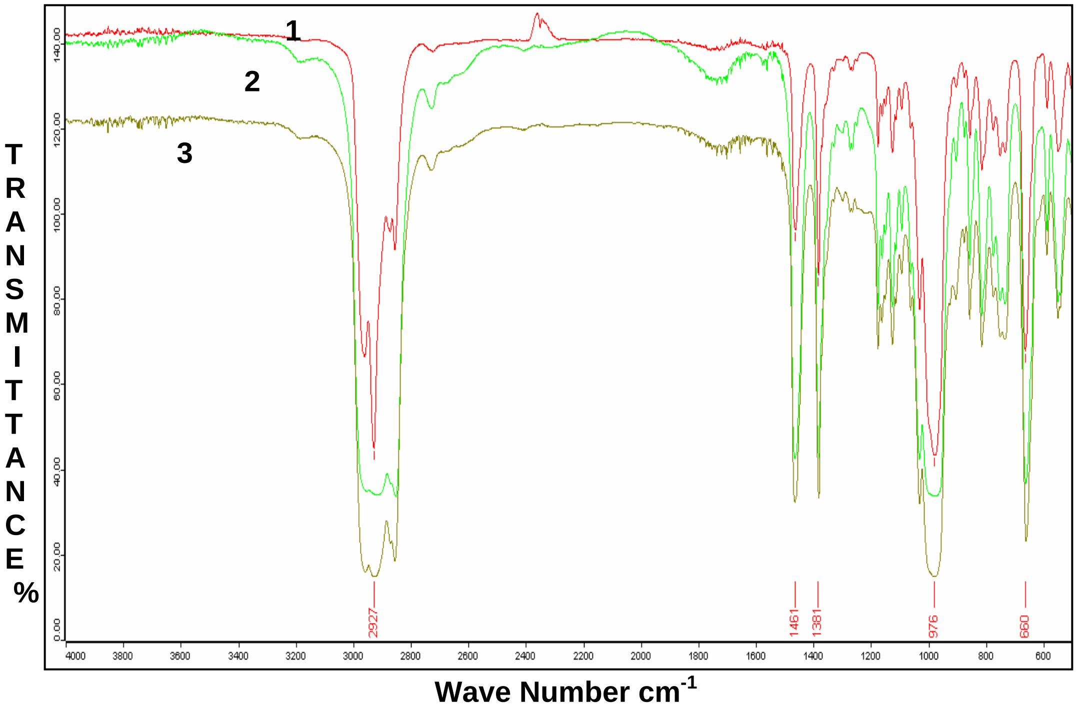

50% ZDDP unbaked	-1
50% ZDDP baked 2hours/150c/N_2	-2
50% ZDDP-FeF_3 baked 2hours/150c/N_2	-3

Figure 6.31 An FT-IR spectrum of ZDDP - FeF_3 baked at 150C for 2 hours in nitrogen (4000-500 cm^{-1})

Most of the peaks associated with phosphorus lie in the fingerprint region which is not clear in fig 6.31. Thus the region 1600-500 cm^{-1} has been zoomed in the figure 6.32.

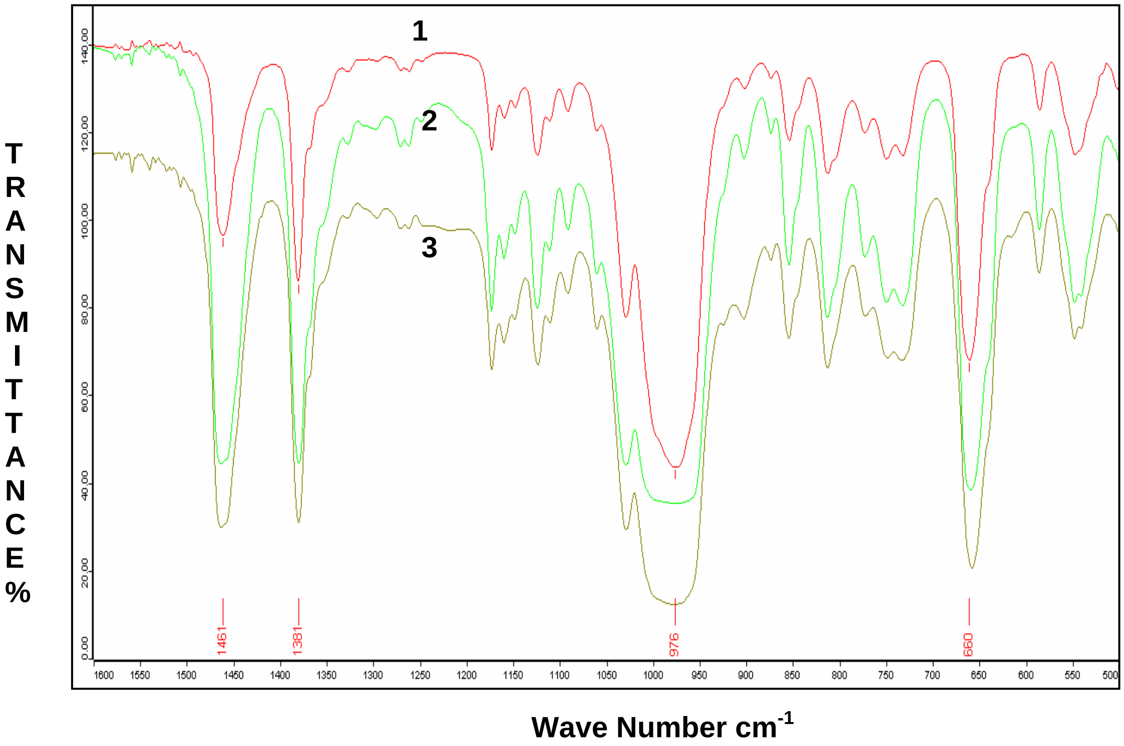

50% ZDDP unbaked -1
50% ZDDP baked 2hours/150c/N_2 -2
50% ZDDP-FeF_3 baked 2hours/150c/N_2 -3

Figure 6.32 An FT-IR spectrum of ZDDP - FeF_3 baked at 150C for 2 hours in nitrogen (1600-500 cm^{-1})

Upon comparison of the above figure 6.31 & 6.32 with figure 6.20 and 6.21 where ZDDP was baked with FeF_3 for 20 min, it's seen no significant changes are reflected in FT-IR spectrum for the same reasons discussed in section 6.1.4. The peaks remain unchanged and can be identified with table 6.9, 6.10, 6.11.

6.3 Effect of air on ZDDP-FeF_3 interaction- oxidative degradation

The findings of new fluorinated phosphorus compounds formed in presence of FeF_3, were all in nitrogen condition. Since ZDDP is known to have antioxidant properties [59, 61] that become equally dominant in presence of oxygen, it was necessary to determine whether the same reactions and compounds form in presence of air or oxygen.

Results pertain to the samples 'a' and 'b' as before (a) 50 wt% of ZDDP in mineral oil baked in a nitrogen environment (as described in section 4) for 20 min and (b) ZDDP (50wt %): FeF_3 (1:0.4) in mineral oil baked in a nitrogen environment for 20 min. Results include

- Phosphorus and fluorine NMR spectrums
- Elemental analysis (Phosphorus, Sulfur, Iron, Zinc, Fluorine)
- Wear performance

6.3.1 Nuclear Magnetic Resonance Spectroscopy

6.3.1.1 Phosphorus NMR – ZDDP baked 20min/150C/air

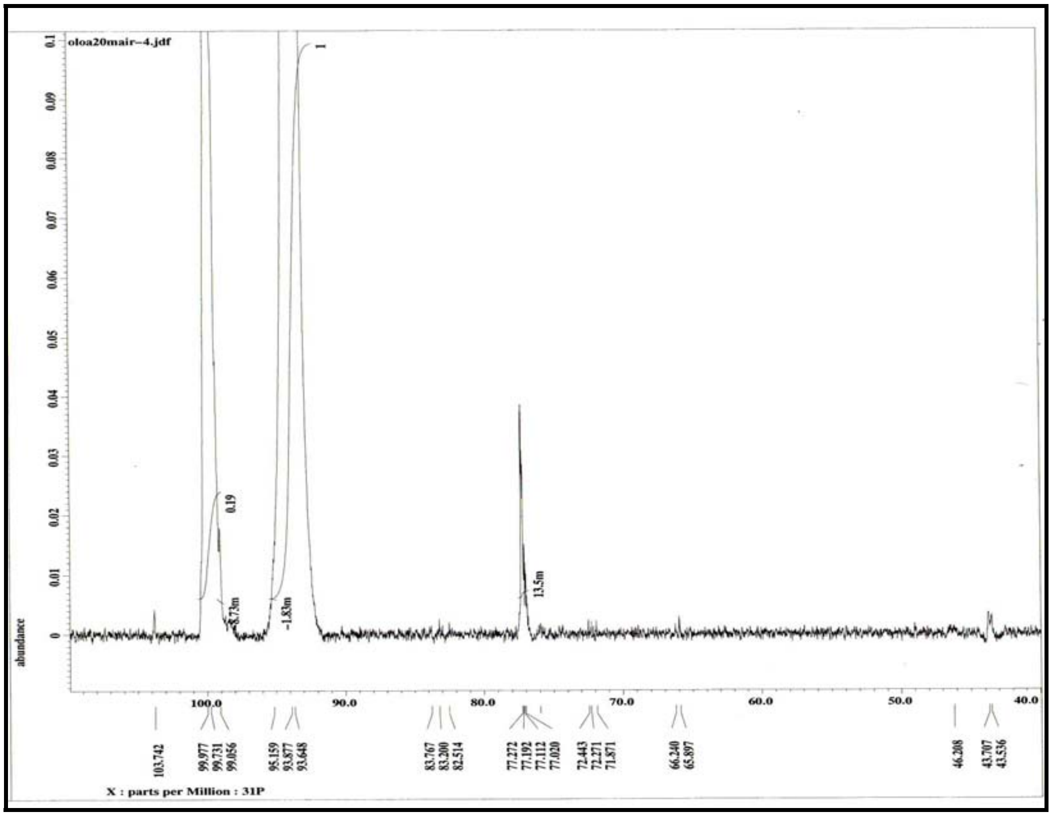

Figure 6.33 Phosphorus NMR of ZDDP baked at 150C for 20 min in air

In Figure 6.33 the new products formed have been attributed to possible compounds tabulated in table 6.15. The impurity peak remains unaffected even in presence of air.

Table 6.15 Phosphorus NMR interpretations from chemical shifts for ZDDP baked at 150C for 20 min in air

S.No	Observed Chemical Shift ppm	Literature values ppm
93.648-95.159	Neutral ZDDP	(93-94)
99.056-99.977	Basic ZDDP	(99-100)
103.742	$(RO)_2P(S)(SR)$ possibility of cage intermediate during interconversion of basic and neutral ZDDP (section	100 103
82.514-83.767	$\{S_2P(OR)_2\}^-H^+$ $(RO)_2PS-Sn-PS(RO)_2$	(1°,86; 2°, 82.4) (78.4-83.4)
77.02-77.272	Impurity	
71.871-72.443	$(RS)_3PO$	(55-65)
65.897-66.24	$(RS)_3PO$	(55-65)
46.208	$(RO)_2P(S)O^-$ $R_3P(O)$, $R>CH_3$	85-93 90,86-85
43	$>P(O)SP(O)<$; $(RS)_2P(O)(OR)$	(38-42) (44)

6.3.1.2 Phosphorus NMR – ZDDP-FeF_3 baked 20min/150C/air

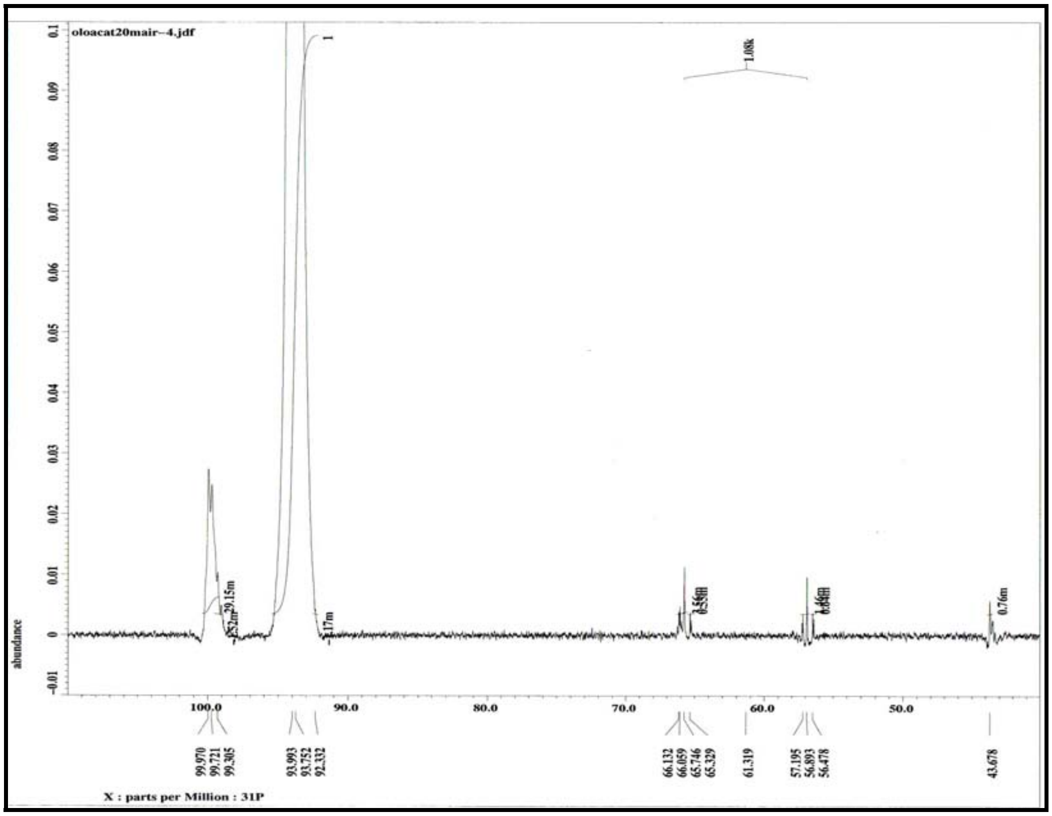

Figure 6.34 Phosphorus NMR of ZDDP - FeF_3 baked at 150 C for 20 min in air

Figure 6.34 shows the formation of FPC even in air environment, signifying the aggressive nature of these compounds. This has an important bearing in that in case of oxidative environments where unfortunately the antiwear property of ZDDP may be reduced due to its antioxidant action, the formation of these compounds can assure antiwear behavior of ZDDP being conserved. The spectrum looks more 'clean' as compared to ZDDP baked for the same time i.e only compounds like FPC unlike several tiny decomposition products in case of baked ZDDP. Moreover the impurity nearly disappears. Products associated with peak at ~46ppm in fig 6.33 for baked ZDDP do not appear here.

Table 6.16 Phosphorus NMR interpretation from chemical shifts for ZDDP - FeF$_3$ baked at 150C for 20min in air

Observed Chemical shift (ppm)	Possible Products	(Literature peak values)
93.730	Neutral ZDDP	(93-94)
99.925	Basic ZDDP	(99-100)
56.9- 65.8 F (splitting, J=1080)	Original Fluorinated phosphorus compounds , (P-F direct bonding)	
42.554	>P(O)SP(O)< (RS)$_2$P(O)(OR)	(38-42) (44)

The intensity of basic ZDDP drops significantly as compared to ZDDP baked alone. A closer look at the twin sets of peaks or FPC upon comparison with those formed in nitrogen environment fig 6.5 reveal that they are identical as observed in fig 6.35

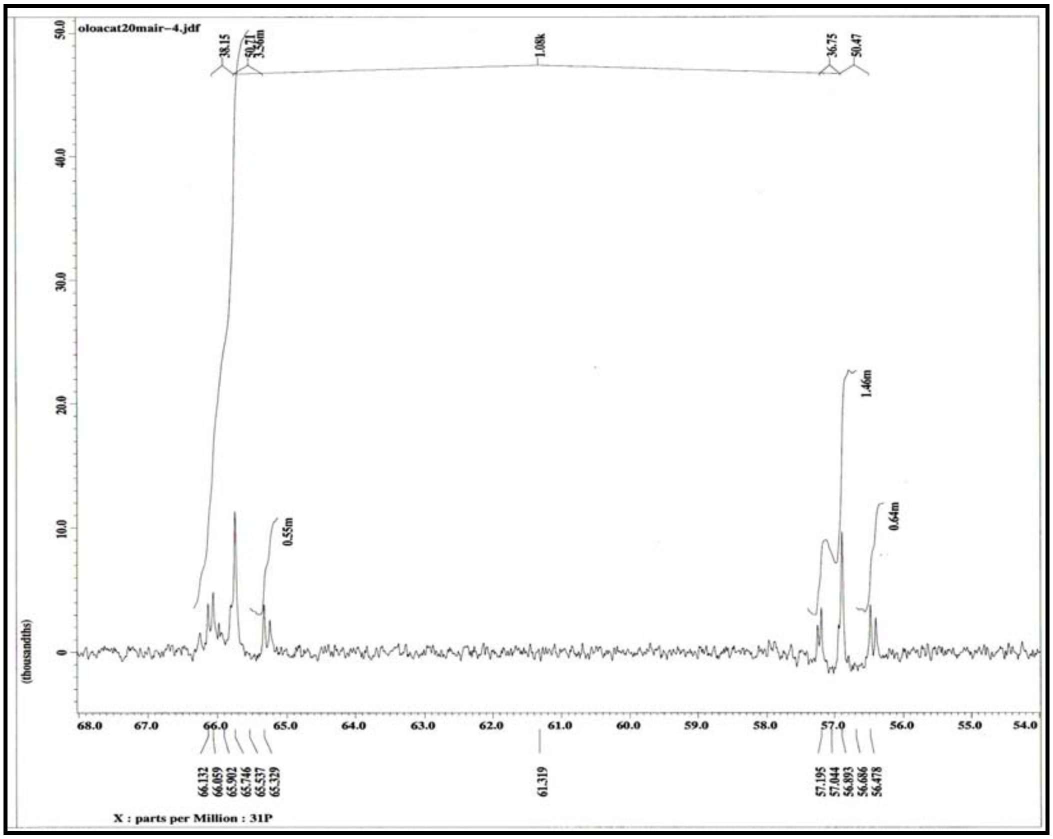

Figure 6.35 A closer view of fluorinated phosphorus compound in phosphorus NMR of ZDDP - FeF_3 baked at 150 C for 20 min in air

A rough estimation of the concentration of compounds can be made from the qualitative NMR spectral intensities for both air (fig 6.33 and 6.34) and nitrogen environments (fig 6.1, 6.2, 6.3), table 6.17. The intensity of the starting parent basic ZDDP was 0.32. The rate of decomposition of ZDDP is reflected in the amount of Basic ZDDP depleted. Upon identical treatments in air and nitrogen and with same amounts of sample used in NMR it's found that the decomposition of ZDDP with and without FeF_3 is accelerated in air. The decomposition is also accelerated in presence of FeF_3 in

N_2. Thus in a condition with both air and FeF_3 simultaneously applied the decomposition of ZDDP is observed to be the fastest.

Table 6.17 Comparison of intensities of basic ZDDP in qualitative NMR spectra obtained for formulations baked at 150C for 20 min in air and nitrogen.

ZDDP Starting material : ~0.32		
Samples	20 min /Nitrogen	20 min/Air
ZDDP Baked	~0.32	0.19
ZDDP-FeF_3	0.14	0.0296

6.3.2 Elemental analysis

From table 6.18 it is observed that zinc levels do not change much in the baked samples and are within experimental error as compared to that of original starting material ZDDP. However the presence of more sulfur is not clear.

Table 6.18 Elemental analysis for unbaked ZDDP, ZDDP and ZDDP-FeF_3 baked at 150C for 20 min in air

S. No	Elements	ZDDP untreated ppm	ZDDP baked 150C/air ppm	ZDDP-FeF_3 baked 150C/air ppm
1	Phosphorus	1000	1000	1000
2	Sulfur	1192	1455	1450
3	Zinc	1087	960	960
4	Iron	0	3	4
5	Fluorine	0	0	~100

6.3.3 Wear performance

Wear performance in terms of wear volume was obtained for the formulations of (a) ZDDP unbaked (b) ZDDP-FeF_3 baked in air at150C for 20min and (c) ZDDP-FeF_3 baked in Nitrogen at 150C for 20 min by the procedure listed in chapter 4 with few modifications in that the test duration was 15000 cycles and base oil used as break in at 24Kg applied load.

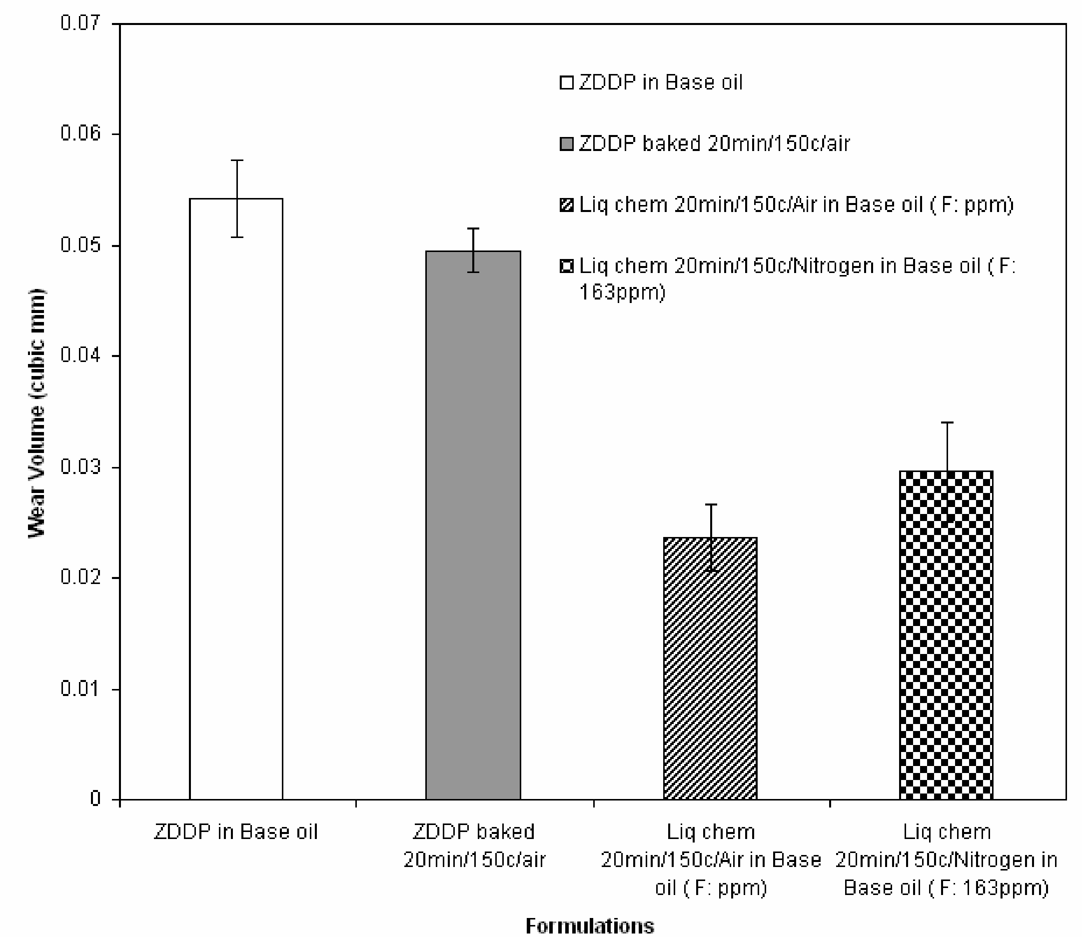

Figure 6.36 Wear volume of formulations at 0.1wt% phosphorus in base stock baked at 150C for 20 min in air tested at 24Kg load 25000 cycles and 700 rpm compared to formulation baked in nitrogen under identical conditions

ZDDP baked in Nitrogen at 150C for 20 min showed a significant improvement in wear performance compared to parent ZDDP (starting material) from fig 6.8. However ZDDP baked in air under identical conditions does not show much improvement within experimental errors in comparison with the baseline fig 6.36. Probably this is due to the fact that the antiwear property of ZDDP suffers greatly once its antioxidant properties are called upon. There is an agreement that when ZDDPs act in their antioxidant/peroxide decomposing role, the species that they form are no longer able to produce effective zinc phosphate antiwear films [3]. With this in mind ZDDP baked in air may not be able to perform as good as ZDDP baked in Nitrogen. However in presence of FeF_3 the scenario is different. There's a dramatic improvement (50-55%) in performance of ZDDP- FeF_3 baked in air over ZDDP baked in air and baseline. The only significant difference between them is the formation of FPC. This can lead us to believe that FPC renders a superior performance to ZDDP even in presence of air.

The performance of ZDDP- FeF_3 in air is slightly better than the same in Nitrogen although the latter has a higher fluorine level of 163ppm as compared to former where it is <100ppm. Probably this can be associated to the products at ~ 82-83 ppm that have a huge signal intensity in case of ZDDP- FeF_3 baked in nitrogen (fig 6.3), however they are absent when the two components are baked in air (fig 6.34). The performance of ZDDP- FeF_3 baked in nitrogen is still better than baked ZDDP although the latter do not contain these products (~82,83ppm). This can be justified by the fact that the presence of FPC compensates for the deleterious effect associated with the phosphorus decomposition products at ~82, 83ppm.

6.4 Optimization of fluorine

Once new chemical species formed in presence of FeF_3 were established in degradation process of ZDDP, optimization of fluorine level with good antiwear performance was desired. The study was carried out at a temperature preferred by industry (~80C) and varying times in two different conditions air and nitrogen. To obtain fluorine content with good wear performance at economically feasible temperatures and times would be the optimum amount of fluorine desired. Results pertain to the samples 'a' to 'f' obtained by procedure listed in chapter 4.

(a) ZDDP (50wt %): FeF_3 (1:0.4) in mineral oil baked in nitrogen environment for 3 hours.

(b) ZDDP (50wt %): FeF_3 (1:0.4) in mineral oil baked in nitrogen environment for 6 hours.

(c) ZDDP (50wt %): FeF_3 (1:0.4) in mineral oil baked in air for 1 hour.

(d) ZDDP (50wt %): FeF_3 (1:0.4) in mineral oil baked in air for 3 hours.

(e) ZDDP (50wt %): FeF_3 (1:0.4) in mineral oil baked in air for 7 hours.

(g) ZDDP (50wt %): FeF_3 (1:0.4) in mineral oil at room temperature for 1 month.

Results include

- Elemental analysis (Phosphorus, Sulfur, Iron, Zinc, Fluorine)
- Wear performance

6.4.1 Elemental analysis

Elemental Analysis included levels of zinc, iron and fluorine for 1000 ppm of phosphorus in the decant of samples.

Table 6.19 Elemental analysis of ZDDP-FeF_3 baked at 80C for different times in air and nitrogen during optimization process of fluorine

Temperature 80C (unless specified)	Phosphorus (ppm)	Fluorine (ppm)	Zinc (ppm)	Iron (ppm)
Room Temperature	1000	<100	1142	5
3 hr/Nitrogen	1000	<100	1130	3
6 hr/ Nitrogen	1000	102	1115	4
1hr/Air	1000	81	1087	2
3 hr/Air	1000	137	106	2
7hr/ Air	1000	96	1075	2

It can be seen that the levels of fluorine obtained under nitrogen conditions increased slowly with time from < 100 ppm at 3hrs to 102 ppm at 6hour. However for samples treated similarly in air, fluorine levels increased from 81 ppm at 1hr to 137 ppm at ~ 3hrs and then steadily declined when heated for longer periods of time for 7 hour. This trend was reproduced when the experiments were repeated.

6.4.2 Wear performance

Wear performance in terms of wear volume was obtained for the formulations by the procedure listed in chapter 4 with few modifications in that the test duration was 15000 cycles and base oil was used as break in at 24kg.

(a) ZDDP (50wt %): FeF_3 (1:0.4) in mineral oil baked in Nitrogen environment at 80c for 6 hours (Phosphorus -1000 ppm; Fluorine ~102 ppm)

(b) ZDDP (50wt %): FeF_3 (1:0.4) in mineral oil baked in air at 80c for 7 hours (Phosphorus -1000 ppm; Fluorine ~ 96 ppm)

(c) ZDDP (50wt %): FeF_3 (1:0.4) in mineral oil baked in air at 80c for 3 hours (Phosphorus -1000 ppm; Fluorine ~137 ppm).

All of these formulations have been compared to the wear performance of unbaked ZDDP in mineral oil at 0.1wt%Phosphorus serving as the baseline. The idea was to compare two formulations (a) and (b) with nearly equal fluorine level but different environmental conditions of nitrogen and air. A comparison could be drawn similarly between same environments (b) and (c) but different fluorine levels.

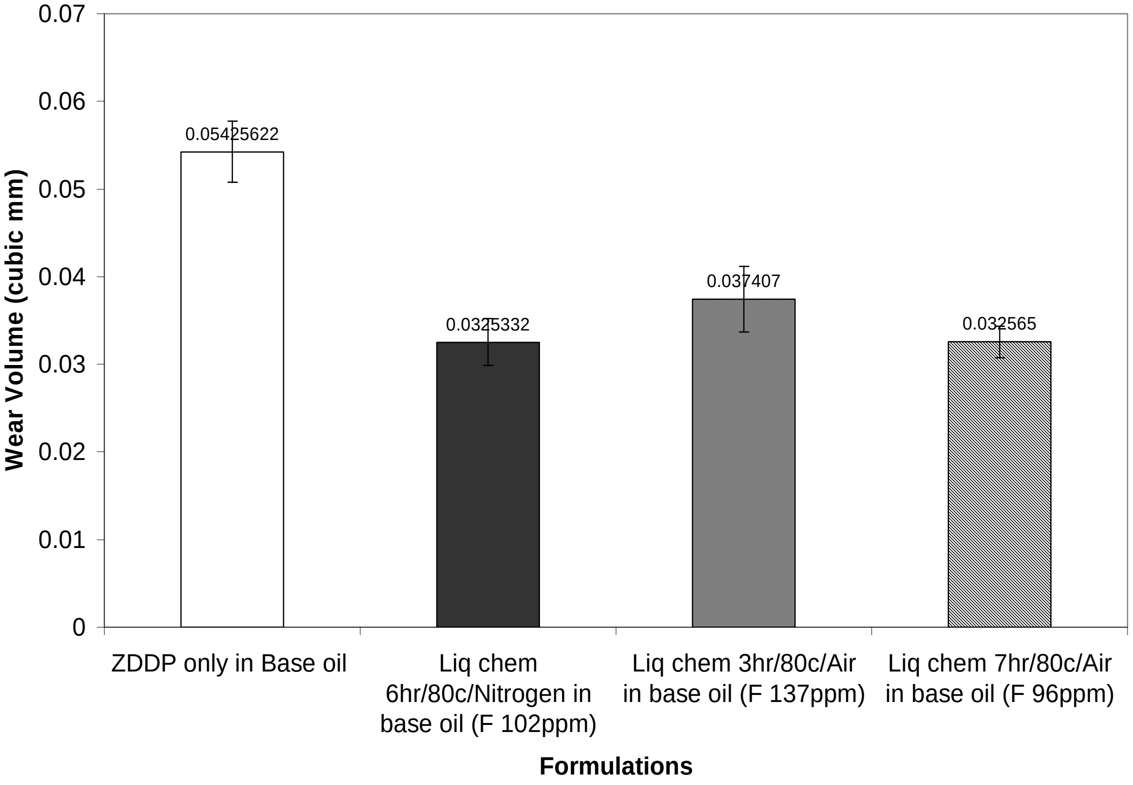

Figure 6.37 Wear volumes of formulations at 0.1wt%P in base stock in the optimization of fluorine process compared to unbaked ZDDP as the baseline

From the wear performance data in the figure 6.37 it can be seen that samples baked for 6 hours in nitrogen and 7 hours in air perform equally. Thus it can be inferred that environment does play a significant role. There was not any improvement in performance for 3 hour sample rather there was a little increase in wear as compared to 6 hour or 7 hours. However the increase in wear volume is within experimental errors and may be regarded to perform nearly equally.

Thus the optimized conditions stand as baking ZDDP (50%) with FeF_3 *at 1:0.4 at 80C for 6 hours in Nitrogen and at least 3 hours in air to give 100 ppm of fluorinated ZDDP resulting in at least 40% improvement in wear performance. .*

6.5 Various conditions for formation of FPC

Different possible conditions have been established that are favorable for the formation of fluorinated phosphorus compounds (FPC). Formation of FPC was assessed by phosphorus NMR. The different conditions include

a. Different temperatures - Room temperature (6months), 150C (20min, nitrogen), 80C (nitrogen & air) and 70C (1hour, air). FPC were found to form under various conditions of temperature and time included below

- ZDDP (50%): FeF_3 (1: 0.4) at room temperature for 6 months, fig 6.38
- ZDDP(50%):FeF_3 (1: 0.4) 150C/20min/nitrogen, fig 6.3
- ZDDP(50%):FeF_3 (1: 0.4) 80C/varying times/air, table 6.19
- ZDDP(50%):FeF_3 (1: 0.4) 70C/1 hour/air, 6.40

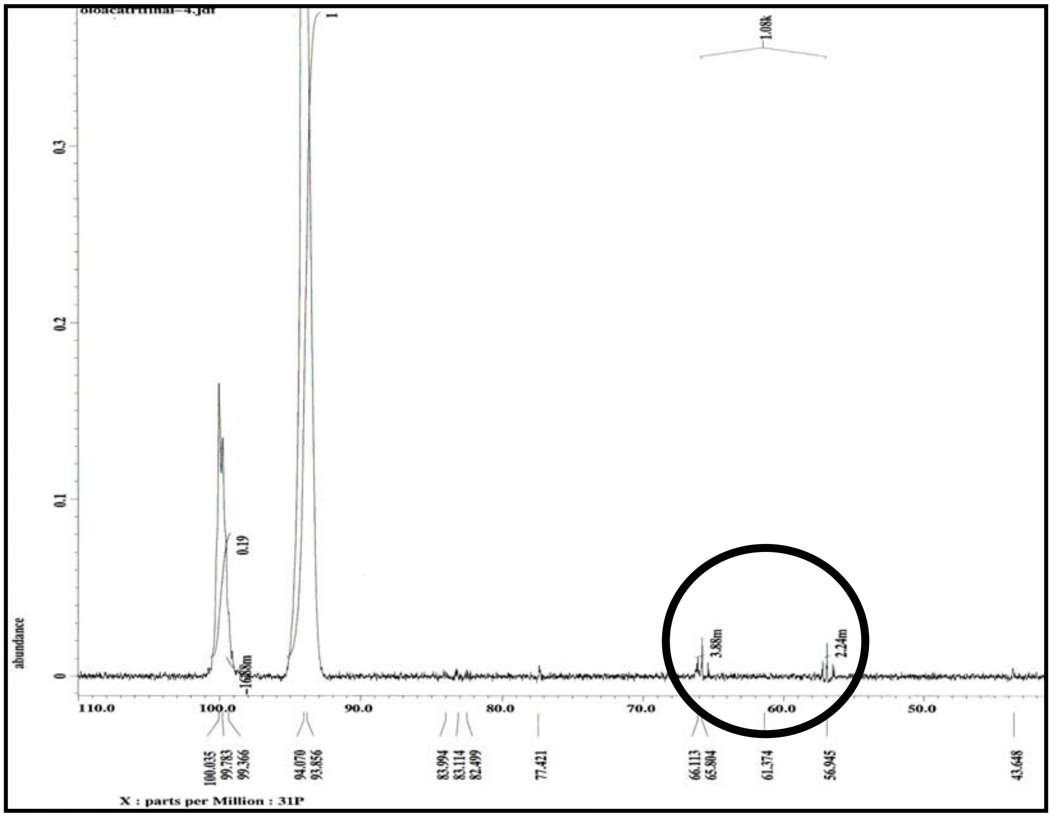

Figure 6.38 Phosphorus NMR of ZDDP - FeF_3 (1:0.4) stored at room temperature for 6 months (versatility of conditions for formation of fluorinated phosphorus compounds)

b. <u>A different ZDDP: FeF_3 ratio (1:0.2) with FeF_3 at lower concentration</u>

In all previous experiments the ZDDP: FeF_3 was 1:0.4. It was interesting to determine whether such species are also formed with a lower concentration of FeF_3. Thus a ZDDP: FeF_3 ratio (1:0.2) was selected and the mixture was baked at 150C for 20min in Nitrogen. The ^{31}P NMR for the sample decant shows the formation of FPC under these conditions.

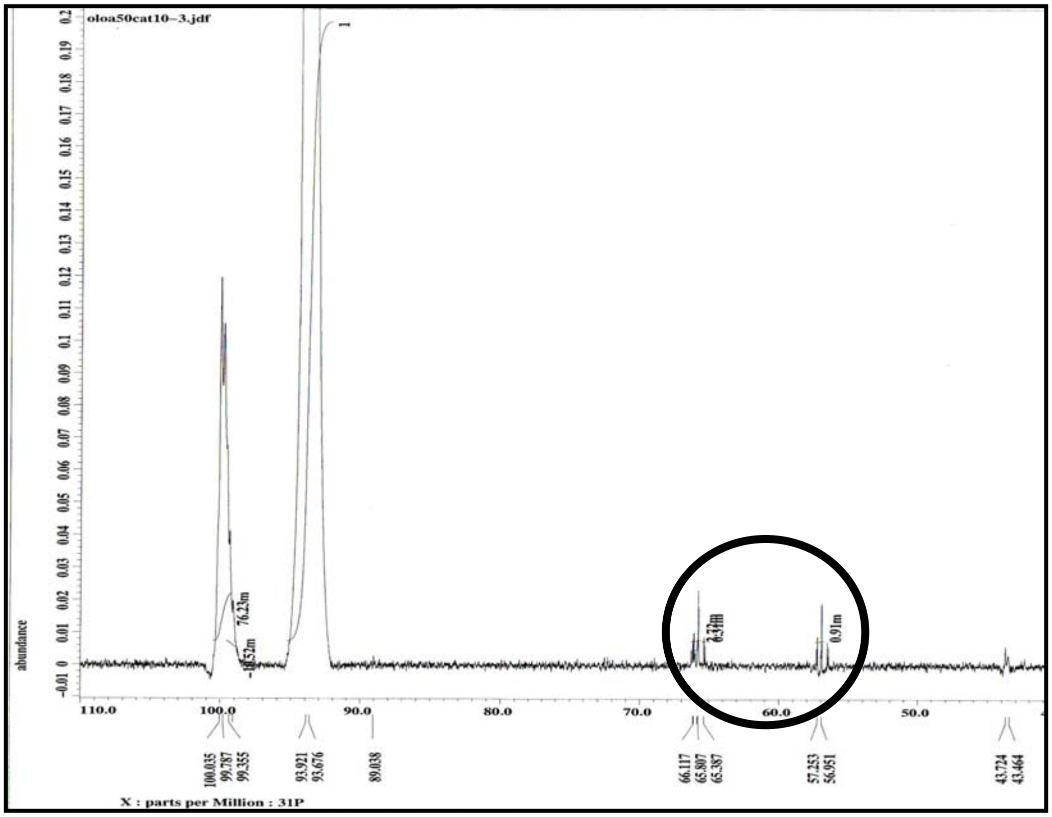

Figure 6.39 Phosphorus NMR of ZDDP - FeF_3 (1:0.2) at lower concentration of FeF_3 baked at 150C for 20 min in nitrogen (versatility of conditions for formation of fluorinated phosphorus compounds)

c. Different type of ZDDP

The type of ZDDP employed in all previous cases was obtained from Chevron (chapter 4). It was a secondary type and was a mixture of basic and neutral ZDDP. Since the reactivity of ZDDP is associated with the type of alkyl groups present in the structure (table 2.5). It was interesting to determine whether ZDDP obtained from a different company consisting of a mixture of primary, secondary, basic and neutral forms also formed FPC. Fluorine NMR of ZDDP baked with FeF_3 (1:0.4) for 70C at 1 hour is shown in fig 6.40. Due to difficulties in exporting the huge file and even printing, picture of the spectrum was obtained using a digital camera.

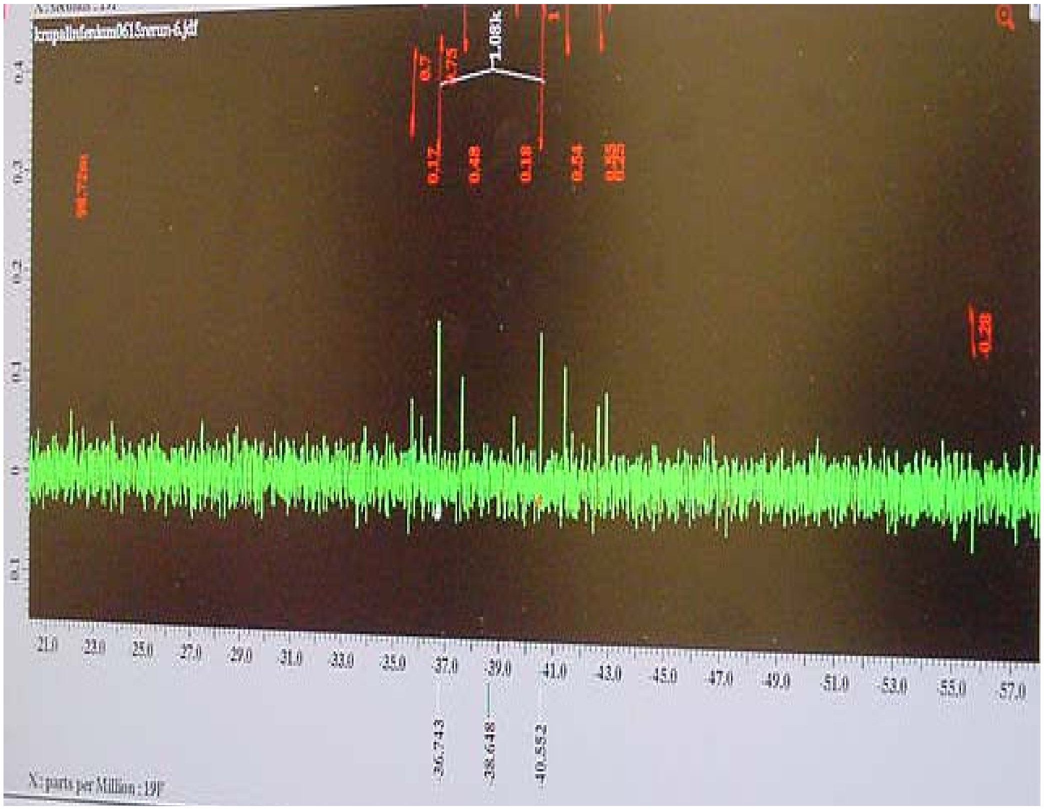

Figure 6.40 Fluorine NMR of a different type of ZDDP (mixture of primary and secondary) baked with FeF_3 (1:0.4) at 70C for 1 hour in air (versatility of conditions for formation of fluorinated phosphorus compounds)

d. Different conditions – nitrogen and air employed

FPC are also found to form when ZDDP is baked with FeF_3 in different environments of Nitrogen or air. This can be found in fig 6.3, 6.36, 6.37. Formation of compounds under different possible conditions lends a versatility of choice in terms of reaction temperature-time, concentrations and type of starting materials that can be used for the production of these compounds.

CHAPTER 7

CONCLUSION

1. New fluorinated phosphorus compounds (FPC) are formed in the early stages ('early intermediates') of the reaction between ZDDP and FeF_3. This conclusion was reached using ^{31}P NMR (decoupled with ^{1}H), ^{19}F NMR and verified by ^{31}P NMR (decoupled with ^{19}F), and fluorine, phosphorus, iron elemental analysis that confirmed the presence of fluorine with phosphorus, sulfur, zinc but no iron in the 'decant' of baked ZDDP- $FeF_{3.}$
2. The 'end products' or 'later intermediates' consist of protective fluorocarbon compounds formed at later stages as a result of direct/indirect reaction between ZDDP and $FeF_{3.}$ This was concluded using ^{31}P NMR and ^{19}F NMR.
3. The strong signal intensity of FPC in NMR spectrum after 20 min baking at 150 C is found to significantly drop after 2 hours of baking at 150 C. At this stage the intensity of fluorocarbons appears and is very intense. It is possible that FPC's serve as precursors for the fluorocarbons, however this was not verified.
4. The wear performance of ZDDP- FeF_3 samples baked for 20 min in Nitrogen at 150 C showed ~ 50% enhancement in performance compared to original ZDDP (unbaked) 0.1wt% P as the baseline. This formulation was found to be superior to original ZDDP, ZDDP-FeF_3 (unbaked) and ZDDP baked in terms of wear performance.

5. The wear performance of ZDDP- FeF_3 samples baked for 20 min in Nitrogen and air at 150 C was consistently better than ZDDP baked under identical conditions by ~ 25 to 30 % in nitrogen and 50% in air. This proves that the improvement in performance is due to the FPC's formed in ZDDP- FeF_3 baked system.
6. Thus it can be said that the early intermediates, FPC provide an early protection to wear during boundary lubrication conditions.
7. The wear performance of <u>baked</u> ZDDP-FeF_3 20 min/150 C/nitrogen was also better compared to <u>unbaked</u> ZDDP- FeF_3. Improved performance is likely to be provided by FPC's from the start of boundary lubrication conditions.
8. The FPC's are found to form even in presence of air when ZDDP's antioxidant property comes into action. This indicates that the formation of these compounds is not suppressed when baked in air.
9. During the optimization of reaction conditions for FPC with antiwear performance at 80 C, it was found that ~100 ppm of fluorine corresponding to baking for ~ 6 hours in Nitrogen or at least 3 hours in air gave good wear performance with an improvement of 40% as compared to original ZDDP at 0.1 wt% phosphorus.
10. In the optimization process the concentration of FPC increased at a fast rate from 1 hr to 3 hours at 80 C in air and then declined from 3 hours to 7 hours.
11. The formation of FPC compounds was found to occur under a wide range of conditions. This lends versatility in choice of reaction conditions like temperature-time, concentration of FeF_3, and type of ZDDP and FeF_3 employed.

12. The formation of FPC seems to follow a 2 stage process where complexation with ZDDP constitutes the first step. This was found to be a governing step. Experiments in which the complexation did not presumably occur (like small surface area, continuous vigorous shaking etc), FPC were not formed even upon baking. Thus the complexed species seem to involve Vanderwaals forces (dipole-dipole type) that are sensitive to temperature, agitation etc.
13. The complexation was again found to be highly dependent on the surface area available for the reaction. It appears that the reaction occurred at the interface of ZDDP-oil soluble material and precipitated FeF_3.
14. The ZDDP-FeF_3 baked formulation containing FPC is ‘a decant’ and this solution was observed to be stable for more than a year with no signs of any precipitation. Thus, the knowledge of mechanism studies led to the development of a liquid chemistry that was successful in solving the dispersion/shelf problems along with great antiwear performance over the current ZDDP (at 0.1wt% phosphorus).

CHAPTER 8

FUTURE WORK

The following things were considered out of scope of this research work because of time constraints. However they need to be addressed as separate projects later. The research work addressed in this thesis will serve as a platform for these projects. Altogether it would constitute a significant advancement in the area of high performance engine oils.

1. Effect of different commercial engine oil additives on Zddp-FeF_3 interaction need to be thoroughly studied.

Engine oil contain several additives added to oil. All of these additives are active chemicals designed for specific functions in a given application. Problems arise when all of these potent chemicals come in contact with each other. Antagonistic interactions are least desired. Compatibility problems can be addressed once the root cause is known. A complete knowledge of the effect and interactions of each additive with the ZDDP-FeF_3 system is necessary. This research has unveiled the interactions between ZDDP and FeF_3 system. It will be useful for addressing the 3 component interactions and will become an integral part of the same.

2. Tribo-film studies need to be addressed

The research addressed chemical interactions between ZDDP and FeF_3 completely from a thermal degradation point of view. This needs to be balanced by studies on tribo films formed on surface by surface characterization techniques in Zddp-FeF_3 system and different additives.

3. The valuable precipitates resulting from thermal degradation studies that could not be analyzed using NMR need to be addressed.

In the present research work, focus was more on soluble degradation products that could be analyzed by NMR. It is clear that FPC are formed upon reaction of ZDDP and FeF3. Other products of this reaction need to be identified in the precipitate. This will help complete the jigsaw puzzle.

APPENDIX A

FUNCTIONS OF DIFFERENT ADDITIVES USED IN ENGINE OILS

(Lubrizol corporation Limited
http://www.lubrizol.com/LubeTheory/theory.asp)

Additive Type	Purpose	Typical Compounds	Functions
Antiwear and EP Agent	Reduce friction and wear and prevent scoring and seizure	Zinc dithiophosphates, organic phosphates, acid phosphates, organic sulfur and chlorine compounds, sulfurized fats, sulfides and disulfides	Chemical reaction with metal surface to form a film with lower shear strength than the metal, thereby preventing metal-to-metal contact
Corrosion and Rust Inhibitor	Prevent corrosion and rusting of metal parts in contact with the lubricant	Zinc dithiophosphates, metal phenolates, basic metal sulfonates, fatty acids and amines	Preferential adsorption of polar constituent on metal surface to provide protective film, or neutralize corrosive acids
Detergent	Keep surfaces free of deposits	Metallo-organic compounds of sodium, calcium and magnesium phenolates, phosphonates and sulfonates	Chemical reaction with sludge and varnish precursors to neutralize them and keep them soluble
Dispersant	Keep insoluble contaminants dispersed in the lubricant	Alkylsuccinimides, alkylsuccinic esters, and mannich reaction products	Contaminants are bonded by polar attraction to dispersant molecules, prevented from agglomerating and kept in suspension due to solubility of dispersant
Antioxidant	Retard oxidative decomposition	Zinc dithiophosphates, hindered phenols, aromatic amines, sulfurized phenols	Decompose peroxides and terminate free-radical reactions
Friction Modifier	Alter coefficient of friction	Organic fatty acids and amides, lard oil, high molecular weight organic phosphorus and phosphoric acid esters	Preferential adsorption of surface-active materials

REFERENCES

1. http://www.findarticles.com/p/articles/mi_m3012/is_5_183/ai_101939317#continue.
2. H.Spedding, R.C Watkins, (Feb. 1982). The antiwear mechanism of ZDDP's Part I, Tribology International, Vol. 15, 1, 9-12.
3. H.Spikes, (Oct 2004). The histroy and Mechanisms of ZDDP, Tribology Letters ,Vol 17, No.3 469-489.
4. N. J. Mosey, M.H Muser, T. K. Woo, (11th March 2005). Molecular Mechanisms for the functionality of lubricant additives, Science, Vol. 307 1612-1615.
5. http://www.how stuff works.com.
6. Jim Fitch, November (Nov 2002). Clean Oil Reduces Engine Fuel Consumption. *Practicing Oil Analysis* Magazine, Issue:200211
7. http://ntrs.nasa.gov/archive/nasa/casi.ntrs.nasa.gov/19960045816_1996077579.pdf.
8. E.S Yamaguchi, S. H Roby, S.W.Yeh, (Jan-March 2005). Time Dependent Film formation from ZnDTPs and Non phosphorus antiwear agents, STLE Tribology Transactions, vol 48, No. 1 57-68.
9. H.A Spikes, (1989). Additive-additive interaction and additive-surface interaction in lubrication, Lubrication Science, Vol. 2, 1, 3-23.

10. F.G. Rounds, (1976). Addtive Interactions and their effect on the performance of a Zinc dilkyl dithiphosphate, ASLE Trans, Vol 21, 2, 91-101.
11. G.S. Kapur, A. Chopra, A.S Sarpal,S.S.V Ramakumar, S.K. Jain, (1999). Studies on competitive interactions between engine oil interactions and blending order of engine oil additives by variable temperature 31P NMR and IR spectroscopy, Tribology Transactions , Vol 42, 4, 807-812.
12. S.S.V Ramakumar, A.M.Rao, S.P Srivastava, (1992). Studies on additive-additive interactions: Formulation of crank case oils towards rationalization, Vol 156, 101-120.
13. K.Patel, (May 2004). Development of low phosphorus engine oils, Thesis, UMI-1421294.
14. Parekh, K., Mourhatch, R., Aswath, P.B., (September 12-16, 2005). ZDDP-Additive-Catalyst Interactions in Engine oil, Proceedings of WTC2005 World Tribology Congress III, Washington, DC., USA.
15. M. Z. Huq, X. Chen, P. B. Aswath, R. L. Elsenbaumer, (June 2005). Thermal degradation behavior of zinc dialkyldithiophosphate in presence of catalyst and detergents in neutral oil, Tribology Letters, Vol 19, No. 2, 127-134.
16. I.M Hutchings, Wear and Lubrication, Encyclopedia of Materials: Science and technology ISBN: 0-08-0431526, 9551-9556.
17. B.A Khorramian, G.R. Iyer, S. Kodali, P. Natarajan, R. Tupil, (1993). Review of antiwear additives for crank case oils, Wear, Vol.169, 1, 87-95.
18. http://www.chevron.com/prodserv/BaseOils/gf4_faq.shtml.

19. W.B. Chamberlin, E.A. Bardasz, Lubrizol Research, Development, (2001). http://64.233.161.104/search?q=cache:iTPT_WRpU2oJ:www.windsorworkshop.ca/2001archive/Transportation/Session_8/3_chamberlin.pdf+W.B+chamberlin+lubrizol&hl=en, Crank case oils and engine design system Technologies for Improving Emissions Performance.
20. Blaine Ballentine, Central Petroleum Company, (July 2003). Motor Oils - Fuel Economy vs. Wear, Machinery Lubrication Magazine, Issue: 200307
21. Jim Fitch, (July 2002). New Lubrication Commandments - Conserve Energy, Protect the Environment, Machinery Lubrication Magazine, Issue: 200207
22. http://www.dowcorning.com/content/molykote/molykoteauto/default.asp
23. http://www.oilamatic.com/engine-tlc.htm.
24. http://www.lubrizol.com/LubeTheory/theory.asp.
25. C. B Davies, (1957-58). A review of boundary Lubrication, Wear, Vol. 1, 244-53.
26. Ph. Kapsa and J.M Martin, (Feb 1982). Boundary Lubricant films: a review, Tribology International,Vol.15, 1, 37-42.
27. http://www.lubrizol.com/LubeTheory/adduse.asp.
28. S.M Hsu, R. S Gates, (2004). Boundary Lubricating films : formation and lubrication mechanism Tribology International , Vol. 38, 3, 1-8.
29. C.M. Allen, D. Drauglis, (1969). Boundary Layer Lubrication: Monolayer or Multilayer, Wear, Vol. 14, 363-384.

30. M. Nicholls, T. Do, P.Norton, M. Kasrai, G.Bancroft, (2005). Review of the lubrication of metallic surfaces by ZincDialkylDithiophosphates, Tribology International, Vol. 38, 15- 39.
31. Don Clason, the Lubrizol Corporation, (Nov 2003)."Zinc-Based Additives Continue to Deliver". Machinery Lubrication Magazine, Issue: 200311
32. P.G Harrison, Thakor Kikabhai, (1987). Proton and Phosphorus 31 NMR study of ZDDP in solution J. Chem Soc. Dalton Trans, 807-813.
33. S. Menzer, J.Phillips, A.Slawin, D. Williams,J.Woolins, (2000). Structural characterization of basic O,O' dialkyl Dithiophosphate and two isomeric examples of zinc monothiophoshate, J.Chem.Soc.,Dalton trans, 3269-3273.
34. F.G.Rounds , (1966).ASLE Transactions Vol. 9, 88.
35. A.D.Brazier, J.S.Elliot, (1967). The thermal stability of Zinc dithiphosphates, Journal of insititute of Petroleum, Vol.53, No.518, 63-76.
36. R.C Coy, R.B Jones, (1981). The thermal degradation and EP performance of oil, ASLE Transactions, Vol.24, 1, 77-90.
37. R.C Coy, R.B Jones, (1981). Chemistry of the thermal degradation of Zinc dialkyl dithiophsophates additives, ASLE Transactions, Vol. 24, 1, 91-97.
38. P.A.Willermet,D.PDailey, R.OCater III, P.J.Schmitz, W.Zhu, (1995). Mechanism of formation of antiwear films from Zinc dialkyl dithiophsophates, Tribology International, Vol 28, 3, 177-187.
39. H. Fujita and H. A Spikes , (2004). Proc. I. Mech. E. Ser.J., Vol. 218, 265.

40. R.C Watkins, Feb. (1982). The antiwear mechanism of ZDDP's Part II, Tribology International.
41. Souminen Fuller ML, Kasrai M, Bancroft GM, Fyfe K, Tan KH., (1998). Solution decomposition of ZDDP and its effects on antiwear and thermal film formation studied by XAS. Tribology international Vol. 31, 10, 627-44.
42. Gaby Nehme, (2004). Performance testing and analysis of anti-wear additives in engine oil for reducing phosphorus content and improving tail pipe emissions , Thesis, University of Texas at Arlington.
43. R.J.Bird, G.D Galvin, (1976). Wear, Vol. 37, 143.
44. Y.C.Lin, H.So, (2004). Limitations on use of ZDDP as an antiwear additive in boundary lubrication, Tribology International, Vol. 37, 25-33.
45. H.So, Y.C.Lin, Antiwear Mechanism of Zinc dialkyl dithiophsophates added to a paraffinic oil in boundary lubrication condition.
46. R. Mourhatch, P. B. Aswath, (2005-06). Boundary Lubrication in Engine Oils (submitted).
47. Grayson, Martin., Griffith, Edward.,(1964-1983). ^{31}P Nuclear Magnetic resonance, Topics in Phosphorus chemistry, Vol 5., New York Interscience publishers,.
48. Douglas A. Skoog, James J. Leary, Principles of Instrumental Analysis, 4th edition, Saunders College Publishing, Harcourt Brace College Publishers.
49. http://www.cem.msu.edu/~reusch/VirtualText/Spectrpy/nmr/nmr1.htm.

50. P. Peng, Hong Shan-Zhen, Lu, Wan, (March 1994). The degradation of Zinc dialkyl Dithiophosphate additives in fully formulated engine oil as studied by ^{31}P NMR spectroscopy, Lubrication Engineering, Vol 50, 3, 230-235.

51. G.L Marshall, (1984). Characterization of lubricants using ^{31}P Fourier transform Nuclear Magnetic Resonance Spectroscopy, Applied Spectrscopy, vol 38, 4, 522-526.

52. Zs. Wittmann, Zs Kovacs, (1985). Phosphorus 31 Nuclear Magnetic Resonance chemical shifts of phosphoric acid derivatives,Talanta, vol 32, 7, 581-582.

53. Emsley, J.W. Feeney, J. and Sutcliffe, L. H., (1965-66) High Resolution Nuclear Magnetic Resonance Spectroscopy, Vol. 2. Oxford, NY, Pergamon Press.

54. J.F. Nixon, R. Schmutzler, (1964) Phosphorus-31 Nuclear Magentic Resonance studies of phosphorus fluorine compounds,Spectrochimica Acta, Vol. 20, 1835-1842.

55. G.S Reddy , R. Schmutzler, (1970), ^{31}P and ^{19}F Nuclear Magentic Resonance Studies of Phosphorus-Fluorine comounds, Zeitschrift Fur Naturforschung, 25b, 1199-1214.

56. Kajal Parekh, Pranesh.B.Aswath, Harold Shaub, Ronald.L Elsenbaumer, (July 14th, 2005). Low Phosphorus Lubricant Additive, Application for US Letters Patent, continuation in part of prior application no. 10/965,686 attorney docket no. 50715/P006CP1/pending.

57. G.C. Smith , J.C Bell, (1999), Multitechnique surface analytical studies of automotive antiwear films, Applied surface science, 144-45, 222-227.
58. J.M Palacios, (1992), The performance of some antiwear additives and interference with other additives, lubrication science, Vol. 4, 201-209.
59. J.L Paddy, N.C lee, J.Waters,D. N Trott,(1990), Zinc dialkyl Dithiophosphate oxidation by cumene hydroperoxide: kinetic studies by Raman and phosphorus -31 NMR spectroscopy, Tribology transactions, Vol. 33, 1, 15-20.
60. J. L Paddy, N.C lee, J.Waters,D. N Trott,(1990), Zinc dialkyl Dithiophosphate oxidation by cumene hydroperoxide: kinetic studies by Raman and phosphorus -31 NMR spectroscopy, Tribology transactions, Vol. 33, 1, 15-20.
61. Mark Barnes, Noria Corporation and Dave Wooton, Wooton Consulting, May 2003 Molecular Spectroscopy - A Precision Lubrication Tool? Practicing Oil Analysis Magazine., Issue Number: 200305.
62. Osin B., Davliatshin D.I., Ogden J.S., (1996), Journal of Flourine chemistry, Vol. 76, 187-192.

BIOGRAPHICAL INFORMATION

The author Kajal Parekh was born and brought up in Kolkata, India. Owing to a deep interest in the field of chemistry she completed Bachelors in Science with chemistry Honors. Awarded as a National Scholar by Govt. of India for B.Sc. results she pursued Polymer science and technology (B.Tech) in University College of science and Technology in Kolkata. Here she had become greatly interested in the field of plastics and pursued projects like Biodegradation of Polyethylene that posed disposal problems. After completing Master's in polymers she came to Unites States and joined Material Science and Engineering program in University of Texas, Arlington in 2003. Here she continued work in an interesting application field, lubrication chemistry. In the process of developing high performance low phosphorus engine oils, she discovered for the first time new fluorinated phosphorus compounds and fluorocarbons in reaction of ZDDP with FeF_3 and later with UTA-Platinum Research Organization, a Dallas based Co. filed a patent on the same. Awarded as a university scholar in UTA she is a member of Tau beta pi and Phi beta delta, engineering honor societies. She is currently working on 2-3 journal papers in the area of ZDDP interactions and wishes to continue working in the field of research and development for an Industry and make a significant contribution to basic science.